Published by IOP Publishing for SISSA

Received: *April 8, 2009*
Accepted: *June 2, 2009*
Published: *June 11, 2009*

JHEP06(2009)041

Event shapes and jet rates in electron-positron annihilation at NNLO

Stefan Weinzierl

Institut für Physik, Universität Mainz,
D-55099 Mainz, Germany

E-mail: stefanw@thep.physik.uni-mainz.de

Abstract: This article gives the perturbative NNLO results for the most commonly used event shape variables associated to three-jet events in electron-positron annihilation: Thrust, heavy jet mass, wide jet broadening, total jet broadening, C parameter and the Durham three-to-two jet transition variable. In addition the NNLO results for the jet rates corresponding to the Durham, Geneva, Jade-E0 and Cambridge jet algorithms are presented.

Keywords: Jets, QCD

ArXiv ePrint: 0904.1077

doi:10.1088/1126-6708/2009/06/041

Contents

JHEP06(2009)041

1 Introduction

The experiments at LEP (CERN), SLC (SLAC) and PETRA (DESY) have collected a wealth of data from electron-positron annihilation with hadronic final state over a wide range of energies. Of particular interest are three-jet events, which can be used to extract the value of the strong coupling. Three-jet events are well suited for this task because the leading term in a perturbative calculation of three-jet observables is already proportional to the strong coupling. In comparing experiments to theory it is important to restrict oneself to infra-red safe observables. For three-jet events in electron-positron annihilation there is a well established set of infra-red safe observables, which is widely used. These are the event shape variables consisting of thrust, heavy jet mass, wide jet broadening, total jet broadening and the C-parameter. In addition there are observables related to a specific jet definition. First of all these are the jet rates associated to the different jet definitions. In this paper the following jet algorithms are considered: Durham, Geneva, Jade-E0 and Cambridge. As the Durham jet algorithm is the most popular one, for this jet algorithm also the three-to-two jet transition variable is studied.

All these observables can be calculated in perturbation theory. In this article I present the next-to-next-to-leading order (NNLO) results for these observables. For completeness I also include the next-to-leading order (NLO) and leading order (LO) results.

Another group published results for these observables earlier on in [1–3], but omitted certain subtraction terms related to soft gluons. The present calculation is based on the numerical Monte Carlo program reported in [4, 5]. The additional soft gluon subtraction terms modify the distributions in the peak region. Meanwhile the other group has added the missing subtraction terms and the two programs are now for the main part of the observables in good agreement. A few remaining differences are discussed in the numerical

section. A detailed account of the subtraction terms used in this calculation is given in a companion paper [6].

For the thrust distribution there exists an independent calculation of the logarithmic terms based on soft-collinear effective theory [7]. This calculation should agree with the NNLO result for small values of $(1-T)$. For large values of $(1-T)$ the logarithmic terms alone are not sufficient to give an accurate result. On the other hand the perturbative calculation of this paper gives the correct NNLO result for large and intermediate values of $(1-T)$, but has its limitations due to the Monte Carlo integration method for very small values of $(1-T)$. This gives a region of overlap where the perturbative NNLO result and the one obtained from SCET should agree, and indeed they do.

This article reports the pure perturbative results for the event shapes. Not included are soft-gluon resummations [7–10] nor power corrections [11, 12].

It should be mentioned that the results of this paper rely heavily on research carried out in the past years: Integration techniques for two-loop amplitudes [13–16], the calculation of the relevant tree-, one- and two-loop-amplitudes [17–29], routines for the numerical evaluation of polylogarithms [30–32], methods to handle infrared singularities [33–51] and experience from the NNLO calculations of $e^+e^- \to 2$ jets and other processes [40, 52–68].

This paper is organised as follows: section 2 gives the definition of the observables related to three-jet events in electron-positron annihilation. Section 3 describes the perturbative calculation of these observables. Section 4 gives the numerical results. Finally, section 5 contains a summary. In an appendix a useful algorithm for the determination of the thrust axis is described.

2 Definition of the observables

The event shape variable thrust [69, 70] is defined by

$$T = \frac{\max\limits_{\vec{n}} \sum\limits_j |\vec{p}_j \cdot \vec{n}|}{\sum\limits_j |\vec{p}_j|}, \tag{2.1}$$

where $\vec{p}_j$ denotes the three-momentum of particle j and the sum runs over all particles in the final state. The thrust variable maximises the total longitudinal momentum along the unit vector $\vec{n}$. The value of $\vec{n}$, for which the maximum is attained is called the thrust axis and denoted by $\vec{n}_T$. The value of thrust ranges between $1/2$ and 1, where $T = 1$ corresponds to an ideal collinear two-jet event and $T = 1/2$ corresponds to a perfectly spherical event. Usually one considers instead of thrust T the variable $(1-T)$, such that the two-jet region corresponds to $(1-T) \to 0$. For three-parton events we have $(1-T) \leq 1/3$.

The plane orthogonal to the thrust axis divides the space into two hemispheres H_1 and H_2. These are used to define the following event shape variables: The hemisphere masses [71] are defined by

$$M_i^2 = \left(\sum_{j \in H_i} p_j \right)^2, \quad i = 1, 2, \tag{2.2}$$

where p_j denotes the four-momentum of particle j. The heavy hemisphere mass M_H and the light hemisphere mass M_L are then defined by

$$M_H^2 = \max\left(M_1^2, M_2^2\right), \quad M_L^2 = \min\left(M_1^2, M_2^2\right). \tag{2.3}$$

The light hemisphere mass is a four-jet observable and vanishes for three partons. For the heavy jet mass it is convenient to introduce the dimensionless quantity

$$\rho = \frac{M_H^2}{Q^2}, \tag{2.4}$$

where Q is the centre-of-mass energy. For three-parton events we have $\rho \leq 1/3$. In leading order the distribution of the heavy jet mass is identical to the distribution of $(1-T)$.

The hemisphere broadenings [72, 73] are defined by

$$B_i = \frac{\sum\limits_{j \in H_i} |\vec{p}_j \times \vec{n}_T|}{2 \sum\limits_k |\vec{p}_k|}, \quad i = 1, 2, \tag{2.5}$$

where the sum over j runs over all particles in one of the hemispheres, whereas the sum over k is over all particles in the final state. The wide jet broadening B_W, the narrow jet broadening B_N and the total jet broadening B_T are defined by

$$B_W = \max\left(B_1, B_2\right), \quad B_N = \min\left(B_1, B_2\right), \quad B_T = B_1 + B_2. \tag{2.6}$$

The narrow jet broadening is a four-jet observable and vanishes for three partons. For three-parton events we have $B_W, B_T \leq 1/(2\sqrt{3})$.

The C- and D-parameters [74, 75] are obtained from the linearised momentum tensor

$$\theta^{ij} = \frac{1}{\sum\limits_l |\vec{p}_l|} \sum_k \frac{p_k^i p_k^j}{|\vec{p}_k|}, \quad i, j = 1, 2, 3, \tag{2.7}$$

where the sum runs over all final state particles and p_k^i is the i-th component of the three-momentum $\vec{p}_k$ of particle k in the c.m. system. The tensor θ is normalised to have unit trace. In terms of the eigenvalues of the θ tensor, λ_1, λ_2, λ_3, with $\lambda_1 + \lambda_2 + \lambda_3 = 1$, one defines

$$\begin{aligned} C &= 3\left(\lambda_1\lambda_2 + \lambda_2\lambda_3 + \lambda_3\lambda_1\right), \\ D &= 27\lambda_1\lambda_2\lambda_3. \end{aligned} \tag{2.8}$$

The range of values is $0 \leq C, D \leq 1$. The D-parameter is again a four-jet observable and vanishes for three partons. For three-parton events we have $C \leq 3/4$. The C-parameter exhibits in perturbation theory a singularity at the three-parton boundary $C = 3/4$ [76].

The production rate for three-jet events is defined by the ratio of the cross section for three-jet events by the total hadronic cross section

$$R_3 = \frac{\sigma_{3-jet}}{\sigma_{\rm tot}}. \tag{2.9}$$

This depends on the definition of the jet algorithm, usually specified through a resolution variable and a recombination prescription. The clustering procedure of a jet algorithm in electron-positron annihilation is in most cases defined through the following steps:

JHEP06(2009)041

1. Define a resolution parameter $y_{\rm cut}$

2. For every pair (p_k, p_l) of final-state particles compute the corresponding resolution variable y_{kl}.

3. If y_{ij} is the smallest value of y_{kl} computed above and $y_{ij} < y_{\rm cut}$ then combine (p_i, p_j) into a single jet ('pseudo-particle') with momentum p_{ij} according to a recombination prescription.

4. Repeat until all pairs of objects (particles and/or pseudo-particles) have $y_{kl} > y_{\rm cut}$.

The various jet algorithms differ in the precise definition of the resolution variable and the recombination prescription. The various recombination prescriptions are:

1. E-scheme:

$$E_{ij} = E_i + E_j, \;\; \vec{p}_{ij} = \vec{p}_i + \vec{p}_j. \tag{2.10}$$

   The E-scheme conserves energy and momentum, but for massless particles i and j the recombined four-momentum is not massless.

2. E0-scheme:

$$E_{ij} = E_i + E_j, \;\; \vec{p}_{ij} = \frac{E_i + E_j}{|\vec{p}_i + \vec{p}_j|} \left(\vec{p}_i + \vec{p}_j\right). \tag{2.11}$$

   The E0-scheme conserves energy, but not momentum. For massless particles i and j is the recombined four-momentum again massless.

3. P-scheme:

$$E_{ij} = \frac{|\vec{p}_i + \vec{p}_j|}{E_i + E_j} \left(E_i + E_j\right) = |\vec{p}_i + \vec{p}_j|\,, \;\; \vec{p}_{ij} = \vec{p}_i + \vec{p}_j. \tag{2.12}$$

   The P-scheme conserves momentum, but not energy. For massless particles i and j is the recombined four-momentum again massless, as in the $E0$-scheme.

For the Durham [77], Geneva [78] and Jade-E0 [79] jet algorithms the resolution variables and the recombination prescriptions are defined as follows:

$$\begin{aligned}
\text{Durham:} \;\; y_{ij} &= \frac{2\min(E_i^2, E_j^2)\left(1 - \cos\theta_{ij}\right)}{Q^2}, \quad \text{E-scheme,} \\
\text{Geneva:} \;\; y_{ij} &= \frac{8}{9} \cdot \frac{2E_iE_j\left(1 - \cos\theta_{ij}\right)}{\left(E_i + E_j\right)^2}, \quad \text{E-scheme,} \\
\text{Jade-E0:} \;\; y_{ij} &= \frac{2E_iE_j\left(1 - \cos\theta_{ij}\right)}{Q^2}, \quad \text{E0-scheme,}
\end{aligned} \tag{2.13}$$

where E_i and E_j are the energies of particles i and j, and θ_{ij} is the angle between $\vec{p}_i$ and $\vec{p}_j$. Q is the centre-of-mass energy. The jet transition variable y_{23} is the value of the jet resolution parameter $y_{\rm cut}$, for which the event changes from a three-jet to a two-jet

JHEP06(2009)041

configuration. Similar, y_{34} is defined as the value of the resolution parameter, where the event changes from a four-jet to a three-jet configuration. The three-jet rate is related to the jet transition variables y_{23} and y_{34}:

$$R_3(y_{\rm cut}) = \int\limits_{y_{\rm cut}}^{1} dy_{23} \frac{d\sigma}{dy_{23}} - \int\limits_{y_{\rm cut}}^{1} dy_{34} \frac{d\sigma}{dy_{34}}. \tag{2.14}$$

The Cambridge algorithm [80] distinguishes an ordering variable v_{ij} and a resolution variable y_{ij}. The Cambridge algorithm is defined as follows:

1. Select a pair of objects (p_i, p_j) with the minimal value of the ordering variable v_{ij}.
2. If $y_{ij} < y_{\rm cut}$ they are combined, one recomputes the relevant values of the ordering variable and goes back to the first step.
3. If $y_{ij} \geq y_{\rm cut}$ and $E_i < E_j$ then i is defined as a resolved jet and deleted from the table.
4. Repeat until only one object is left in the table. This object is also defined as a jet and clustering is finished.

As ordering variable

$$v_{ij} = 2\,(1 - \cos\theta_{ij}) \tag{2.15}$$

is used. The resolution variable is as in the Durham algorithm

$$y_{ij} = \frac{2\min(E_i^2, E_j^2)\,(1 - \cos\theta_{ij})}{Q^2} \tag{2.16}$$

and the E-scheme is used as recombination prescription.

3 Perturbative expansion

The perturbative expansion of a differential distribution for any infrared-safe observable $\mathcal{O}$ for the process $e^+e^- \to 3$ jets can be written up to NNLO as

$$\frac{\mathcal{O}^n}{\sigma_{\rm tot}(\mu)} \frac{d\sigma(\mu)}{d\mathcal{O}} = \frac{\alpha_s(\mu)}{2\pi} \frac{\mathcal{O}^n d\bar{A}_{\mathcal{O}}(\mu)}{d\mathcal{O}} + \left(\frac{\alpha_s(\mu)}{2\pi}\right)^2 \frac{\mathcal{O}^n d\bar{B}_{\mathcal{O}}(\mu)}{d\mathcal{O}} + \left(\frac{\alpha_s(\mu)}{2\pi}\right)^3 \frac{\mathcal{O}^n d\bar{C}_{\mathcal{O}}(\mu)}{d\mathcal{O}}. \tag{3.1}$$

$\bar{A}_{\mathcal{O}}$ gives the LO result, $\bar{B}_{\mathcal{O}}$ the NLO correction and $\bar{C}_{\mathcal{O}}$ the NNLO correction. The variable n denotes the moment of the distribution. Unless stated otherwise, the value $n = 1$ is used as default. $\sigma_{\rm tot}$ denotes the total hadronic cross section calculated up to the relevant order. The arbitrary renormalisation scale is denoted by μ. The n-th moment is given by

$$\langle \mathcal{O}^n \rangle = \frac{1}{\sigma_{\rm tot}} \int \mathcal{O}^n \frac{d\sigma}{d\mathcal{O}} d\mathcal{O}. \tag{3.2}$$

In practise the numerical program computes the distribution

$$\frac{\mathcal{O}^n}{\sigma_0(\mu)} \frac{d\sigma(\mu)}{d\mathcal{O}} = \frac{\alpha_s(\mu)}{2\pi} \frac{\mathcal{O}^n dA_{\mathcal{O}}(\mu)}{d\mathcal{O}} + \left(\frac{\alpha_s(\mu)}{2\pi}\right)^2 \frac{\mathcal{O}^n dB_{\mathcal{O}}(\mu)}{d\mathcal{O}} + \left(\frac{\alpha_s(\mu)}{2\pi}\right)^3 \frac{\mathcal{O}^n dC_{\mathcal{O}}(\mu)}{d\mathcal{O}}, \tag{3.3}$$

JHEP06(2009)041

normalised to σ_0, which is the LO cross section for $e^+e^- \to$ hadrons, instead of the normalisation to $\sigma_{\rm tot}$. There is a simple relation between the two distributions: The functions $A_{\mathcal{O}}$, $B_{\mathcal{O}}$ and $C_{\mathcal{O}}$ are related to the functions $\bar{A}_{\mathcal{O}}$, $\bar{B}_{\mathcal{O}}$ and $\bar{C}_{\mathcal{O}}$ by

$$\begin{aligned}
\bar{A}_{\mathcal{O}} &= A_{\mathcal{O}}, \\
\bar{B}_{\mathcal{O}} &= B_{\mathcal{O}} - A_{\rm tot} A_{\mathcal{O}}, \\
\bar{C}_{\mathcal{O}} &= C_{\mathcal{O}} - A_{\rm tot} B_{\mathcal{O}} - \left(B_{\rm tot} - A_{\rm tot}^2\right) A_{\mathcal{O}},
\end{aligned}$$

where

$$\begin{aligned}
A_{\rm tot} &= \frac{3(N_c^2-1)}{4N_c}, \\
B_{\rm tot} &= \frac{N_c^2-1}{8N_c}\left[\left(\frac{243}{4} - 44\zeta_3\right) N_c + \frac{3}{4N_c} + (8\zeta_3 - 11)\, N_f\right].
\end{aligned}$$

N_c denotes the number of colours and N_f the number of light quark flavours. $A_{\rm tot}$ and $B_{\rm tot}$ are obtained from the perturbative expansion of $\sigma_{\rm tot}$ [81–83]:

$$\sigma_{\rm tot} = \sigma_0 \left(1 + \frac{\alpha_s}{2\pi} A_{\rm tot} + \left(\frac{\alpha_s}{2\pi}\right)^2 B_{\rm tot} + \mathcal{O}(\alpha_s^3)\right). \tag{3.4}$$

The perturbative calculation of the inclusive hadronic cross section $\langle\sigma\rangle^{(tot)}$ is actually known to $\mathcal{O}(\alpha_s^3)$ [84, 85], although we need here only the coefficients up to $\mathcal{O}(\alpha_s^2)$.

It is sufficient to calculate the functions $\bar{A}_{\mathcal{O}}$, $\bar{B}_{\mathcal{O}}$ and $\bar{C}_{\mathcal{O}}$ for a fixed renormalisation scale μ_0, which can be taken conveniently to be equal to the centre-of-mass energy: $\mu_0 = Q$. The scale variation can be restored from the renormalisation group equation

$$\begin{aligned}
\mu^2 \frac{d}{d\mu^2}\left(\frac{\alpha_S}{2\pi}\right) &= -\frac{1}{2}\beta_0 \left(\frac{\alpha_S}{2\pi}\right)^2 - \frac{1}{4}\beta_1 \left(\frac{\alpha_S}{2\pi}\right)^3 - \frac{1}{8}\beta_2 \left(\frac{\alpha_S}{2\pi}\right)^4 + \mathcal{O}(\alpha_s^5), \qquad (3.5) \\
\beta_0 &= \frac{11}{3} C_A - \frac{4}{3} T_R N_f, \\
\beta_1 &= \frac{34}{3} C_A^2 - 4\left(\frac{5}{3} C_A + C_F\right) T_R N_f, \\
\beta_2 &= \frac{2857}{54} C_A^3 - \left(\frac{1415}{27} C_A^2 + \frac{205}{9} C_A C_F - 2C_F^2\right) T_R N_f \\
&\qquad + \left(\frac{158}{27} C_A + \frac{44}{9} C_F\right) T_R^2 N_f^2.
\end{aligned}$$

The colour factors are defined as usual by

$$C_A = N_c, \quad C_F = \frac{N_c^2 - 1}{2N_c}, \quad T_R = \frac{1}{2}. \tag{3.6}$$

The values of the functions $\bar{A}_{\mathcal{O}}$, $\bar{B}_{\mathcal{O}}$ and $\bar{C}_{\mathcal{O}}$ at a scale μ are then obtained from the ones at the scale μ_0 by

$$\begin{aligned}
\bar{A}_{\mathcal{O}}(\mu) &= \bar{A}_{\mathcal{O}}(\mu_0), \\
\bar{B}_{\mathcal{O}}(\mu) &= \bar{B}_{\mathcal{O}}(\mu_0) + \frac{1}{2}\beta_0 \ln\left(\frac{\mu^2}{\mu_0^2}\right) \bar{A}_{\mathcal{O}}(\mu_0), \\
\bar{C}_{\mathcal{O}}(\mu) &= \bar{C}_{\mathcal{O}}(\mu_0) + \beta_0 \ln\left(\frac{\mu^2}{\mu_0^2}\right) \bar{B}_{\mathcal{O}}(\mu_0) + \frac{1}{4}\left[\beta_1 + \beta_0^2 \ln\left(\frac{\mu^2}{\mu_0^2}\right)\right] \ln\left(\frac{\mu^2}{\mu_0^2}\right) \bar{A}_{\mathcal{O}}(\mu_0).
\end{aligned} \tag{3.7}$$

JHEP06(2009)041

Finally, an approximate solution of eq. (3.5) for α_s is given by

$$\frac{\alpha_s(\mu)}{2\pi} = \frac{2}{\beta_0 L}\left\{1 - \frac{\beta_1}{\beta_0^2}\frac{\ln L}{L} + \frac{\beta_1^2}{\beta_0^4 L^2}\left[\left(\frac{1}{2} - \ln L\right)^2 + \frac{\beta_0\beta_2}{\beta_1^2} - \frac{5}{4}\right]\right\}, \tag{3.8}$$

where $L = \ln(\mu^2/\Lambda^2)$.

The function $C_{\mathcal{O}}$ can be decomposed into six colour pieces

$$C_{\mathcal{O}} = \frac{(N_c^2-1)}{8N_c}\left[N_c^2 C_{\mathcal{O}}^{\mathrm{lc}} + C_{\mathcal{O}}^{\mathrm{sc}} + \frac{1}{N_c^2}C_{\mathcal{O}}^{\mathrm{ssc}} + N_f N_c C_{\mathcal{O}}^{\mathrm{nf}} + \frac{N_f}{N_c}C_{\mathcal{O}}^{\mathrm{nfsc}} + N_f^2 C_{\mathcal{O}}^{\mathrm{nfnf}}\right]. \tag{3.9}$$

In addition, there are singlet contributions, which arise from interference terms of amplitudes, where the electro-weak boson couples to two different fermion lines. These singlet contributions are expected to be numerically small [28, 86, 87] and neglected in the present calculation. We define

$$C_{\mathcal{O}}|_{\mathrm{lc}} = \frac{(N_c^2-1)}{8N_c}N_c^2 C_{\mathcal{O}}^{\mathrm{lc}}, \qquad C_{\mathcal{O}}|_{\mathrm{sc}} = \frac{(N_c^2-1)}{8N_c}C_{\mathcal{O}}^{\mathrm{sc}}, \qquad C_{\mathcal{O}}|_{\mathrm{ssc}} = \frac{(N_c^2-1)}{8N_c}\frac{1}{N_c^2}C_{\mathcal{O}}^{\mathrm{ssc}},$$
$$C_{\mathcal{O}}|_{\mathrm{nf}} = \frac{(N_c^2-1)}{8N_c}N_f N_c C_{\mathcal{O}}^{\mathrm{nf}}, \quad C_{\mathcal{O}}|_{\mathrm{nfsc}} = \frac{(N_c^2-1)}{8N_c}\frac{N_f}{N_c}C_{\mathcal{O}}^{\mathrm{nfsc}}, \quad C_{\mathcal{O}}|_{\mathrm{nfnf}} = \frac{(N_c^2-1)}{8N_c}N_f^2 C_{\mathcal{O}}^{\mathrm{nfnf}}, \tag{3.10}$$

e.g. the function $C_{\mathcal{O}}|_{\mathrm{lc}}$ includes the colour factors.

The functions $A_{\mathcal{O}}$, $B_{\mathcal{O}}$ and $C_{\mathcal{O}}$ are calculated for a fixed renormalisation scale equal to the centre-of-mass energy: $\mu_0 = Q$. They depend only on the value of the observable $\mathcal{O}$. Since only QCD corrections with non-singlet quark couplings are taken into account and singlet contributions to $C_{\mathcal{O}}$ are neglected, the functions $A_{\mathcal{O}}$, $B_{\mathcal{O}}$ and $C_{\mathcal{O}}$ do not depend on electro-weak couplings.

4 Numerical results

In this section I present the numerical results for the event shape variables and jet rates at next-to-next-to-leading order. All results have been obtained by numerical Monte Carlo integration. The Monte Carlo integration introduces a statistical error, which will be quoted with all results. For the infrared singularities a hybrid method between subtraction and slicing has been used. Unless stated otherwise all results have been obtained with the slicing parameter

$$\eta = \frac{s_{\min}}{Q^2} = 10^{-5}. \tag{4.1}$$

It should be noted that the slicing procedure introduces in addition a systematic error. The size of this error can be estimated by varying the slicing parameter η. However, lowering the slicing parameter will increase the statistical error. A practical criteria is to require that the variation due to the slicing parameter is smaller than the statistical error, with the possible exception for the boundaries of the distributions. Imposing this criteria $\eta = 10^{-5}$ turns out to be a good compromise between accuracy and efficiency. The

JHEP06(2009)041

boundaries of the distributions close to the two-jet region deserve special attention: There the value of the observable is comparable to η and one expects sizable corrections. I will discuss the dependence on the slicing parameter in the close-to-two-jet region in detail for a few examples.

In a first series of plots I show the comparison of the NNLO results with the NLO and LO results for the LEP I centre-of-mass energy $\sqrt{Q^2} = m_Z$ with $\alpha_S = 0.118$. The results for the event shape variables thrust, heavy jet mass, wide jet broadening, total jet broadening, C parameter and three-to-two jet transition variable y_{23} are shown in figures 1 to 6. For each of these observable the distribution weighted by the observable and normalised to the total hadronic cross section is shown, e.g. for thrust the distribution

$$\frac{1-T}{\sigma}\frac{d\sigma}{d(1-T)} \tag{4.2}$$

is shown. The corresponding plots for the jet rates for the jet algorithms of Durham, Geneva, Jade-E0 and Cambridge are shown in figures 7 to 10. In all these plots is the leading-order prediction shown in light blue, the next-to-leading-order prediction is shown in pink and the next-to-next-to-leading order prediction is shown in dark blue. The bands give the range for the theoretical prediction obtained from varying the renormalisation scale from $\mu = Q/2$ to $\mu = 2Q$. In addition the experimental data points [88] from the Aleph experiment (where available) are also shown in these plot. Note that the theory predictions in these plots are the pure perturbative predictions. Power corrections or soft gluon resummation effects are not included in these results.

Numerical results for centre-of-mass energies different from $\sqrt{Q^2} = m_Z$ are also easily obtained. As an example I show in figure 11 the thrust distribution at centre-of-mass energies of $\sqrt{Q^2} = 91.2\text{GeV}$, 133GeV, 161GeV, 172GeV, 183GeV, 189GeV, 200GeV, 206GeV, again with experimental data points from the Aleph experiment. As for the LEP II energies the bin size of the experimental data is rather large, I show in figure 11 the distribution

$$\frac{1}{\sigma}\frac{d\sigma}{d(1-T)} \tag{4.3}$$

without an additional factor $(1-T)$.

The most important results of this paper are the perturbative coefficients $A_{\mathcal{O}}$, $B_{\mathcal{O}}$ and $C_{\mathcal{O}}$. For the six event shape variables (thrust, heavy jet mass, wide jet broadening, total jet broadening, C-parameter and the three-to-two jet transition variable) the numerical values for the LO functions $A_{\mathcal{O}}$, the NLO functions $B_{\mathcal{O}}$ and the NNLO functions $C_{\mathcal{O}}$, all weighted by $\mathcal{O}$, are given in tables 1 to 7. The corresponding values for the jet rates defined according to the Durham, Geneva, Jade-E0 or Cambridge algorithms are given in tables 8 to 11. These values are obtained by Monte Carlo integration and the statistical Monte Carlo integration error is indicated in these tables. The systematic error due to the slicing parameter η is not included in these tables, but will be discussed below. The values for the Durham jet rate have already been given in ref. [4]. Due to a typo in the numerical program which was corrected after publication of [4] the corrected values are repeated here.

For the six event shape variables the LO functions $A_{\mathcal{O}}$, the NLO functions $B_{\mathcal{O}}$ and the NNLO functions $C_{\mathcal{O}}$ are also shown in in figures 12 to 17. The leading-order function $A_{\mathcal{O}}$

JHEP06(2009)041

and the next-to-leading order function $B_{\mathcal{O}}$ can be computed with high precision and the graphs are shown simply with solid lines in figures 12, 17. For the next-to-next-to-leading order function $C_{\mathcal{O}}$ the Monte Carlo integration errors are typically at the per cent level, and this function is shown with errorbars corresponding to the Monte Carlo integration errors in figures 12–17.

The NNLO function $C_{\mathcal{O}}$ can be split up into the contributions from the individual colour factors

$$C_{\mathcal{O}}|_{\mathrm{lc}}\,, \quad C_{\mathcal{O}}|_{\mathrm{sc}}\,, \quad C_{\mathcal{O}}|_{\mathrm{ssc}}\,, \quad C_{\mathcal{O}}|_{\mathrm{nf}}\,, \quad C_{\mathcal{O}}|_{\mathrm{nfsc}}\,, \quad C_{\mathcal{O}}|_{\mathrm{nfnf}} \tag{4.4}$$

defined in eq. (3.10). For the event shape variables the contributions from the individual colour factors to $C_{\mathcal{O}}$ are given in tables 12 to 18. For the jet rates the contributions from the individual colour factors to $C_{\mathcal{O}}$ are given in tables 19 to 20. In addition the individual colour contributions are plotted for the six event shape variables in figures 18–23.

In figure 24–26 the results for the thrust distribution are compared with the calculation of Becher and Schwartz based on soft-collinear effective theory [7]. The leading-order, next-to-leading-order and next-to-next-to-leading order coefficients A_{1-T}, B_{1-T} and C_{1-T} are compared in figure 24. The individual colour factors of the coefficient C_{1-T} are compared in figure 25. The effective theory gives a good description of the thrust distribution for small values of $(1-T)$. For values of $(1-T)$ close to 1 the effective theory is not valid and deviations from the perturbative result can be seen. On the other hand the perturbative result obtained from Monte Carlo integration has its limitation through the slicing parameter introduced to handle the infrared singularities. The deviations of the numerical Monte Carlo results for the C_{1-T} coefficient from the SCET results for values of $(1-T) < 0.003$ are an artefact of the slicing parameter. In figures 24 and 25 the value $\eta = 10^{-5}$ was used for the slicing parameter. To study the situation in more detail, I show in figure 26 the variation of the numerical result for the leading colour factor of C_{1-T} with the slicing parameter η. The numerical results for $\eta = 10^{-5}$, $\eta = 10^{-7}$ and $\eta = 10^{-9}$ are plotted. For smaller values of η the SCET result is approached.

As a further example I also show the dependence on the slicing parameter η for the colour factor N_c^2 for the next-to-next-to-leading order coefficient $C_{y_{23}}$ for the three-to-two jet transition distribution in figure 27. In this plot the numerical results for $\eta = 10^{-5}$, $\eta = 10^{-7}$ and $\eta = 10^{-9}$ are shown.

Figure 28 compares the results of this calculation to the updated ones from ref. [1]. For the six event shape distributions one observes good agreement with the exception of the three-to-two jet transition distribution at very small values of y_{23}. The discrepancy at small values of y_{23} can be traced back to the colour factor N_c^2 and could have an explanation in terms of a systematic error due to the slicing parameter. The study of the η-dependence in figure 27 gives hints in this direction, but does not give a conclusive answer. Although in figure 27 the three results for $\eta = 10^{-5}$, $\eta = 10^{-7}$ and $\eta = 10^{-9}$ are consistent with each other, using $\eta = 10^{-9}$ instead of $\eta = 10^{-5}$ for the comparison with ref. [1] would reduce the discrepancy significantly (but also enlarge the errorbars). Given the complexity of the calculation the agreement of the two numerical programs in all other distributions is remarkable.

JHEP06(2009)041

5 Conclusions

In this article I reported on the NNLO calculation of observables associated to three-jet events in electron-positron annihilation. I provided NNLO results for the event shape variables thrust, heavy jet mass, wide jet broadening, total jet broadening, C parameter and the Durham three-to-two jet transition variable. In addition the NNLO results for the jet rates defined in the schemes of Durham, Geneva, Jade-E0 and Cambridge were given. The results of this paper will be useful for an extraction of α_s from three-jet quantities.

Acknowledgments

I would like to thank Th. Gehrmann, G. Heinrich, S. Kluth, Ch. Pahl and J. Schieck for useful discussions. In particular I would like to thank E. Schömer for pointing out the method for the determination of the thrust axis to me. The computer support from the Max-Planck-Institut for Physics is greatly acknowledged.

A Calculation of the thrust for a single parton event

For the event shape variable thrust and the ones related to it, it is necessary to determine the maximum

$$\max_{\vec{n}} \sum_j |\vec{p}_j \cdot \vec{n}| \tag{A.1}$$

over all orientations of the unit vector $\vec{n}$. The sum runs over all final state particles j. For the NNLO calculation we have either 3, 4 or 5 partons in the final state. Of course there are numerical algorithms which can be used to find a local maximum. However the computational cost for such a minimisation/maximisation is comparable to the cost for the matrix elements and therefore not negligible. Furthermore it is non-trivial to ensure that the found maximum is actually the global maximum.

There is a better way to calculate thrust and the thrust axis for a small number of final state particles. This method finds the exact global maximum in $2^{N-1}-1$ steps for N final state particles. Let us define N signs $s_j \in \{-1, 1\}$ by

$$\vec{p}_j \cdot \vec{n} = s_j \, |\vec{p}_j \cdot \vec{n}| \, . \tag{A.2}$$

Of course the correct values for the signs s_j are only known once the thrust axis $\vec{n}$ is known. But we know in advance that the N-tuple $(s_1, s_2, \ldots, s_N)$ will be one configuration out of the 2^N possible ones. We can now step over all 2^N possibilities $(s_1, s_2, \ldots, s_N)$. For a given N-tuple $(s_1, s_2, \ldots, s_N)$ we define

$$\vec{P} = s_1\vec{p}_1 + s_2\vec{p}_2 + \ldots + s_N\vec{p}_N. \tag{A.3}$$

We then have

$$\max_{\vec{n}} \sum_j |\vec{p}_j \cdot \vec{n}| = \max_{\vec{n}} \sum_j s_j \vec{p}_j \cdot \vec{n} = \max_{\vec{n}} \; \vec{P} \cdot \vec{n} \tag{A.4}$$

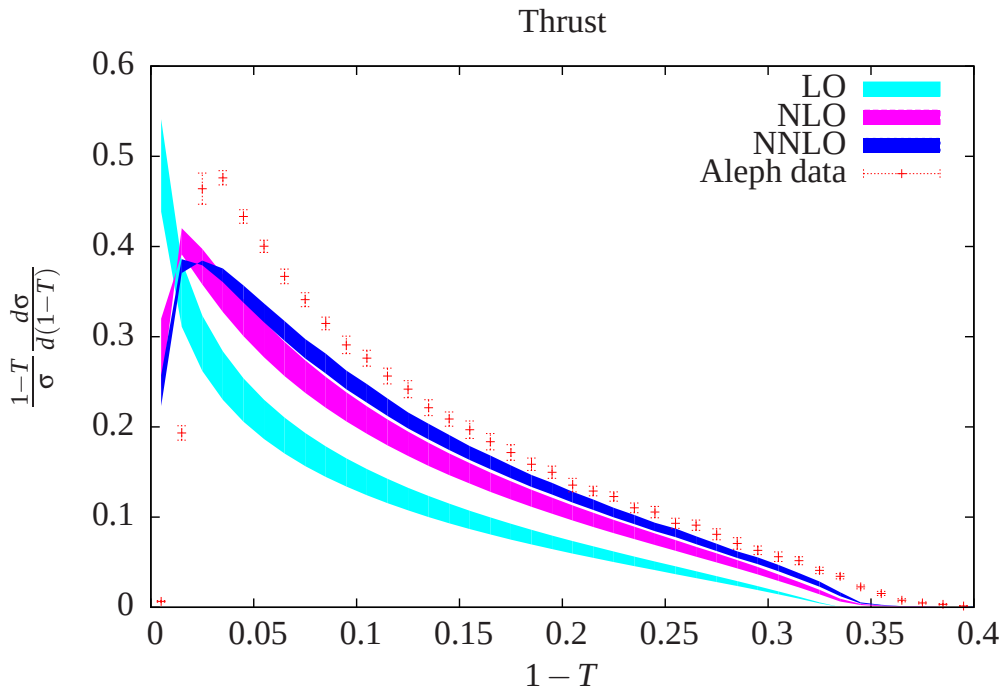

Figure 1. The thrust distribution at LO, NLO and NNLO at $\sqrt{Q^2} = m_Z$ with $\alpha_s(m_Z) = 0.118$. The bands give the range for the theoretical prediction obtained from varying the renormalisation scale from $\mu = m_Z/2$ to $\mu = 2m_Z$. In addition the experimental data points from the Aleph experiment are shown.

This expression is maximised for $\vec{n} = \vec{P}/|\vec{P}|$. Next, one checks if the N-tuple $(s_1, s_2, \ldots, s_N)$ is actually allowed by verifying eq. (A.2) for all $j = 1, \ldots, N$. The maximum is then given by the maximum value obtained from all allowed N-tuples. It is actually sufficient to restrict the search to $2^{N-1} - 1$ possibilities, since thrust is invariant under

$$\vec{n} \to -\vec{n}, \tag{A.5}$$

and the two cases where all signs are equal can be excluded due to momentum conservation. With this algorithm we have to check for five-parton final states 15 configurations to find the global maximum, whereas for four-parton final states 7 configurations have to be checked. For the case of three massless particles in the final state the algorithm does not need to be used, since there is a general formula for the thrust axis: The thrust axis is given in this case by the direction of the most energetic particle [89].

JHEP06(2009)041

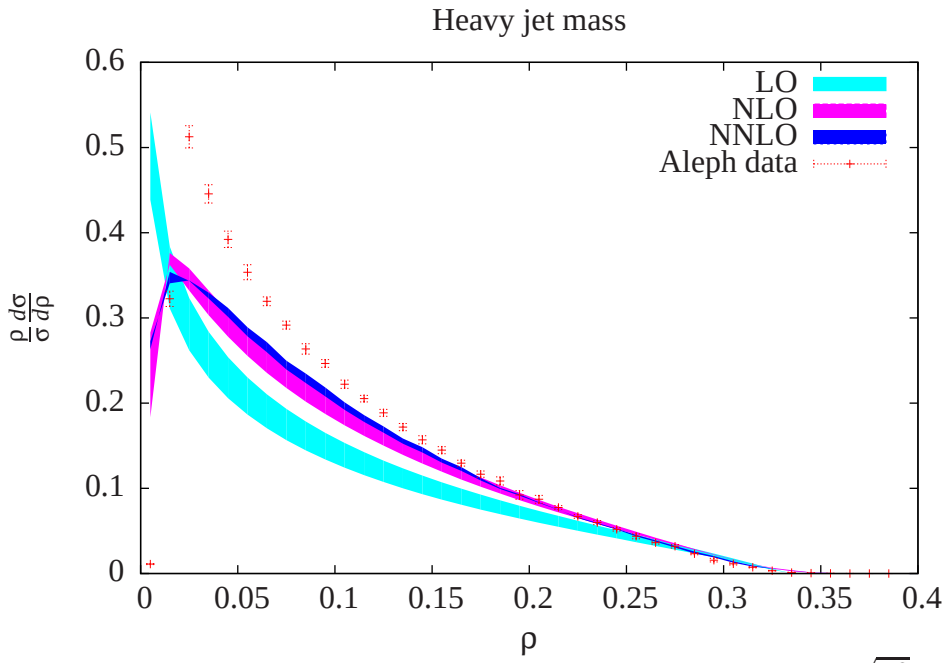

Figure 2. The distribution of the heavy jet mass at LO, NLO and NNLO at $\sqrt{Q^2} = m_Z$ with $\alpha_s(m_Z) = 0.118$. The bands give the range for the theoretical prediction obtained from varying the renormalisation scale from $\mu = m_Z/2$ to $\mu = 2m_Z$. In addition the experimental data points from the Aleph experiment are shown.

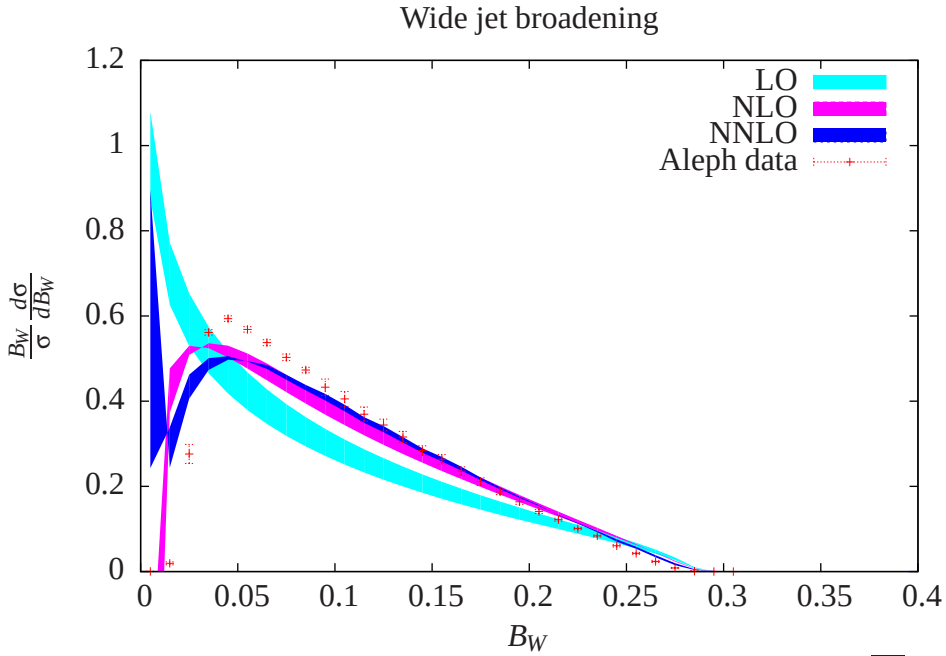

Figure 3. The wide jet broadening distribution at LO, NLO and NNLO at $\sqrt{Q^2} = m_Z$ with $\alpha_s(m_Z) = 0.118$. The bands give the range for the theoretical prediction obtained from varying the renormalisation scale from $\mu = m_Z/2$ to $\mu = 2m_Z$. In addition the experimental data points from the Aleph experiment are shown.

JHEP06(2009)041

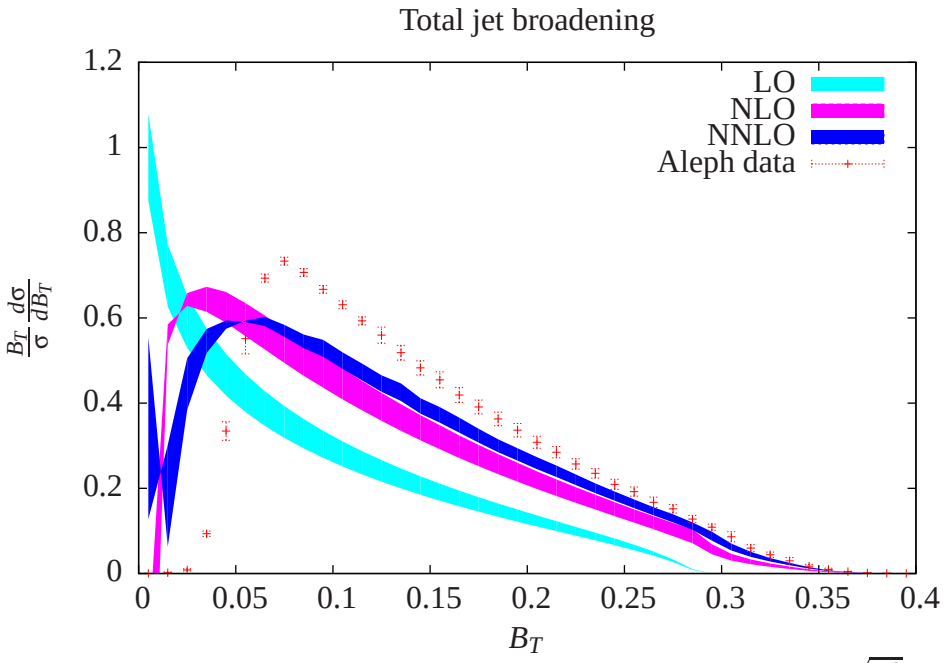

Figure 4. The total jet broadening distribution at LO, NLO and NNLO at $\sqrt{Q^2} = m_Z$ with $\alpha_s(m_Z) = 0.118$. The bands give the range for the theoretical prediction obtained from varying the renormalisation scale from $\mu = m_Z/2$ to $\mu = 2m_Z$. In addition the experimental data points from the Aleph experiment are shown.

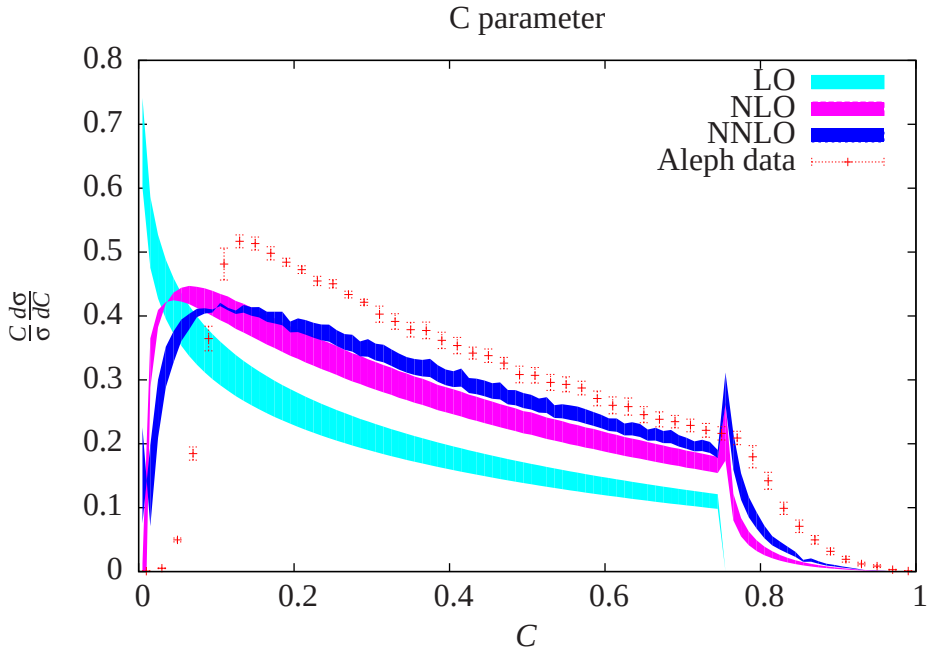

Figure 5. The C-parameter distribution at LO, NLO and NNLO at $\sqrt{Q^2} = m_Z$ with $\alpha_s(m_Z) = 0.118$. The bands give the range for the theoretical prediction obtained from varying the renormalisation scale from $\mu = m_Z/2$ to $\mu = 2m_Z$. In addition the experimental data points from the Aleph experiment are shown.

JHEP06(2009)041

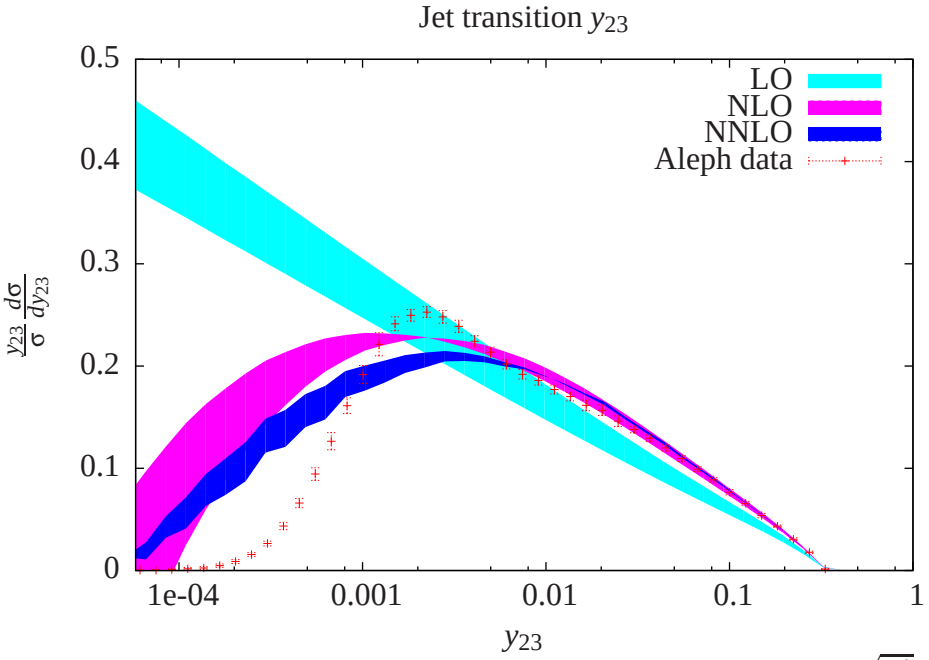

Figure 6. The three-to-two jet transition distribution at LO, NLO and NNLO at $\sqrt{Q^2} = m_Z$ with $\alpha_s(m_Z) = 0.118$. The bands give the range for the theoretical prediction obtained from varying the renormalisation scale from $\mu = m_Z/2$ to $\mu = 2m_Z$. In addition the experimental data points from the Aleph experiment are shown.

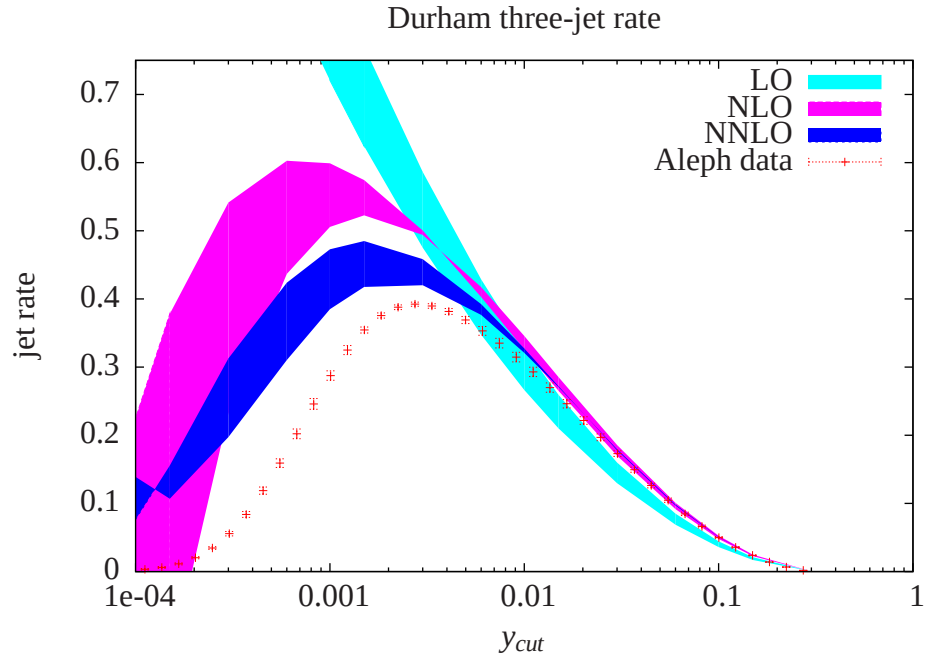

Figure 7. The three jet rate with the Durham jet algorithm at LO, NLO and NNLO at $\sqrt{Q^2} = m_Z$ with $\alpha_s(m_Z) = 0.118$. The bands give the range for the theoretical prediction obtained from varying the renormalisation scale from $\mu = m_Z/2$ to $\mu = 2m_Z$. In addition the experimental data points from the Aleph experiment are shown.

JHEP06(2009)041

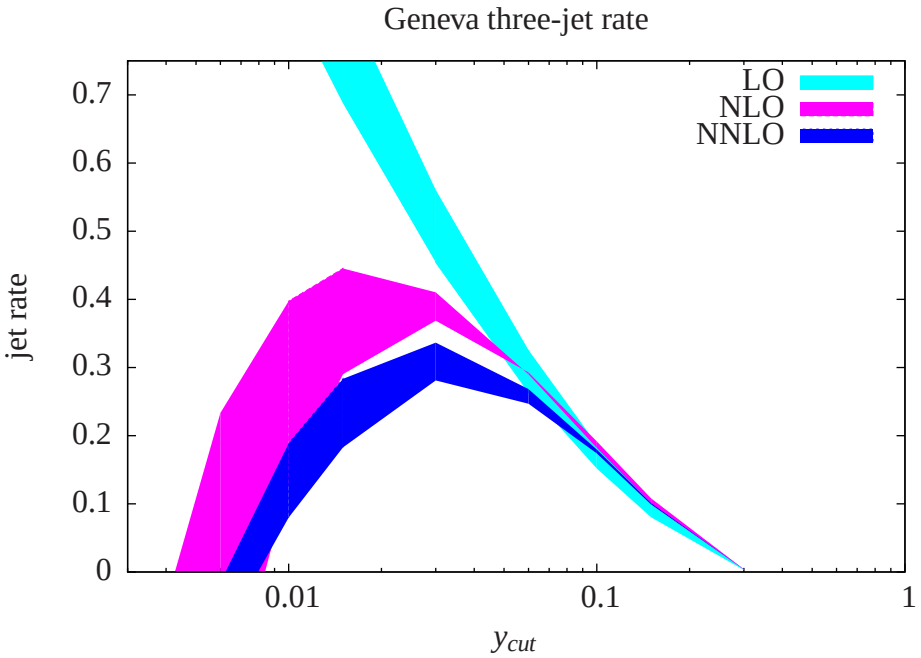

Figure 8. The three jet rate with the Geneva jet algorithm at LO, NLO and NNLO at $\sqrt{Q^2} = m_Z$ with $\alpha_s(m_Z) = 0.118$. The bands give the range for the theoretical prediction obtained from varying the renormalisation scale from $\mu = m_Z/2$ to $\mu = 2m_Z$.

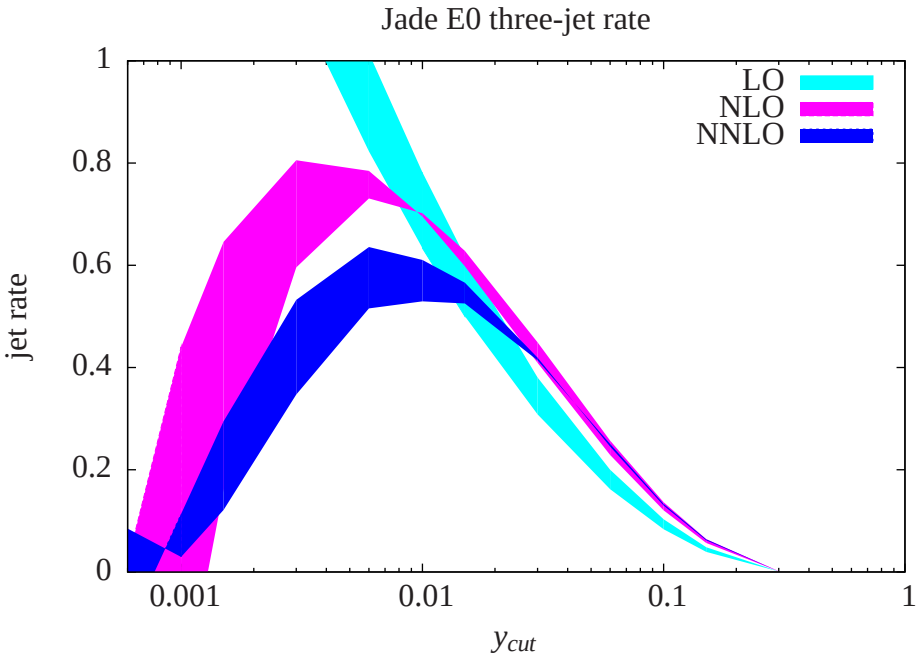

Figure 9. The three jet rate with the Jade E0 jet algorithm at LO, NLO and NNLO at $\sqrt{Q^2} = m_Z$ with $\alpha_s(m_Z) = 0.118$. The bands give the range for the theoretical prediction obtained from varying the renormalisation scale from $\mu = m_Z/2$ to $\mu = 2m_Z$.

JHEP06(2009)041

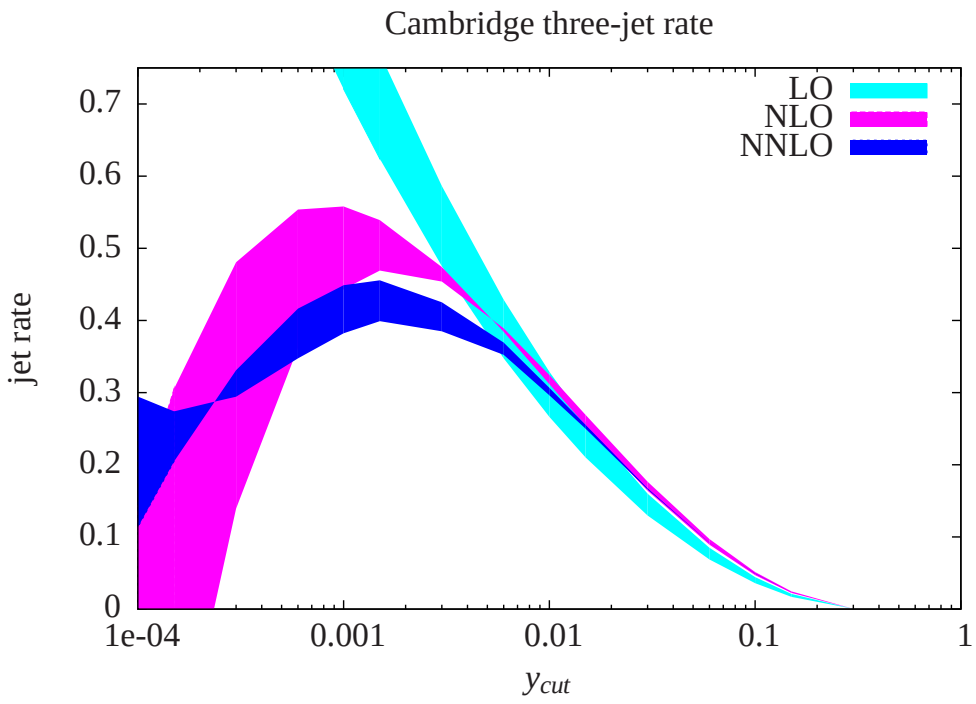

Figure 10. The three jet rate with the Cambridge jet algorithm at LO, NLO and NNLO at $\sqrt{Q^2} = m_Z$ with $\alpha_s(m_Z) = 0.118$. The bands give the range for the theoretical prediction obtained from varying the renormalisation scale from $\mu = m_Z/2$ to $\mu = 2m_Z$.

JHEP06(2009)041

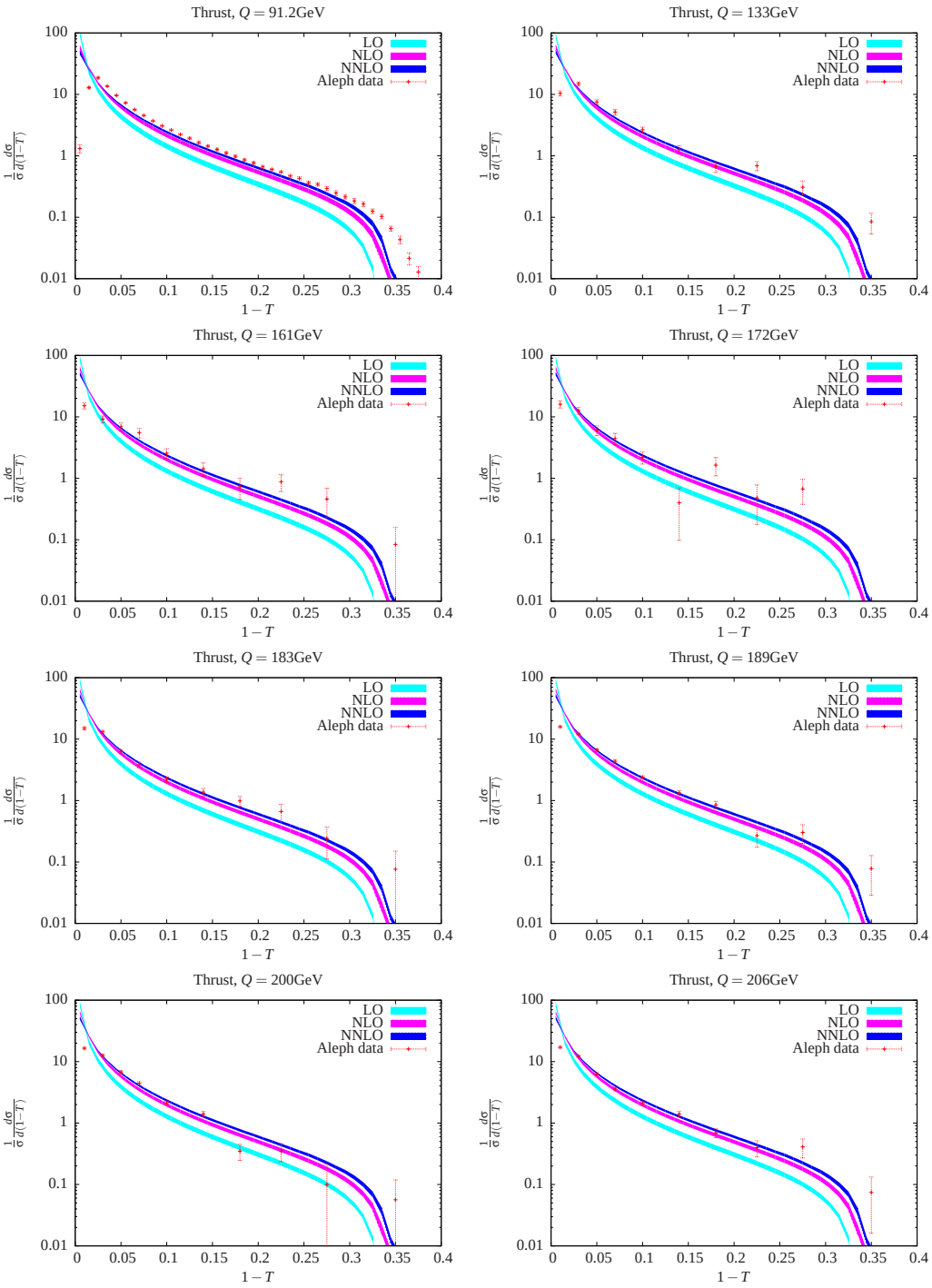

Figure 11. The thrust distribution at LO, NLO and NNLO at various values of $\sqrt{Q^2}$. The bands correspond to a variation of the renormalisation scale from $\mu = m_Z/2$ to $\mu = 2m_Z$. The experimental data points are from the Aleph experiment.

JHEP06(2009)041

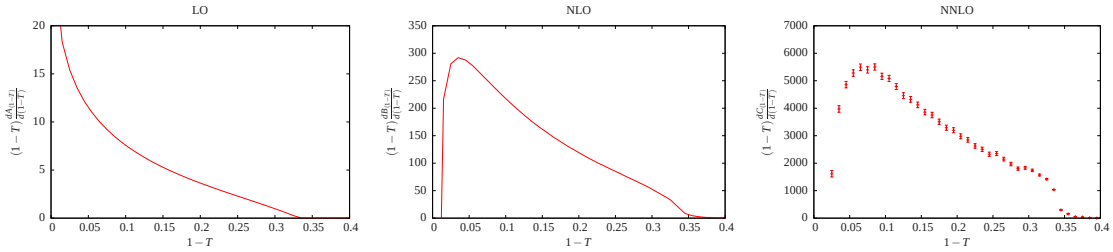

Figure 12. Coefficients of the leading-order ($A_{(1-T)}$, left), next-to-leading-order ($B_{(1-T)}$, middle) and next-to-next-to-leading order ($C_{(1-T)}$, right) contributions to the thrust distribution, all weighted by $(1-T)$. For the coefficient $C_{(1-T)}$ the Monte Carlo integration errors are also shown.

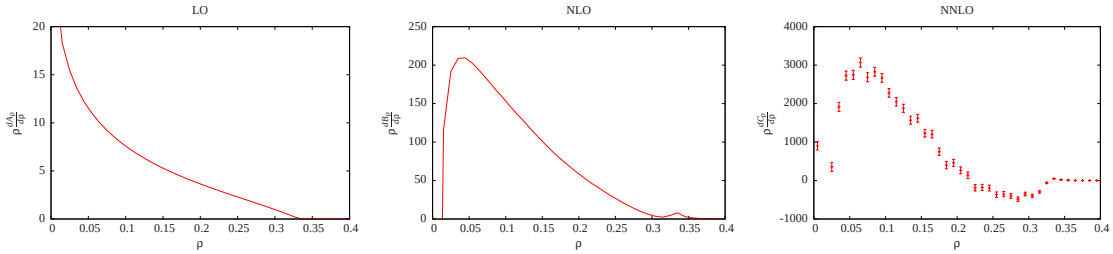

Figure 13. Coefficients of the leading-order (A_ρ, left), next-to-leading-order (B_ρ, middle) and next-to-next-to-leading order (C_ρ, right) contributions to the heavy jet mass distribution, all weighted by ρ. For the coefficient C_ρ the Monte Carlo integration errors are also shown.

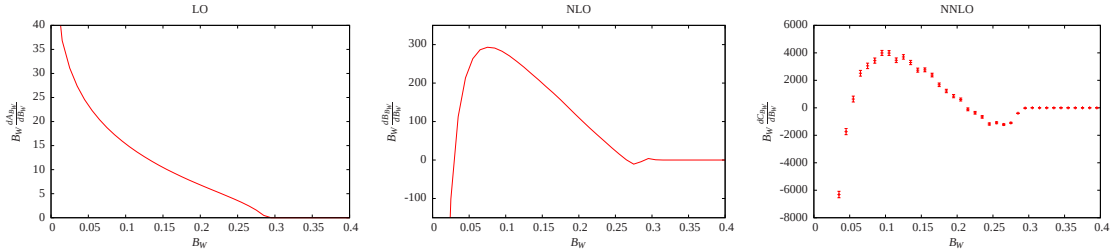

Figure 14. Coefficients of the leading-order (A_{B_W}, left), next-to-leading-order (B_{B_W}, middle) and next-to-next-to-leading order (C_{B_W}, right) contributions to the wide jet broadening distribution, all weighted by B_W. For the coefficient C_{B_W} the Monte Carlo integration errors are also shown.

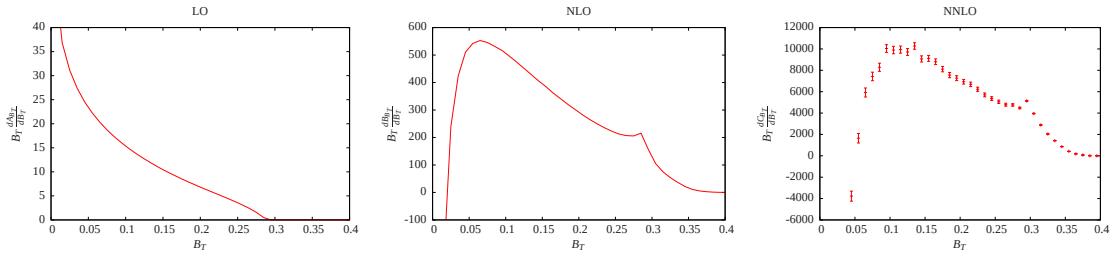

Figure 15. Coefficients of the leading-order (A_{B_T}, left), next-to-leading-order (B_{B_T}, middle) and next-to-next-to-leading order (C_{B_T}, right) contributions to the total jet broadening distribution, all weighted by B_T. For the coefficient C_{B_T} the Monte Carlo integration errors are also shown.

JHEP06(2009)041

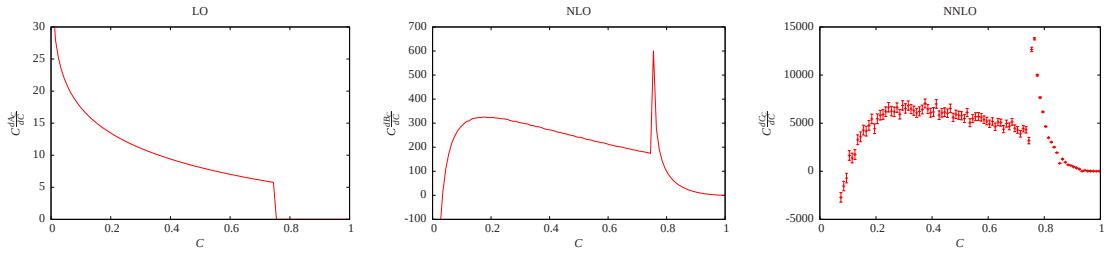

Figure 16. Coefficients of the leading-order (A_C, left), next-to-leading-order (B_C, middle) and next-to-next-to-leading order (C_C, right) contributions to the C-parameter distribution, all weighted by C. For the coefficient C_C the Monte Carlo integration errors are also shown.

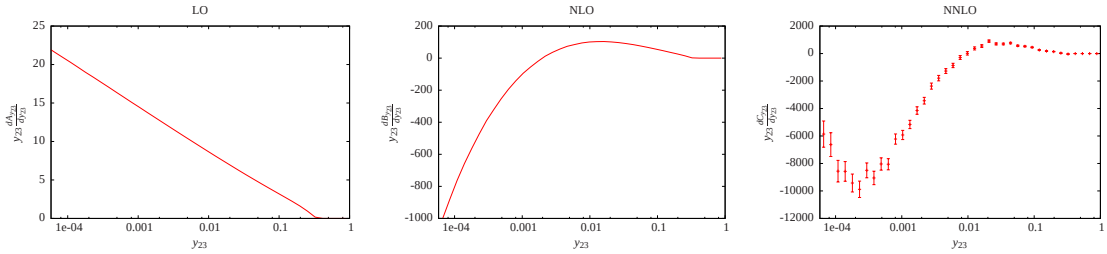

Figure 17. Coefficients of the leading-order ($A_{y_{23}}$, left), next-to-leading-order ($B_{y_{23}}$, middle) and next-to-next-to-leading order ($C_{y_{23}}$, right) contributions to the three-to-two jet transition distribution, all weighted by y_{23}. For the coefficient $C_{y_{23}}$ the Monte Carlo integration errors are also shown.

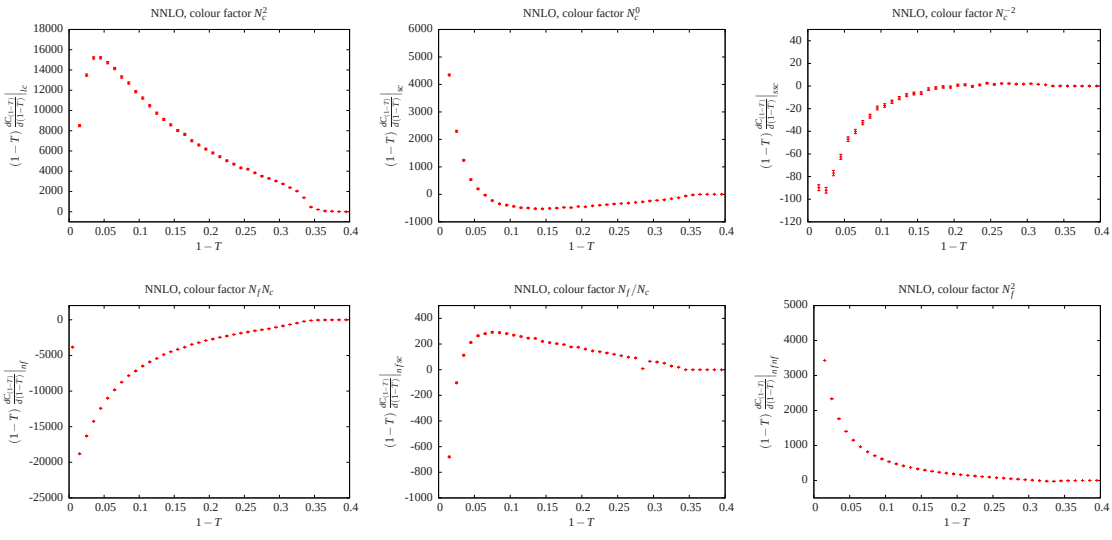

Figure 18. The NNLO coefficient $C_{(1-T)}$ for the thrust distribution split up into individual colour factors.

JHEP06(2009)041

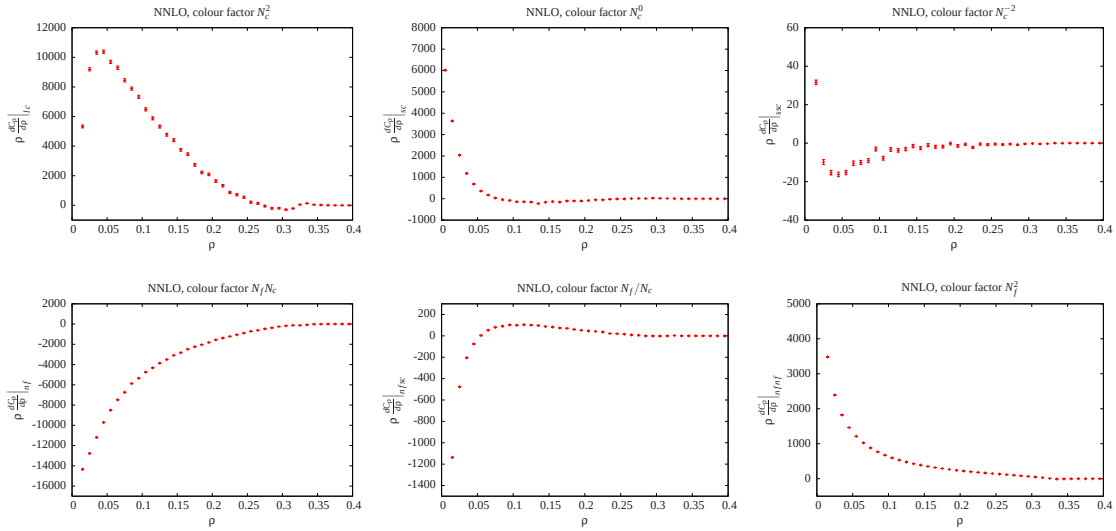

Figure 19. The NNLO coefficient C_ρ for the heavy jet mass distribution split up into individual colour factors.

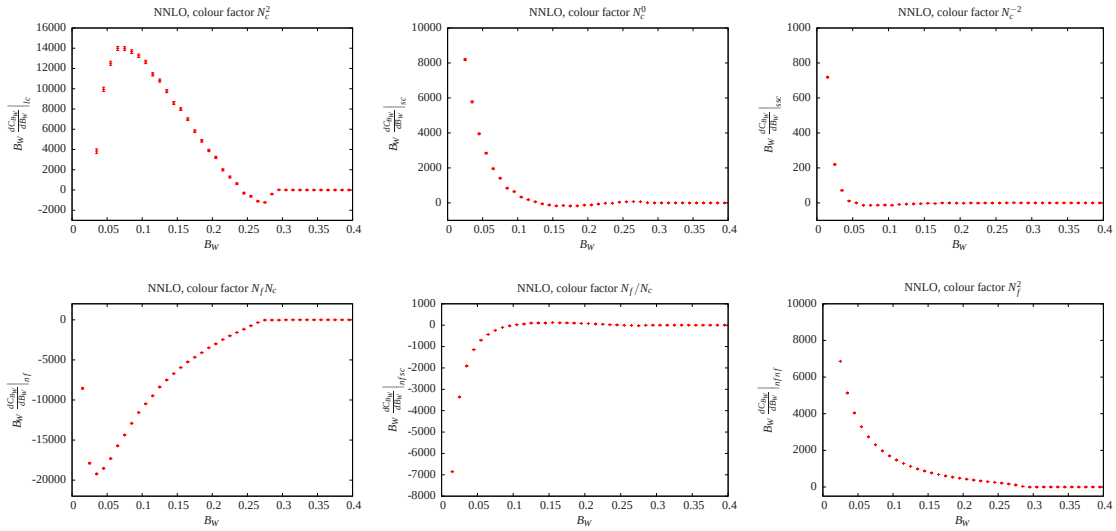

Figure 20. The NNLO coefficient C_{B_W} for the wide jet broadening distribution split up into individual colour factors.

JHEP06(2009)041

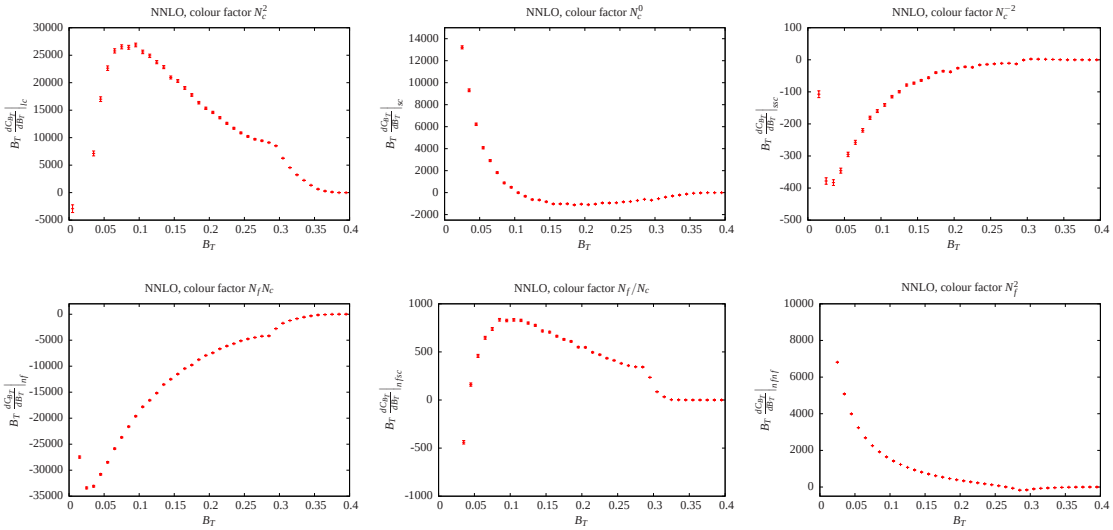

Figure 21. The NNLO coefficient C_{B_T} for the total jet broadening distribution split up into individual colour factors.

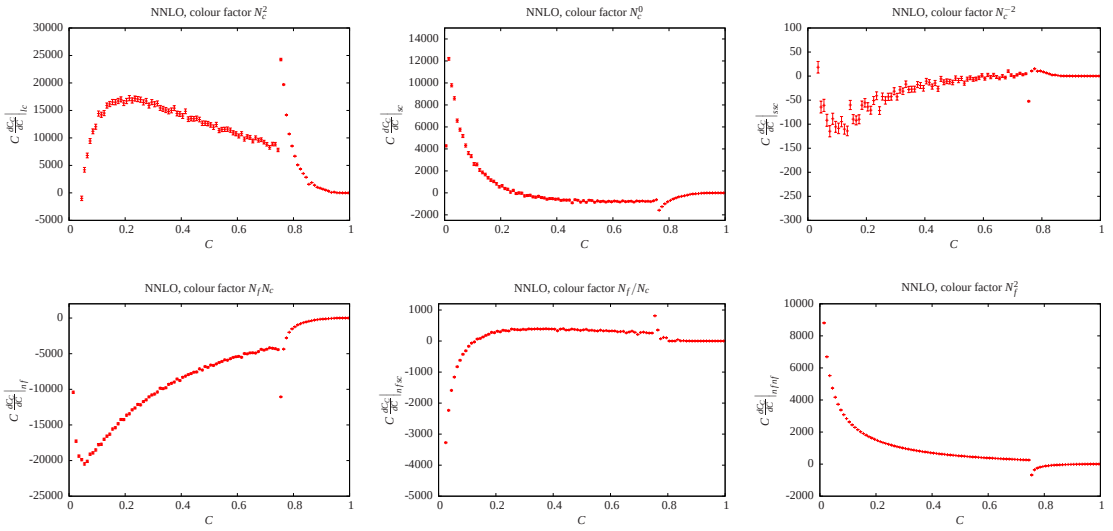

Figure 22. The NNLO coefficient C_C for the C-parameter distribution split up into individual colour factors.

JHEP06(2009)041

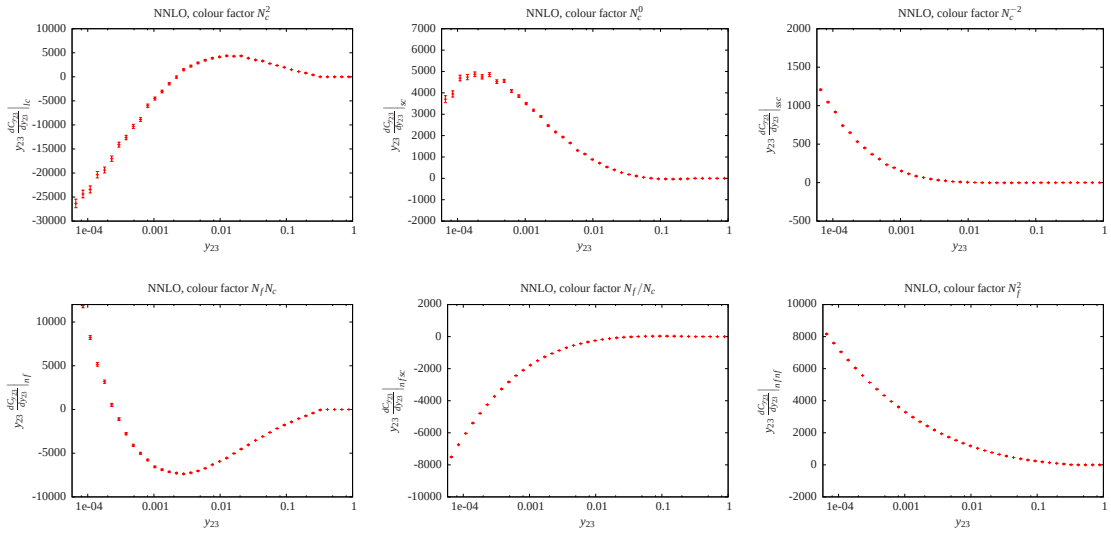

Figure 23. The NNLO coefficient $C_{y_{23}}$ for the three-to-two jet transition distribution split up into individual colour factors.

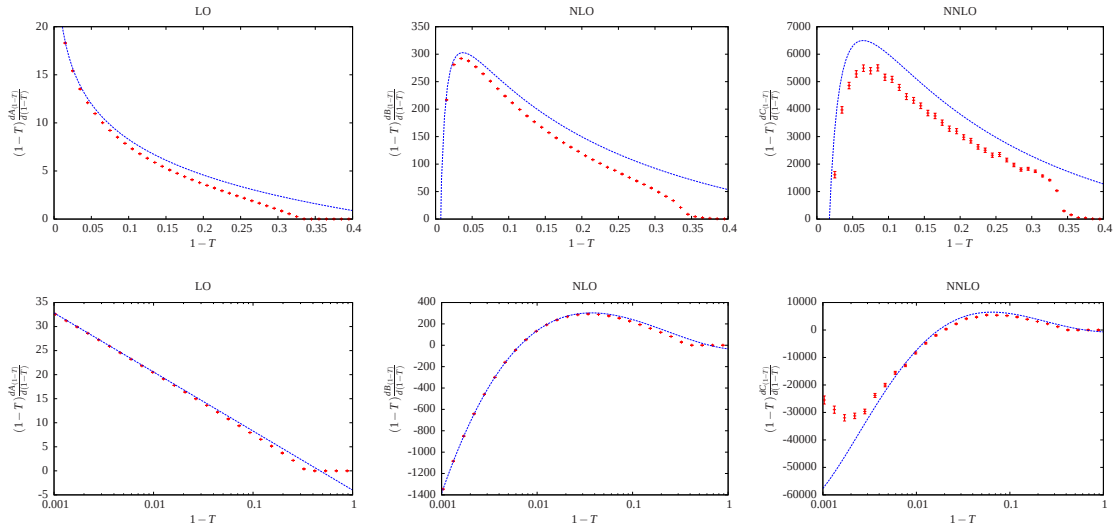

Figure 24. Comparison of the results for the coefficients of the leading-order ($A_{(1-T)}$, left), next-to-leading-order ($B_{(1-T)}$, middle) and next-to-next-to-leading order ($C_{(1-T)}$, right) contributions to the thrust distribution from perturbative QCD (red) and SCET (blue line). The upper row shows the distribution with a linear scale for $(1-T)$, the lower row shows the distribution with a logarithmic scale for $(1-T)$.

JHEP06(2009)041

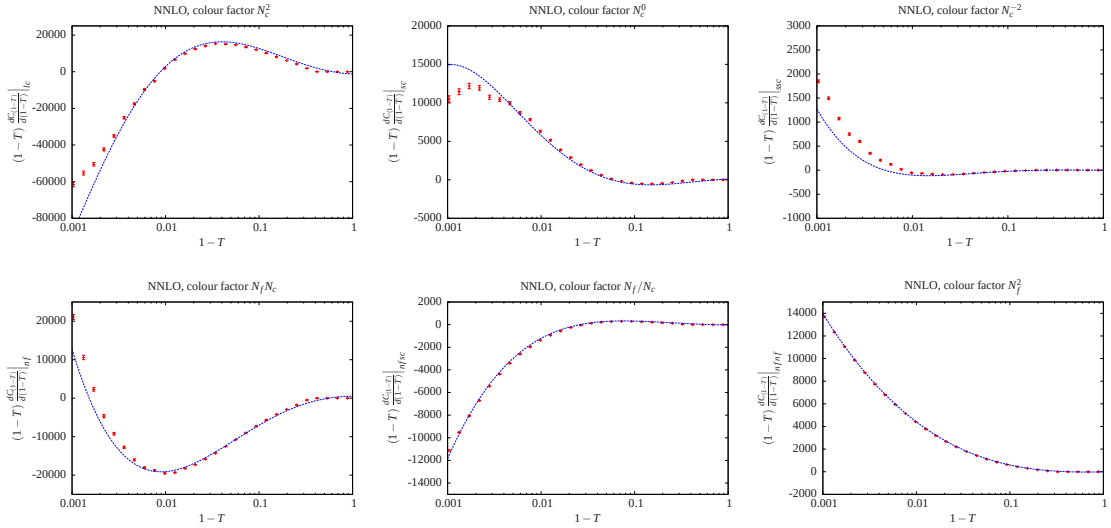

Figure 25. Comparison of the individual colour factors of the next-to-next-to-leading order coefficient $C_{(1-T)}$ for the thrust distribution between perturbative QCD (red) and SCET (blue line). The distributions are shown with a logarithmic scale for $(1-T)$. The deviations of the Monte Carlo results for small values of $(1-T)$ are due to the slicing procedure.

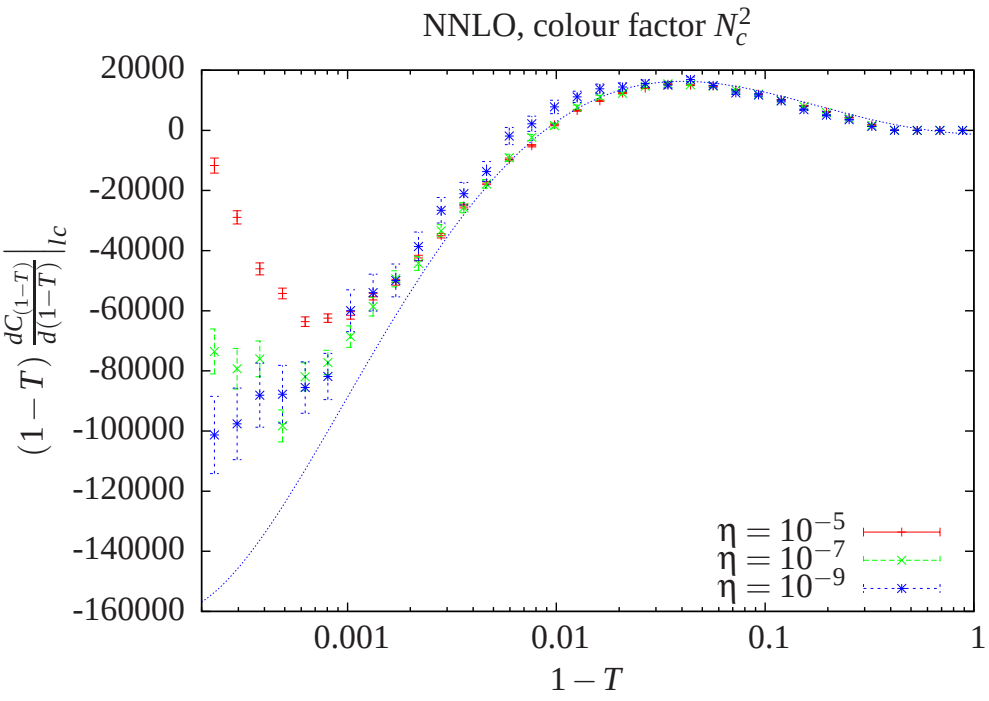

Figure 26. Comparison of the next-to-next-to-leading order coefficient $C_{(1-T)}$ for the colour factor N_c^2 for the thrust distribution between the numerical Monte Carlo program for various values of η and SCET (blue line).

JHEP06(2009)041

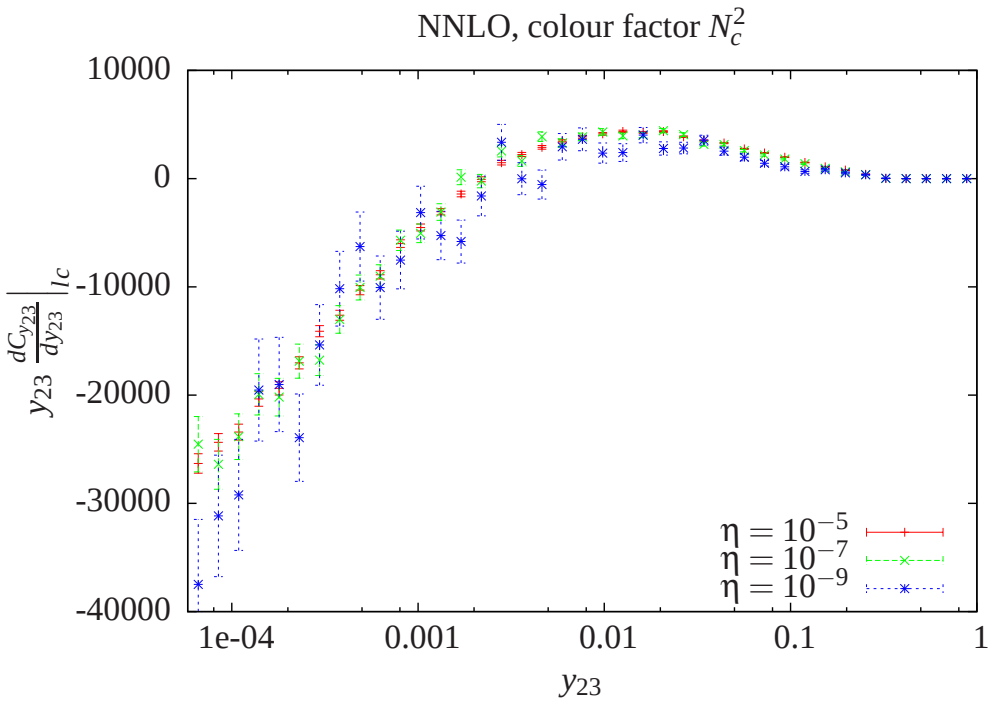

Figure 27. Dependence of the numerical Monte Carlo result for the next-to-next-to-leading order coefficient $C_{y_{23}}$ for the colour factor N_c^2 for the three-to-two jet transition distribution on the slicing parameter η.

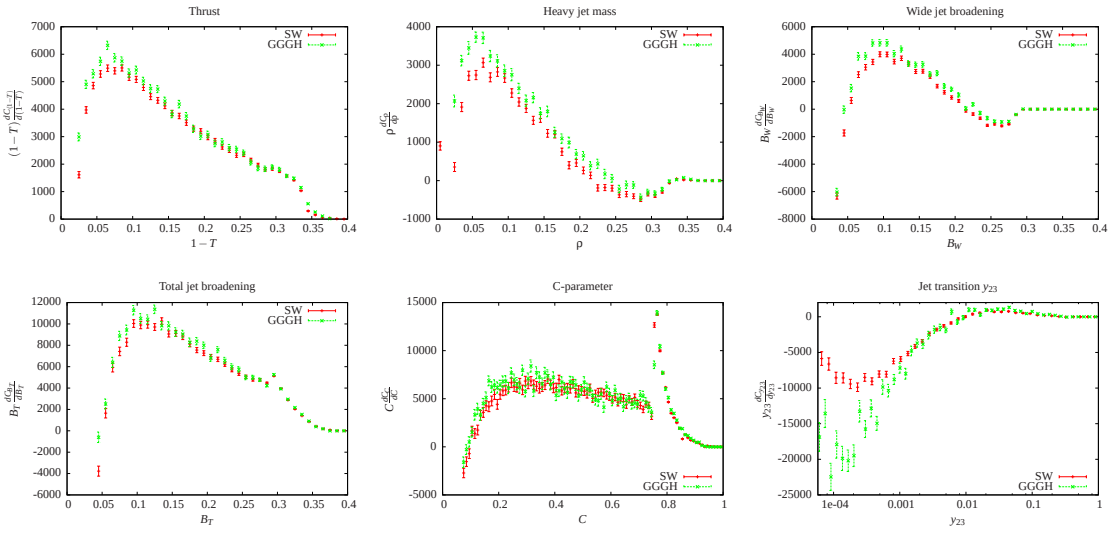

Figure 28. Comparison of the next-to-next-to-leading order coefficient $C_{\mathcal{O}}$ for the six distributions between ref. [1] and the present work.

JHEP06(2009)041

$(1-T)$	$(1-T)\frac{dA_{(1-T)}}{d(1-T)}$	$(1-T)\frac{dB_{(1-T)}}{d(1-T)}$	$(1-T)\frac{dC_{(1-T)}}{d(1-T)}$
0.005	$2.5797(2)\cdot 10^{1}$	$-4.957(3)\cdot 10^{2}$	$-9.0(1)\cdot 10^{3}$
0.015	$1.8299(1)\cdot 10^{1}$	$2.166(3)\cdot 10^{2}$	$-3.3(1)\cdot 10^{3}$
0.025	$1.5411(1)\cdot 10^{1}$	$2.809(3)\cdot 10^{2}$	$1.6(1)\cdot 10^{3}$
0.035	$1.35230(9)\cdot 10^{1}$	$2.920(3)\cdot 10^{2}$	$4.0(1)\cdot 10^{3}$
0.045	$1.21030(9)\cdot 10^{1}$	$2.877(2)\cdot 10^{2}$	$4.9(1)\cdot 10^{3}$
0.055	$1.09692(8)\cdot 10^{1}$	$2.772(2)\cdot 10^{2}$	$5.3(1)\cdot 10^{3}$
0.065	$1.00228(8)\cdot 10^{1}$	$2.638(2)\cdot 10^{2}$	$5.5(1)\cdot 10^{3}$
0.075	$9.2112(7)\cdot 10^{0}$	$2.505(2)\cdot 10^{2}$	$5.4(1)\cdot 10^{3}$
0.085	$8.5022(7)\cdot 10^{0}$	$2.371(2)\cdot 10^{2}$	$5.5(1)\cdot 10^{3}$
0.095	$7.8724(7)\cdot 10^{0}$	$2.240(2)\cdot 10^{2}$	$5.2(1)\cdot 10^{3}$
0.105	$7.3045(6)\cdot 10^{0}$	$2.113(2)\cdot 10^{2}$	$5.1(1)\cdot 10^{3}$
0.115	$6.7891(6)\cdot 10^{0}$	$1.993(2)\cdot 10^{2}$	$4.8(1)\cdot 10^{3}$
0.125	$6.3179(6)\cdot 10^{0}$	$1.878(2)\cdot 10^{2}$	$4.5(1)\cdot 10^{3}$
0.135	$5.8820(6)\cdot 10^{0}$	$1.768(2)\cdot 10^{2}$	$4.3(1)\cdot 10^{3}$
0.145	$5.4791(6)\cdot 10^{0}$	$1.666(2)\cdot 10^{2}$	$4.1(1)\cdot 10^{3}$
0.155	$5.1030(5)\cdot 10^{0}$	$1.572(2)\cdot 10^{2}$	$3.9(1)\cdot 10^{3}$
0.165	$4.7484(5)\cdot 10^{0}$	$1.475(2)\cdot 10^{2}$	$3.8(1)\cdot 10^{3}$
0.175	$4.4141(5)\cdot 10^{0}$	$1.393(2)\cdot 10^{2}$	$3.5(1)\cdot 10^{3}$
0.185	$4.0962(5)\cdot 10^{0}$	$1.306(2)\cdot 10^{2}$	$3.29(9)\cdot 10^{3}$
0.195	$3.7931(5)\cdot 10^{0}$	$1.231(2)\cdot 10^{2}$	$3.20(9)\cdot 10^{3}$
0.205	$3.5028(4)\cdot 10^{0}$	$1.153(2)\cdot 10^{2}$	$2.98(9)\cdot 10^{3}$
0.215	$3.2220(4)\cdot 10^{0}$	$1.081(2)\cdot 10^{2}$	$2.85(9)\cdot 10^{3}$
0.225	$2.9494(4)\cdot 10^{0}$	$1.011(2)\cdot 10^{2}$	$2.63(8)\cdot 10^{3}$
0.235	$2.6826(4)\cdot 10^{0}$	$9.47(1)\cdot 10^{1}$	$2.50(8)\cdot 10^{3}$
0.245	$2.4223(4)\cdot 10^{0}$	$8.82(1)\cdot 10^{1}$	$2.33(8)\cdot 10^{3}$
0.255	$2.1634(3)\cdot 10^{0}$	$8.21(1)\cdot 10^{1}$	$2.35(7)\cdot 10^{3}$
0.265	$1.9062(3)\cdot 10^{0}$	$7.54(1)\cdot 10^{1}$	$2.15(7)\cdot 10^{3}$
0.275	$1.6470(3)\cdot 10^{0}$	$6.94(1)\cdot 10^{1}$	$1.97(6)\cdot 10^{3}$
0.285	$1.3841(3)\cdot 10^{0}$	$6.30(1)\cdot 10^{1}$	$1.80(6)\cdot 10^{3}$
0.295	$1.1169(2)\cdot 10^{0}$	$5.64(1)\cdot 10^{1}$	$1.83(5)\cdot 10^{3}$
0.305	$8.415(2)\cdot 10^{-1}$	$4.888(9)\cdot 10^{1}$	$1.74(5)\cdot 10^{3}$
0.315	$5.567(2)\cdot 10^{-1}$	$4.135(8)\cdot 10^{1}$	$1.57(4)\cdot 10^{3}$
0.325	$2.593(1)\cdot 10^{-1}$	$3.353(5)\cdot 10^{1}$	$1.42(2)\cdot 10^{3}$
0.335	$1.706(3)\cdot 10^{-2}$	$2.108(3)\cdot 10^{1}$	$1.03(1)\cdot 10^{3}$
0.345	0	$8.570(8)\cdot 10^{0}$	$2.96(5)\cdot 10^{2}$
0.355	0	$4.474(5)\cdot 10^{0}$	$1.55(3)\cdot 10^{2}$
0.365	0	$2.434(3)\cdot 10^{0}$	$5.3(1)\cdot 10^{1}$
0.375	0	$1.301(2)\cdot 10^{0}$	$3.57(7)\cdot 10^{1}$
0.385	0	$6.44(1)\cdot 10^{-1}$	$1.09(2)\cdot 10^{1}$
0.395	0	$2.818(8)\cdot 10^{-1}$	$1.8(2)\cdot 10^{-1}$
0.405	0	$5.12(3)\cdot 10^{-2}$	$-1.0(1)\cdot 10^{-3}$
0.415	0	$1.45987(8)\cdot 10^{-5}$	$-1.950(2)\cdot 10^{-1}$
0.425	0	$4.66279(3)\cdot 10^{-5}$	$-9(4)\cdot 10^{-3}$
0.435	0	0	$-1(1)\cdot 10^{-3}$
0.445	0	0	0

Table 1. Coefficients of the leading-order ($A_{(1-T)}$), next-to-leading-order ($B_{(1-T)}$) and next-to-next-to-leading order ($C_{(1-T)}$) contributions to the thrust distribution.

JHEP06(2009)041

ρ	$\rho\frac{dA_\rho}{d\rho}$	$\rho\frac{dB_\rho}{d\rho}$	$\rho\frac{dC_\rho}{d\rho}$
0.005	$2.5797(2)\cdot 10^{1}$	$-6.243(3)\cdot 10^{2}$	$9(1)\cdot 10^{2}$
0.015	$1.8299(1)\cdot 10^{1}$	$1.162(3)\cdot 10^{2}$	$-3.0(1)\cdot 10^{3}$
0.025	$1.5411(1)\cdot 10^{1}$	$1.917(3)\cdot 10^{2}$	$4(1)\cdot 10^{2}$
0.035	$1.35230(9)\cdot 10^{1}$	$2.088(3)\cdot 10^{2}$	$1.9(1)\cdot 10^{3}$
0.045	$1.21030(9)\cdot 10^{1}$	$2.092(2)\cdot 10^{2}$	$2.7(1)\cdot 10^{3}$
0.055	$1.09692(8)\cdot 10^{1}$	$2.020(2)\cdot 10^{2}$	$2.7(1)\cdot 10^{3}$
0.065	$1.00228(8)\cdot 10^{1}$	$1.918(2)\cdot 10^{2}$	$3.1(1)\cdot 10^{3}$
0.075	$9.2112(7)\cdot 10^{0}$	$1.809(2)\cdot 10^{2}$	$2.7(1)\cdot 10^{3}$
0.085	$8.5022(7)\cdot 10^{0}$	$1.695(2)\cdot 10^{2}$	$2.8(1)\cdot 10^{3}$
0.095	$7.8724(7)\cdot 10^{0}$	$1.590(2)\cdot 10^{2}$	$2.7(1)\cdot 10^{3}$
0.105	$7.3045(6)\cdot 10^{0}$	$1.476(2)\cdot 10^{2}$	$2.3(1)\cdot 10^{3}$
0.115	$6.7891(6)\cdot 10^{0}$	$1.370(2)\cdot 10^{2}$	$2.0(1)\cdot 10^{3}$
0.125	$6.3179(6)\cdot 10^{0}$	$1.269(2)\cdot 10^{2}$	$1.9(1)\cdot 10^{3}$
0.135	$5.8820(6)\cdot 10^{0}$	$1.161(2)\cdot 10^{2}$	$1.6(1)\cdot 10^{3}$
0.145	$5.4791(6)\cdot 10^{0}$	$1.060(2)\cdot 10^{2}$	$1.6(1)\cdot 10^{3}$
0.155	$5.1030(5)\cdot 10^{0}$	$9.63(1)\cdot 10^{1}$	$1.2(1)\cdot 10^{3}$
0.165	$4.7484(5)\cdot 10^{0}$	$8.67(1)\cdot 10^{1}$	$1.2(1)\cdot 10^{3}$
0.175	$4.4141(5)\cdot 10^{0}$	$7.81(1)\cdot 10^{1}$	$8(1)\cdot 10^{2}$
0.185	$4.0962(5)\cdot 10^{0}$	$7.01(1)\cdot 10^{1}$	$4.0(9)\cdot 10^{2}$
0.195	$3.7931(5)\cdot 10^{0}$	$6.23(1)\cdot 10^{1}$	$4.6(9)\cdot 10^{2}$
0.205	$3.5028(4)\cdot 10^{0}$	$5.50(1)\cdot 10^{1}$	$2.7(9)\cdot 10^{2}$
0.215	$3.2220(4)\cdot 10^{0}$	$4.79(1)\cdot 10^{1}$	$1.4(9)\cdot 10^{2}$
0.225	$2.9494(4)\cdot 10^{0}$	$4.17(1)\cdot 10^{1}$	$-1.9(8)\cdot 10^{2}$
0.235	$2.6826(4)\cdot 10^{0}$	$3.55(1)\cdot 10^{1}$	$-1.8(8)\cdot 10^{2}$
0.245	$2.4223(4)\cdot 10^{0}$	$2.96(1)\cdot 10^{1}$	$-2.0(8)\cdot 10^{2}$
0.255	$2.1634(3)\cdot 10^{0}$	$2.411(9)\cdot 10^{1}$	$-3.7(7)\cdot 10^{2}$
0.265	$1.9062(3)\cdot 10^{0}$	$1.871(9)\cdot 10^{1}$	$-3.5(7)\cdot 10^{2}$
0.275	$1.6470(3)\cdot 10^{0}$	$1.398(8)\cdot 10^{1}$	$-4.1(6)\cdot 10^{2}$
0.285	$1.3841(3)\cdot 10^{0}$	$9.63(8)\cdot 10^{0}$	$-4.9(6)\cdot 10^{2}$
0.295	$1.1169(2)\cdot 10^{0}$	$6.11(7)\cdot 10^{0}$	$-3.5(5)\cdot 10^{2}$
0.305	$8.415(2)\cdot 10^{-1}$	$3.48(6)\cdot 10^{0}$	$-4.0(4)\cdot 10^{2}$
0.315	$5.567(2)\cdot 10^{-1}$	$2.43(5)\cdot 10^{0}$	$-3.0(3)\cdot 10^{2}$
0.325	$2.593(1)\cdot 10^{-1}$	$4.67(3)\cdot 10^{0}$	$-6(2)\cdot 10^{1}$
0.335	$1.706(3)\cdot 10^{-2}$	$8.08(2)\cdot 10^{0}$	$4.8(5)\cdot 10^{1}$
0.345	0	$3.189(5)\cdot 10^{0}$	$2.1(1)\cdot 10^{1}$
0.355	0	$1.498(3)\cdot 10^{0}$	$9.2(6)\cdot 10^{0}$
0.365	0	$7.22(2)\cdot 10^{-1}$	$2.7(2)\cdot 10^{0}$
0.375	0	$3.24(1)\cdot 10^{-1}$	$1.0(2)\cdot 10^{-1}$
0.385	0	$1.154(5)\cdot 10^{-1}$	$-7.0(4)\cdot 10^{-2}$
0.395	0	$1.71(1)\cdot 10^{-2}$	$-2.7(2)\cdot 10^{-3}$
0.405	0	$1.29995(4)\cdot 10^{-6}$	$-3.7(4)\cdot 10^{-3}$
0.415	0	$1.647637(6)\cdot 10^{-5}$	$-1.0(4)\cdot 10^{-1}$
0.425	0	0	0

Table 2. Coefficients of the leading-order (A_ρ), next-to-leading-order (B_ρ) and next-to-next-to-leading order (C_ρ) contributions to the heavy jet mass distribution.

JHEP06(2009)041

B_W	$B_W \frac{dA_{B_W}}{dB_W}$	$B_W \frac{dB_{B_W}}{dB_W}$	$B_W \frac{dC_{B_W}}{dB_W}$
0.005	$5.146(1) \cdot 10^1$	$-4.194(2) \cdot 10^3$	$1.433(7) \cdot 10^5$
0.015	$3.6823(4) \cdot 10^1$	$-6.385(7) \cdot 10^2$	$-2.33(3) \cdot 10^4$
0.025	$3.1132(3) \cdot 10^1$	$-1.015(5) \cdot 10^2$	$-1.34(2) \cdot 10^4$
0.035	$2.7389(2) \cdot 10^1$	$1.126(5) \cdot 10^2$	$-6.3(2) \cdot 10^3$
0.045	$2.4563(2) \cdot 10^1$	$2.136(4) \cdot 10^2$	$-1.7(2) \cdot 10^3$
0.055	$2.2291(2) \cdot 10^1$	$2.634(4) \cdot 10^2$	$6(2) \cdot 10^2$
0.065	$2.0389(2) \cdot 10^1$	$2.867(4) \cdot 10^2$	$2.5(2) \cdot 10^3$
0.075	$1.8734(1) \cdot 10^1$	$2.931(3) \cdot 10^2$	$3.1(2) \cdot 10^3$
0.085	$1.7273(1) \cdot 10^1$	$2.910(3) \cdot 10^2$	$3.4(2) \cdot 10^3$
0.095	$1.5966(1) \cdot 10^1$	$2.827(3) \cdot 10^2$	$4.0(2) \cdot 10^3$
0.105	$1.4778(1) \cdot 10^1$	$2.709(3) \cdot 10^2$	$4.0(2) \cdot 10^3$
0.115	$1.3686(1) \cdot 10^1$	$2.565(3) \cdot 10^2$	$3.5(2) \cdot 10^3$
0.125	$1.2685(1) \cdot 10^1$	$2.413(3) \cdot 10^2$	$3.7(2) \cdot 10^3$
0.135	$1.17528(9) \cdot 10^1$	$2.246(2) \cdot 10^2$	$3.3(2) \cdot 10^3$
0.145	$1.08786(9) \cdot 10^1$	$2.083(2) \cdot 10^2$	$2.7(1) \cdot 10^3$
0.155	$1.00548(8) \cdot 10^1$	$1.911(2) \cdot 10^2$	$2.8(1) \cdot 10^3$
0.165	$9.2782(8) \cdot 10^0$	$1.744(2) \cdot 10^2$	$2.4(1) \cdot 10^3$
0.175	$8.5406(7) \cdot 10^0$	$1.567(2) \cdot 10^2$	$1.7(1) \cdot 10^3$
0.185	$7.8351(7) \cdot 10^0$	$1.379(2) \cdot 10^2$	$1.2(1) \cdot 10^3$
0.195	$7.1576(6) \cdot 10^0$	$1.191(2) \cdot 10^2$	$9(1) \cdot 10^2$
0.205	$6.4999(6) \cdot 10^0$	$1.009(2) \cdot 10^2$	$6(1) \cdot 10^2$
0.215	$5.8549(6) \cdot 10^0$	$8.29(2) \cdot 10^1$	$-1(1) \cdot 10^2$
0.225	$5.2173(5) \cdot 10^0$	$6.57(1) \cdot 10^1$	$-4(1) \cdot 10^2$
0.235	$4.5744(5) \cdot 10^0$	$4.89(1) \cdot 10^1$	$-6.6(9) \cdot 10^2$
0.245	$3.9151(4) \cdot 10^0$	$3.19(1) \cdot 10^1$	$-1.18(8) \cdot 10^3$
0.255	$3.2206(4) \cdot 10^0$	$1.57(1) \cdot 10^1$	$-1.08(7) \cdot 10^3$
0.265	$2.4584(3) \cdot 10^0$	$4.8(9) \cdot 10^{-1}$	$-1.22(6) \cdot 10^3$
0.275	$1.5815(3) \cdot 10^0$	$-1.062(7) \cdot 10^1$	$-1.10(4) \cdot 10^3$
0.285	$4.942(2) \cdot 10^{-1}$	$-4.38(4) \cdot 10^0$	$-4.0(2) \cdot 10^2$
0.295	0	$3.961(6) \cdot 10^0$	$-2.1(1) \cdot 10^1$
0.305	0	$6.95(1) \cdot 10^{-1}$	$1.41(9) \cdot 10^0$
0.315	0	$4.06(2) \cdot 10^{-2}$	$-9(7) \cdot 10^{-4}$
0.325	0	$3.88459(5) \cdot 10^{-6}$	$-6(3) \cdot 10^{-2}$
0.335	0	0	0

Table 3. Coefficients of the leading-order (A_{B_W}), next-to-leading-order (B_{B_W}) and next-to-next-to-leading order (C_{B_W}) contributions to the wide jet broadening distribution.

JHEP06(2009)041

B_T	$B_T \frac{dA_{B_T}}{dB_T}$	$B_T \frac{dB_{B_T}}{dB_T}$	$B_T \frac{dC_{B_T}}{dB_T}$
0.005	$5.146(1) \cdot 10^1$	$-3.776(2) \cdot 10^3$	$9.16(8) \cdot 10^4$
0.015	$3.6823(4) \cdot 10^1$	$-2.65(2) \cdot 10^2$	$-5.59(5) \cdot 10^4$
0.025	$3.1132(3) \cdot 10^1$	$2.40(2) \cdot 10^2$	$-2.77(5) \cdot 10^4$
0.035	$2.7389(2) \cdot 10^1$	$4.24(2) \cdot 10^2$	$-1.24(5) \cdot 10^4$
0.045	$2.4563(2) \cdot 10^1$	$5.11(1) \cdot 10^2$	$-3.8(5) \cdot 10^3$
0.055	$2.2291(2) \cdot 10^1$	$5.42(1) \cdot 10^2$	$1.6(4) \cdot 10^3$
0.065	$2.0389(2) \cdot 10^1$	$5.53(1) \cdot 10^2$	$5.9(4) \cdot 10^3$
0.075	$1.8734(1) \cdot 10^1$	$5.46(1) \cdot 10^2$	$7.4(4) \cdot 10^3$
0.085	$1.7273(1) \cdot 10^1$	$5.32(1) \cdot 10^2$	$8.3(4) \cdot 10^3$
0.095	$1.5966(1) \cdot 10^1$	$5.164(9) \cdot 10^2$	$1.00(4) \cdot 10^4$
0.105	$1.4778(1) \cdot 10^1$	$4.960(8) \cdot 10^2$	$9.9(3) \cdot 10^3$
0.115	$1.3686(1) \cdot 10^1$	$4.744(8) \cdot 10^2$	$9.9(3) \cdot 10^3$
0.125	$1.2685(1) \cdot 10^1$	$4.515(7) \cdot 10^2$	$9.7(3) \cdot 10^3$
0.135	$1.17528(9) \cdot 10^1$	$4.288(7) \cdot 10^2$	$1.03(3) \cdot 10^4$
0.145	$1.08786(9) \cdot 10^1$	$4.056(6) \cdot 10^2$	$9.1(3) \cdot 10^3$
0.155	$1.00548(8) \cdot 10^1$	$3.850(6) \cdot 10^2$	$9.1(3) \cdot 10^3$
0.165	$9.2782(8) \cdot 10^0$	$3.615(6) \cdot 10^2$	$8.8(3) \cdot 10^3$
0.175	$8.5406(7) \cdot 10^0$	$3.409(6) \cdot 10^2$	$8.1(3) \cdot 10^3$
0.185	$7.8351(7) \cdot 10^0$	$3.203(5) \cdot 10^2$	$7.6(2) \cdot 10^3$
0.195	$7.1576(6) \cdot 10^0$	$3.016(5) \cdot 10^2$	$7.3(2) \cdot 10^3$
0.205	$6.4999(6) \cdot 10^0$	$2.825(5) \cdot 10^2$	$6.9(2) \cdot 10^3$
0.215	$5.8549(6) \cdot 10^0$	$2.654(5) \cdot 10^2$	$6.7(2) \cdot 10^3$
0.225	$5.2173(5) \cdot 10^0$	$2.496(4) \cdot 10^2$	$6.2(2) \cdot 10^3$
0.235	$4.5744(5) \cdot 10^0$	$2.353(4) \cdot 10^2$	$5.7(2) \cdot 10^3$
0.245	$3.9151(4) \cdot 10^0$	$2.228(4) \cdot 10^2$	$5.4(2) \cdot 10^3$
0.255	$3.2206(4) \cdot 10^0$	$2.124(4) \cdot 10^2$	$5.1(2) \cdot 10^3$
0.265	$2.4584(3) \cdot 10^0$	$2.067(3) \cdot 10^2$	$4.8(1) \cdot 10^3$
0.275	$1.5815(3) \cdot 10^0$	$2.057(3) \cdot 10^2$	$4.8(1) \cdot 10^3$
0.285	$4.942(2) \cdot 10^{-1}$	$2.158(2) \cdot 10^2$	$4.48(8) \cdot 10^3$
0.295	0	$1.5624(7) \cdot 10^2$	$5.13(4) \cdot 10^3$
0.305	0	$1.0481(4) \cdot 10^2$	$3.95(3) \cdot 10^3$
0.315	0	$7.527(3) \cdot 10^1$	$2.88(2) \cdot 10^3$
0.325	0	$5.412(2) \cdot 10^1$	$2.04(2) \cdot 10^3$
0.335	0	$3.710(2) \cdot 10^1$	$1.42(1) \cdot 10^3$
0.345	0	$2.203(1) \cdot 10^1$	$8.57(9) \cdot 10^2$
0.355	0	$1.1206(7) \cdot 10^1$	$4.15(6) \cdot 10^2$
0.365	0	$5.581(4) \cdot 10^0$	$1.81(3) \cdot 10^2$
0.375	0	$2.611(3) \cdot 10^0$	$7.0(1) \cdot 10^1$
0.385	0	$1.018(2) \cdot 10^0$	$4.0(2) \cdot 10^0$
0.395	0	$2.247(7) \cdot 10^{-1}$	$9(1) \cdot 10^{-2}$
0.405	0	$1.70679(8) \cdot 10^{-5}$	$-7.35(5) \cdot 10^{-2}$
0.415	0	0	0

Table 4. Coefficients of the leading-order (A_{B_T}), next-to-leading-order (B_{B_T}) and next-to-next-to-leading order (C_{B_T}) contributions to the total jet broadening distribution.

JHEP06(2009)041

C	$C\frac{dA_C}{dC}$	$C\frac{dB_C}{dC}$	$C\frac{dC_C}{dC}$
0.005	$3.5327(6)\cdot 10^1$	$-2.151(1)\cdot 10^3$	$3.06(4)\cdot 10^4$
0.015	$2.7963(3)\cdot 10^1$	$-4.75(1)\cdot 10^2$	$-3.04(4)\cdot 10^4$
0.025	$2.5124(3)\cdot 10^1$	$-1.45(1)\cdot 10^2$	$-2.15(4)\cdot 10^4$
0.035	$2.3269(2)\cdot 10^1$	$1.3(1)\cdot 10^1$	$-1.48(4)\cdot 10^4$
0.045	$2.1887(2)\cdot 10^1$	$1.09(1)\cdot 10^2$	$-1.12(5)\cdot 10^4$
0.055	$2.0774(2)\cdot 10^1$	$1.71(1)\cdot 10^2$	$-7.6(5)\cdot 10^3$
0.065	$1.9831(2)\cdot 10^1$	$2.15(1)\cdot 10^2$	$-5.3(5)\cdot 10^3$
0.075	$1.9042(2)\cdot 10^1$	$2.44(1)\cdot 10^2$	$-2.7(5)\cdot 10^3$
0.085	$1.8340(2)\cdot 10^1$	$2.67(1)\cdot 10^2$	$-1.5(5)\cdot 10^3$
0.095	$1.7710(2)\cdot 10^1$	$2.83(1)\cdot 10^2$	$-7(5)\cdot 10^2$
0.105	$1.7152(2)\cdot 10^1$	$2.95(1)\cdot 10^2$	$1.6(5)\cdot 10^3$
0.115	$1.6637(2)\cdot 10^1$	$3.06(1)\cdot 10^2$	$1.4(5)\cdot 10^3$
0.125	$1.6154(2)\cdot 10^1$	$3.10(1)\cdot 10^2$	$1.7(5)\cdot 10^3$
0.135	$1.5713(2)\cdot 10^1$	$3.18(1)\cdot 10^2$	$3.3(5)\cdot 10^3$
0.145	$1.5312(2)\cdot 10^1$	$3.21(1)\cdot 10^2$	$3.6(5)\cdot 10^3$
0.155	$1.4933(2)\cdot 10^1$	$3.23(1)\cdot 10^2$	$4.3(5)\cdot 10^3$
0.165	$1.4572(2)\cdot 10^1$	$3.24(1)\cdot 10^2$	$4.2(5)\cdot 10^3$
0.175	$1.4228(2)\cdot 10^1$	$3.26(1)\cdot 10^2$	$4.8(5)\cdot 10^3$
0.185	$1.3915(2)\cdot 10^1$	$3.241(9)\cdot 10^2$	$5.4(5)\cdot 10^3$
0.195	$1.3609(2)\cdot 10^1$	$3.227(9)\cdot 10^2$	$4.4(5)\cdot 10^3$
0.205	$1.3321(2)\cdot 10^1$	$3.242(9)\cdot 10^2$	$5.5(5)\cdot 10^3$
0.215	$1.3039(2)\cdot 10^1$	$3.214(9)\cdot 10^2$	$5.8(5)\cdot 10^3$
0.225	$1.2779(2)\cdot 10^1$	$3.208(9)\cdot 10^2$	$5.9(5)\cdot 10^3$
0.235	$1.2524(2)\cdot 10^1$	$3.184(9)\cdot 10^2$	$6.2(5)\cdot 10^3$
0.245	$1.2281(2)\cdot 10^1$	$3.179(9)\cdot 10^2$	$6.7(5)\cdot 10^3$
0.255	$1.2046(2)\cdot 10^1$	$3.156(9)\cdot 10^2$	$6.3(5)\cdot 10^3$
0.265	$1.1823(2)\cdot 10^1$	$3.113(9)\cdot 10^2$	$6.2(5)\cdot 10^3$
0.275	$1.1608(2)\cdot 10^1$	$3.079(9)\cdot 10^2$	$6.6(5)\cdot 10^3$
0.285	$1.1392(2)\cdot 10^1$	$3.078(9)\cdot 10^2$	$5.9(5)\cdot 10^3$
0.295	$1.1197(2)\cdot 10^1$	$3.029(8)\cdot 10^2$	$6.8(5)\cdot 10^3$
0.305	$1.1000(2)\cdot 10^1$	$3.008(8)\cdot 10^2$	$6.5(5)\cdot 10^3$
0.315	$1.0812(2)\cdot 10^1$	$2.980(8)\cdot 10^2$	$6.8(5)\cdot 10^3$
0.325	$1.0627(2)\cdot 10^1$	$2.964(8)\cdot 10^2$	$6.5(5)\cdot 10^3$
0.335	$1.0451(1)\cdot 10^1$	$2.908(8)\cdot 10^2$	$6.3(5)\cdot 10^3$
0.345	$1.0273(1)\cdot 10^1$	$2.897(8)\cdot 10^2$	$6.1(5)\cdot 10^3$
0.355	$1.0110(1)\cdot 10^1$	$2.856(8)\cdot 10^2$	$6.2(5)\cdot 10^3$
0.365	$9.946(1)\cdot 10^0$	$2.843(8)\cdot 10^2$	$6.4(5)\cdot 10^3$
0.375	$9.787(1)\cdot 10^0$	$2.804(8)\cdot 10^2$	$7.0(5)\cdot 10^3$
0.385	$9.628(1)\cdot 10^0$	$2.752(8)\cdot 10^2$	$6.5(5)\cdot 10^3$
0.395	$9.484(1)\cdot 10^0$	$2.732(8)\cdot 10^2$	$6.1(5)\cdot 10^3$
0.405	$9.332(1)\cdot 10^0$	$2.711(8)\cdot 10^2$	$6.2(5)\cdot 10^3$
0.415	$9.190(1)\cdot 10^0$	$2.685(7)\cdot 10^2$	$7.0(5)\cdot 10^3$
0.425	$9.049(1)\cdot 10^0$	$2.636(7)\cdot 10^2$	$5.8(4)\cdot 10^3$
0.435	$8.914(1)\cdot 10^0$	$2.616(7)\cdot 10^2$	$6.1(4)\cdot 10^3$
0.445	$8.779(1)\cdot 10^0$	$2.580(7)\cdot 10^2$	$6.2(4)\cdot 10^3$
0.455	$8.645(1)\cdot 10^0$	$2.555(7)\cdot 10^2$	$6.0(4)\cdot 10^3$
0.465	$8.518(1)\cdot 10^0$	$2.518(7)\cdot 10^2$	$6.5(4)\cdot 10^3$
0.475	$8.392(1)\cdot 10^0$	$2.491(7)\cdot 10^2$	$5.6(4)\cdot 10^3$
0.485	$8.269(1)\cdot 10^0$	$2.465(7)\cdot 10^2$	$5.9(4)\cdot 10^3$
0.495	$8.152(1)\cdot 10^0$	$2.415(7)\cdot 10^2$	$5.8(4)\cdot 10^3$

Table 5. Coefficients of the leading-order (A_C), next-to-leading-order (B_C) and next-to-next-to-leading order (C_C) contributions to the C-parameter distribution.

JHEP06(2009)041

C	$C\frac{dA_C}{dC}$	$C\frac{dB_C}{dC}$	$C\frac{dC_C}{dC}$
0.505	$8.033(1)\cdot 10^0$	$2.417(7)\cdot 10^2$	$5.8(4)\cdot 10^3$
0.515	$7.918(1)\cdot 10^0$	$2.376(7)\cdot 10^2$	$5.5(4)\cdot 10^3$
0.525	$7.804(1)\cdot 10^0$	$2.326(7)\cdot 10^2$	$6.1(4)\cdot 10^3$
0.535	$7.691(1)\cdot 10^0$	$2.312(7)\cdot 10^2$	$5.0(4)\cdot 10^3$
0.545	$7.589(1)\cdot 10^0$	$2.285(7)\cdot 10^2$	$5.5(4)\cdot 10^3$
0.555	$7.476(1)\cdot 10^0$	$2.247(7)\cdot 10^2$	$5.7(4)\cdot 10^3$
0.565	$7.377(1)\cdot 10^0$	$2.227(7)\cdot 10^2$	$5.7(4)\cdot 10^3$
0.575	$7.271(1)\cdot 10^0$	$2.190(7)\cdot 10^2$	$5.6(4)\cdot 10^3$
0.585	$7.172(1)\cdot 10^0$	$2.180(7)\cdot 10^2$	$5.4(4)\cdot 10^3$
0.595	$7.073(1)\cdot 10^0$	$2.143(7)\cdot 10^2$	$5.2(4)\cdot 10^3$
0.605	$6.976(1)\cdot 10^0$	$2.105(7)\cdot 10^2$	$4.9(4)\cdot 10^3$
0.615	$6.880(1)\cdot 10^0$	$2.084(7)\cdot 10^2$	$5.2(4)\cdot 10^3$
0.625	$6.788(1)\cdot 10^0$	$2.046(7)\cdot 10^2$	$4.6(4)\cdot 10^3$
0.635	$6.692(1)\cdot 10^0$	$2.025(7)\cdot 10^2$	$5.1(4)\cdot 10^3$
0.645	$6.600(1)\cdot 10^0$	$2.009(7)\cdot 10^2$	$5.1(4)\cdot 10^3$
0.655	$6.515(1)\cdot 10^0$	$1.977(7)\cdot 10^2$	$4.4(4)\cdot 10^3$
0.665	$6.426(1)\cdot 10^0$	$1.947(7)\cdot 10^2$	$5.0(4)\cdot 10^3$
0.675	$6.337(1)\cdot 10^0$	$1.924(7)\cdot 10^2$	$4.7(4)\cdot 10^3$
0.685	$6.253(1)\cdot 10^0$	$1.892(7)\cdot 10^2$	$5.1(4)\cdot 10^3$
0.695	$6.171(1)\cdot 10^0$	$1.877(7)\cdot 10^2$	$4.5(4)\cdot 10^3$
0.705	$6.0874(9)\cdot 10^0$	$1.840(7)\cdot 10^2$	$4.3(3)\cdot 10^3$
0.715	$6.0103(9)\cdot 10^0$	$1.826(7)\cdot 10^2$	$3.9(3)\cdot 10^3$
0.725	$5.9266(9)\cdot 10^0$	$1.800(7)\cdot 10^2$	$4.4(3)\cdot 10^3$
0.735	$5.8474(9)\cdot 10^0$	$1.775(7)\cdot 10^2$	$4.3(3)\cdot 10^3$
0.745	$5.7695(9)\cdot 10^0$	$1.745(8)\cdot 10^2$	$3.2(3)\cdot 10^3$
0.755	0	$6.011(5)\cdot 10^2$	$1.27(2)\cdot 10^4$
0.765	0	$2.771(2)\cdot 10^2$	$1.38(1)\cdot 10^4$
0.775	0	$1.905(1)\cdot 10^2$	$9.99(9)\cdot 10^3$
0.785	0	$1.4246(7)\cdot 10^2$	$7.66(7)\cdot 10^3$
0.795	0	$1.1124(6)\cdot 10^2$	$6.17(6)\cdot 10^3$
0.805	0	$8.895(5)\cdot 10^1$	$4.65(5)\cdot 10^3$
0.815	0	$7.228(4)\cdot 10^1$	$3.49(4)\cdot 10^3$
0.825	0	$5.913(3)\cdot 10^1$	$3.02(4)\cdot 10^3$
0.835	0	$4.876(3)\cdot 10^1$	$2.50(3)\cdot 10^3$
0.845	0	$4.037(2)\cdot 10^1$	$1.93(3)\cdot 10^3$
0.855	0	$3.336(2)\cdot 10^1$	$8.2(2)\cdot 10^2$
0.865	0	$2.754(2)\cdot 10^1$	$1.26(2)\cdot 10^3$
0.875	0	$2.270(2)\cdot 10^1$	$9.4(2)\cdot 10^2$
0.885	0	$1.856(1)\cdot 10^1$	$6.8(1)\cdot 10^2$
0.895	0	$1.506(1)\cdot 10^1$	$5.9(1)\cdot 10^2$
0.905	0	$1.212(1)\cdot 10^1$	$4.57(9)\cdot 10^2$
0.915	0	$9.587(9)\cdot 10^0$	$3.50(7)\cdot 10^2$
0.925	0	$7.458(8)\cdot 10^0$	$2.19(5)\cdot 10^2$
0.935	0	$5.645(7)\cdot 10^0$	$1.0(2)\cdot 10^1$
0.945	0	$4.125(6)\cdot 10^0$	$1.01(2)\cdot 10^2$
0.955	0	$2.875(5)\cdot 10^0$	$2.59(8)\cdot 10^1$
0.965	0	$1.835(4)\cdot 10^0$	$2.26(5)\cdot 10^1$
0.975	0	$1.008(3)\cdot 10^0$	$3.9(1)\cdot 10^0$
0.985	0	$3.99(1)\cdot 10^{-1}$	$-4.886(1)\cdot 10^{-1}$
0.995	0	$1.8841(2)\cdot 10^{-2}$	$-1.443(2)\cdot 10^{-1}$

Table 6. Coefficients of the leading-order (A_C), next-to-leading-order (B_C) and next-to-next-to-leading order (C_C) contributions to the C-parameter distribution.

JHEP06(2009)041

$\ln y_{23}$	$y_{23}\frac{dA_{y_{23}}}{dy_{23}}$	$y_{23}\frac{dB_{y_{23}}}{dy_{23}}$	$y_{23}\frac{dC_{y_{23}}}{dy_{23}}$
-9.875	$2.222(1)\cdot 10^{1}$	$-1.133(3)\cdot 10^{3}$	$-2(1)\cdot 10^{3}$
-9.625	$2.157(1)\cdot 10^{1}$	$-1.004(3)\cdot 10^{3}$	$-6(1)\cdot 10^{3}$
-9.375	$2.094(1)\cdot 10^{1}$	$-8.81(3)\cdot 10^{2}$	$-6.6(9)\cdot 10^{3}$
-9.125	$2.031(1)\cdot 10^{1}$	$-7.63(2)\cdot 10^{2}$	$-8.6(8)\cdot 10^{3}$
-8.875	$1.9650(8)\cdot 10^{1}$	$-6.58(2)\cdot 10^{2}$	$-8.6(7)\cdot 10^{3}$
-8.625	$1.8987(7)\cdot 10^{1}$	$-5.63(2)\cdot 10^{2}$	$-9.4(7)\cdot 10^{3}$
-8.375	$1.8361(6)\cdot 10^{1}$	$-4.74(2)\cdot 10^{2}$	$-9.9(6)\cdot 10^{3}$
-8.125	$1.7707(6)\cdot 10^{1}$	$-3.90(1)\cdot 10^{2}$	$-8.5(5)\cdot 10^{3}$
-7.875	$1.7061(5)\cdot 10^{1}$	$-3.21(1)\cdot 10^{2}$	$-9.1(5)\cdot 10^{3}$
-7.625	$1.6405(4)\cdot 10^{1}$	$-2.54(1)\cdot 10^{2}$	$-8.0(4)\cdot 10^{3}$
-7.375	$1.5758(4)\cdot 10^{1}$	$-1.94(1)\cdot 10^{2}$	$-8.1(4)\cdot 10^{3}$
-7.125	$1.5099(3)\cdot 10^{1}$	$-1.415(9)\cdot 10^{2}$	$-6.2(4)\cdot 10^{3}$
-6.875	$1.4457(3)\cdot 10^{1}$	$-9.45(8)\cdot 10^{1}$	$-5.9(3)\cdot 10^{3}$
-6.625	$1.3806(2)\cdot 10^{1}$	$-5.56(7)\cdot 10^{1}$	$-5.2(3)\cdot 10^{3}$
-6.375	$1.3163(2)\cdot 10^{1}$	$-2.00(6)\cdot 10^{1}$	$-4.1(3)\cdot 10^{3}$
-6.125	$1.2520(2)\cdot 10^{1}$	$1.21(5)\cdot 10^{1}$	$-3.4(2)\cdot 10^{3}$
-5.875	$1.1876(2)\cdot 10^{1}$	$3.61(5)\cdot 10^{1}$	$-2.4(2)\cdot 10^{3}$
-5.625	$1.1235(1)\cdot 10^{1}$	$5.67(4)\cdot 10^{1}$	$-1.8(2)\cdot 10^{3}$
-5.375	$1.0598(1)\cdot 10^{1}$	$7.36(4)\cdot 10^{1}$	$-1.3(2)\cdot 10^{3}$
-5.125	$9.965(1)\cdot 10^{0}$	$8.47(3)\cdot 10^{1}$	$-9(2)\cdot 10^{2}$
-4.875	$9.3336(9)\cdot 10^{0}$	$9.48(3)\cdot 10^{1}$	$-3(1)\cdot 10^{2}$
-4.625	$8.7098(8)\cdot 10^{0}$	$1.005(2)\cdot 10^{2}$	$0(1)\cdot 10^{1}$
-4.375	$8.0890(7)\cdot 10^{0}$	$1.027(2)\cdot 10^{2}$	$4(1)\cdot 10^{2}$
-4.125	$7.4721(6)\cdot 10^{0}$	$1.033(2)\cdot 10^{2}$	$5(1)\cdot 10^{2}$
-3.875	$6.8622(5)\cdot 10^{0}$	$1.009(2)\cdot 10^{2}$	$9.1(9)\cdot 10^{2}$
-3.625	$6.2583(5)\cdot 10^{0}$	$9.70(1)\cdot 10^{1}$	$7.0(8)\cdot 10^{2}$
-3.375	$5.6606(4)\cdot 10^{0}$	$9.10(1)\cdot 10^{1}$	$7.0(7)\cdot 10^{2}$
-3.125	$5.0728(4)\cdot 10^{0}$	$8.39(1)\cdot 10^{1}$	$7.6(6)\cdot 10^{2}$
-2.875	$4.4922(3)\cdot 10^{0}$	$7.551(8)\cdot 10^{1}$	$5.7(5)\cdot 10^{2}$
-2.625	$3.9202(3)\cdot 10^{0}$	$6.652(7)\cdot 10^{1}$	$5.2(4)\cdot 10^{2}$
-2.375	$3.3538(2)\cdot 10^{0}$	$5.674(6)\cdot 10^{1}$	$4.5(3)\cdot 10^{2}$
-2.125	$2.7894(2)\cdot 10^{0}$	$4.676(4)\cdot 10^{1}$	$2.6(3)\cdot 10^{2}$
-1.875	$2.2184(2)\cdot 10^{0}$	$3.635(3)\cdot 10^{1}$	$1.8(2)\cdot 10^{2}$
-1.625	$1.6189(1)\cdot 10^{0}$	$2.590(2)\cdot 10^{1}$	$1.4(2)\cdot 10^{2}$
-1.375	$9.4172(8)\cdot 10^{-1}$	$1.479(2)\cdot 10^{1}$	$3(1)\cdot 10^{1}$
-1.125	$1.6678(3)\cdot 10^{-1}$	$1.704(6)\cdot 10^{0}$	$-4.0(4)\cdot 10^{1}$
-0.875	0	0	0

Table 7. Coefficients of the leading-order ($A_{y_{23}}$), next-to-leading-order ($B_{y_{23}}$) and next-to-next-to-leading order ($C_{y_{23}}$) contributions to the three-to-two jet transition distribution.

JHEP06(2009)041

$y_{\rm cut}$	$A_{3-jet,Durham}$	$B_{3-jet,Durham}$	$C_{3-jet,Durham}$
0.3	$2.2301(9)\cdot 10^{-2}$	$1.35(2)\cdot 10^{-1}$	$-6(3)\cdot 10^{0}$
0.15	$1.0028(3)\cdot 10^{0}$	$1.582(3)\cdot 10^{1}$	$5(1)\cdot 10^{1}$
0.1	$2.1150(6)\cdot 10^{0}$	$3.415(7)\cdot 10^{1}$	$1.7(2)\cdot 10^{2}$
0.06	$4.046(1)\cdot 10^{0}$	$6.57(1)\cdot 10^{1}$	$4.1(3)\cdot 10^{2}$
0.03	$7.627(2)\cdot 10^{0}$	$1.141(2)\cdot 10^{2}$	$5.0(6)\cdot 10^{2}$
0.015	$1.2359(3)\cdot 10^{1}$	$1.495(3)\cdot 10^{2}$	$-1.2(9)\cdot 10^{2}$
0.01	$1.5671(4)\cdot 10^{1}$	$1.531(4)\cdot 10^{2}$	$-1.3(1)\cdot 10^{3}$
0.006	$2.0430(5)\cdot 10^{1}$	$1.238(5)\cdot 10^{2}$	$-3.6(2)\cdot 10^{3}$
0.003	$2.7947(7)\cdot 10^{1}$	$-5.5(7)\cdot 10^{0}$	$-9.0(3)\cdot 10^{3}$
0.0015	$3.6694(8)\cdot 10^{1}$	$-2.93(1)\cdot 10^{2}$	$-1.63(5)\cdot 10^{4}$
0.001	$4.2386(9)\cdot 10^{1}$	$-5.62(1)\cdot 10^{2}$	$-2.16(6)\cdot 10^{4}$
0.0006	$5.016(1)\cdot 10^{1}$	$-1.032(2)\cdot 10^{3}$	$-2.84(8)\cdot 10^{4}$
0.0003	$6.181(1)\cdot 10^{1}$	$-1.967(2)\cdot 10^{3}$	$-3.1(1)\cdot 10^{4}$
0.00015	$7.471(2)\cdot 10^{1}$	$-3.333(2)\cdot 10^{3}$	$-1.8(3)\cdot 10^{4}$
0.0001	$8.285(2)\cdot 10^{1}$	$-4.368(3)\cdot 10^{3}$	$6(4)\cdot 10^{3}$

Table 8. Coefficients of the leading-order ($A_{3-jet,Durham}$), next-to-leading-order ($B_{3-jet,Durham}$) and next-to-next-to-leading order ($C_{3-jet,Durham}$) contributions to the Durham three-jet rate for various values of $y_{\rm cut}$.

$y_{\rm cut}$	$A_{3-jet,Geneva}$	$B_{3-jet,Geneva}$	$C_{3-jet,Geneva}$
0.3	$1.7615(7)\cdot 10^{-1}$	$2.10(1)\cdot 10^{0}$	$-1.3(6)\cdot 10^{1}$
0.15	$4.7265(9)\cdot 10^{0}$	$5.45(1)\cdot 10^{1}$	$-4.4(6)\cdot 10^{2}$
0.1	$8.922(1)\cdot 10^{0}$	$7.51(2)\cdot 10^{1}$	$-1.3(1)\cdot 10^{3}$
0.06	$1.5520(3)\cdot 10^{1}$	$3.87(4)\cdot 10^{1}$	$-5.0(2)\cdot 10^{3}$
0.03	$2.6717(4)\cdot 10^{1}$	$-2.403(7)\cdot 10^{2}$	$-1.35(4)\cdot 10^{4}$
0.015	$4.0440(5)\cdot 10^{1}$	$-9.725(7)\cdot 10^{2}$	$-2.53(7)\cdot 10^{4}$
0.01	$4.9627(6)\cdot 10^{1}$	$-1.709(2)\cdot 10^{3}$	$-2.86(8)\cdot 10^{4}$
0.006	$6.2446(7)\cdot 10^{1}$	$-3.072(3)\cdot 10^{3}$	$-2.5(1)\cdot 10^{4}$
0.003	$8.204(1)\cdot 10^{1}$	$-5.937(5)\cdot 10^{3}$	$1.4(2)\cdot 10^{4}$
0.0015	$1.0418(1)\cdot 10^{2}$	$-1.0300(6)\cdot 10^{4}$	$1.53(4)\cdot 10^{5}$
0.001	$1.1833(1)\cdot 10^{2}$	$-1.3736(9)\cdot 10^{4}$	$2.81(5)\cdot 10^{5}$

Table 9. Coefficients of the leading-order ($A_{3-jet,Geneva}$), next-to-leading-order ($B_{3-jet,Geneva}$) and next-to-next-to-leading order ($C_{3-jet,Geneva}$) contributions to the Durham three-jet rate for various values of $y_{\rm cut}$.

$y_{\rm cut}$	$A_{3-jet,Jade-E0}$	$B_{3-jet,Jade-E0}$	$C_{3-jet,Jade-E0}$
0.3	$5.393(2)\cdot 10^{-2}$	$1.119(5)\cdot 10^{0}$	$9(8)\cdot 10^{0}$
0.15	$2.3086(5)\cdot 10^{0}$	$5.293(6)\cdot 10^{1}$	$5.3(4)\cdot 10^{2}$
0.1	$4.9170(9)\cdot 10^{0}$	$1.118(1)\cdot 10^{2}$	$9(1)\cdot 10^{2}$
0.06	$9.527(2)\cdot 10^{0}$	$1.994(2)\cdot 10^{2}$	$1.5(2)\cdot 10^{3}$
0.03	$1.8137(3)\cdot 10^{1}$	$2.885(4)\cdot 10^{2}$	$-8(3)\cdot 10^{2}$
0.015	$2.9425(4)\cdot 10^{1}$	$2.397(8)\cdot 10^{2}$	$-9.1(6)\cdot 10^{3}$
0.01	$3.7257(5)\cdot 10^{1}$	$9.1(1)\cdot 10^{1}$	$-1.88(6)\cdot 10^{4}$
0.006	$4.8389(6)\cdot 10^{1}$	$-2.92(2)\cdot 10^{2}$	$-2.9(1)\cdot 10^{4}$
0.003	$6.5768(9)\cdot 10^{1}$	$-1.300(3)\cdot 10^{3}$	$-4.6(2)\cdot 10^{4}$
0.0015	$8.572(1)\cdot 10^{1}$	$-3.092(4)\cdot 10^{3}$	$-4.6(2)\cdot 10^{4}$
0.001	$9.859(1)\cdot 10^{1}$	$-4.603(5)\cdot 10^{3}$	$-2.9(4)\cdot 10^{4}$
0.0006	$1.1607(1)\cdot 10^{2}$	$-7.143(7)\cdot 10^{3}$	$3.2(4)\cdot 10^{4}$
0.0003	$1.4199(2)\cdot 10^{2}$	$-1.190(1)\cdot 10^{4}$	$2.30(8)\cdot 10^{5}$

Table 10. Coefficients of the leading-order ($A_{3-jet,Jade-E0}$), next-to-leading-order ($B_{3-jet,Jade-E0}$) and next-to-next-to-leading order ($C_{3-jet,Jade-E0}$) contributions to the Durham three-jet rate for various values of $y_{\rm cut}$.

JHEP06(2009)041

$y_{\rm cut}$	$A_{3-jet,Cambridge}$	$B_{3-jet,Cambridge}$	$C_{3-jet,Cambridge}$
0.3	$2.2301(9) \cdot 10^{-2}$	$1.35(2) \cdot 10^{-1}$	$-7(3) \cdot 10^{0}$
0.15	$1.0028(3) \cdot 10^{0}$	$1.525(3) \cdot 10^{1}$	$2(3) \cdot 10^{1}$
0.1	$2.1150(6) \cdot 10^{0}$	$3.156(6) \cdot 10^{1}$	$9(6) \cdot 10^{1}$
0.06	$4.046(1) \cdot 10^{0}$	$5.72(1) \cdot 10^{1}$	$4(9) \cdot 10^{1}$
0.03	$7.627(2) \cdot 10^{0}$	$9.33(2) \cdot 10^{1}$	$-2(2) \cdot 10^{2}$
0.015	$1.2359(3) \cdot 10^{1}$	$1.127(3) \cdot 10^{2}$	$-1.1(2) \cdot 10^{3}$
0.01	$1.5671(4) \cdot 10^{1}$	$1.048(4) \cdot 10^{2}$	$-2.3(3) \cdot 10^{3}$
0.006	$2.0430(5) \cdot 10^{1}$	$5.96(6) \cdot 10^{1}$	$-3.9(4) \cdot 10^{3}$
0.003	$2.7947(7) \cdot 10^{1}$	$-9.66(7) \cdot 10^{1}$	$-9.6(6) \cdot 10^{3}$
0.0015	$3.6694(8) \cdot 10^{1}$	$-4.15(1) \cdot 10^{2}$	$-1.41(8) \cdot 10^{4}$
0.001	$4.2386(9) \cdot 10^{1}$	$-7.03(1) \cdot 10^{2}$	$-1.7(1) \cdot 10^{4}$
0.0006	$5.016(1) \cdot 10^{1}$	$-1.201(2) \cdot 10^{3}$	$-1.8(1) \cdot 10^{4}$
0.0003	$6.181(1) \cdot 10^{1}$	$-2.177(2) \cdot 10^{3}$	$-1.3(2) \cdot 10^{4}$
0.00015	$7.471(2) \cdot 10^{1}$	$-3.584(3) \cdot 10^{3}$	$9(2) \cdot 10^{3}$
0.0001	$8.285(2) \cdot 10^{1}$	$-4.656(4) \cdot 10^{3}$	$3.3(3) \cdot 10^{4}$

Table 11. Coefficients of the leading-order ($A_{3-jet,Cambridge}$), next-to-leading-order ($B_{3-jet,Cambridge}$) and next-to-next-to-leading order ($C_{3-jet,Cambridge}$) contributions to the Durham three-jet rate for various values of $y_{\rm cut}$.

JHEP06(2009)041

$(1-T)$	N_c^2	N_c^0	N_c^{-2}	$N_f N_c$	N_f/N_c	N_f^2
0.005	$-1.67(1)\cdot 10^4$	$8.14(2)\cdot 10^3$	$5.73(2)\cdot 10^2$	$-3.85(4)\cdot 10^3$	$-5.412(5)\cdot 10^3$	$8.3281(6)\cdot 10^3$
0.015	$8.5(1)\cdot 10^3$	$4.35(3)\cdot 10^3$	$-9.0(3)\cdot 10^1$	$-1.880(4)\cdot 10^4$	$-6.80(6)\cdot 10^2$	$3.4298(3)\cdot 10^3$
0.025	$1.35(1)\cdot 10^4$	$2.30(3)\cdot 10^3$	$-9.2(3)\cdot 10^1$	$-1.632(4)\cdot 10^4$	$-1.02(6)\cdot 10^2$	$2.3354(3)\cdot 10^3$
0.035	$1.52(1)\cdot 10^4$	$1.24(3)\cdot 10^3$	$-7.7(2)\cdot 10^1$	$-1.425(4)\cdot 10^4$	$1.12(6)\cdot 10^2$	$1.7636(3)\cdot 10^3$
0.045	$1.52(1)\cdot 10^4$	$5.4(3)\cdot 10^2$	$-6.3(2)\cdot 10^1$	$-1.243(4)\cdot 10^4$	$2.12(6)\cdot 10^2$	$1.4027(3)\cdot 10^3$
0.055	$1.47(1)\cdot 10^4$	$2.0(2)\cdot 10^2$	$-4.7(2)\cdot 10^1$	$-1.101(4)\cdot 10^4$	$2.65(6)\cdot 10^2$	$1.1509(3)\cdot 10^3$
0.065	$1.41(1)\cdot 10^4$	$-3(2)\cdot 10^1$	$-4.0(2)\cdot 10^1$	$-9.83(4)\cdot 10^3$	$2.81(5)\cdot 10^2$	$9.646(3)\cdot 10^2$
0.075	$1.33(1)\cdot 10^4$	$-2.3(2)\cdot 10^2$	$-3.2(2)\cdot 10^1$	$-8.76(4)\cdot 10^3$	$2.92(5)\cdot 10^2$	$8.209(2)\cdot 10^2$
0.085	$1.27(1)\cdot 10^4$	$-3.4(2)\cdot 10^2$	$-2.7(2)\cdot 10^1$	$-7.84(4)\cdot 10^3$	$2.89(5)\cdot 10^2$	$7.070(2)\cdot 10^2$
0.095	$1.19(1)\cdot 10^4$	$-3.9(2)\cdot 10^2$	$-1.9(2)\cdot 10^1$	$-7.18(3)\cdot 10^3$	$2.81(5)\cdot 10^2$	$6.142(2)\cdot 10^2$
0.105	$1.12(1)\cdot 10^4$	$-4.4(2)\cdot 10^2$	$-1.7(2)\cdot 10^1$	$-6.49(3)\cdot 10^3$	$2.69(5)\cdot 10^2$	$5.374(2)\cdot 10^2$
0.115	$1.05(1)\cdot 10^4$	$-4.9(2)\cdot 10^2$	$-1.4(2)\cdot 10^1$	$-5.91(3)\cdot 10^3$	$2.59(5)\cdot 10^2$	$4.733(2)\cdot 10^2$
0.125	$9.7(1)\cdot 10^3$	$-5.0(2)\cdot 10^2$	$-1.1(1)\cdot 10^1$	$-5.44(3)\cdot 10^3$	$2.46(4)\cdot 10^2$	$4.182(2)\cdot 10^2$
0.135	$9.1(1)\cdot 10^3$	$-5.2(2)\cdot 10^2$	$-8(1)\cdot 10^0$	$-4.88(3)\cdot 10^3$	$2.44(4)\cdot 10^2$	$3.705(2)\cdot 10^2$
0.145	$8.6(1)\cdot 10^3$	$-5.3(2)\cdot 10^2$	$-7(1)\cdot 10^0$	$-4.48(3)\cdot 10^3$	$2.21(4)\cdot 10^2$	$3.298(2)\cdot 10^2$
0.155	$8.0(1)\cdot 10^3$	$-5.1(2)\cdot 10^2$	$-6(1)\cdot 10^0$	$-4.15(3)\cdot 10^3$	$2.11(4)\cdot 10^2$	$2.937(2)\cdot 10^2$
0.165	$7.64(9)\cdot 10^3$	$-5.0(1)\cdot 10^2$	$-3(1)\cdot 10^0$	$-3.85(3)\cdot 10^3$	$2.03(4)\cdot 10^2$	$2.620(2)\cdot 10^2$
0.175	$7.01(9)\cdot 10^3$	$-4.7(1)\cdot 10^2$	$-2(1)\cdot 10^0$	$-3.46(3)\cdot 10^3$	$1.96(3)\cdot 10^2$	$2.338(2)\cdot 10^2$
0.185	$6.59(9)\cdot 10^3$	$-4.8(1)\cdot 10^2$	$-1(1)\cdot 10^0$	$-3.20(3)\cdot 10^3$	$1.77(3)\cdot 10^2$	$2.079(2)\cdot 10^2$
0.195	$6.19(9)\cdot 10^3$	$-4.4(1)\cdot 10^2$	$-9(9)\cdot 10^{-1}$	$-2.91(3)\cdot 10^3$	$1.75(3)\cdot 10^2$	$1.848(2)\cdot 10^2$
0.205	$5.81(9)\cdot 10^3$	$-4.5(1)\cdot 10^2$	$7(9)\cdot 10^{-1}$	$-2.70(3)\cdot 10^3$	$1.60(3)\cdot 10^2$	$1.639(2)\cdot 10^2$
0.215	$5.44(8)\cdot 10^3$	$-4.2(1)\cdot 10^2$	$1.1(8)\cdot 10^0$	$-2.46(2)\cdot 10^3$	$1.47(3)\cdot 10^2$	$1.446(2)\cdot 10^2$
0.225	$5.04(8)\cdot 10^3$	$-4.0(1)\cdot 10^2$	$-3(8)\cdot 10^{-1}$	$-2.28(2)\cdot 10^3$	$1.40(2)\cdot 10^2$	$1.266(2)\cdot 10^2$
0.235	$4.70(8)\cdot 10^3$	$-3.7(1)\cdot 10^2$	$1.0(7)\cdot 10^0$	$-2.06(2)\cdot 10^3$	$1.30(2)\cdot 10^2$	$1.097(2)\cdot 10^2$
0.245	$4.33(7)\cdot 10^3$	$-3.49(9)\cdot 10^2$	$2.5(6)\cdot 10^0$	$-1.87(2)\cdot 10^3$	$1.20(2)\cdot 10^2$	$9.38(2)\cdot 10^1$
0.255	$4.20(7)\cdot 10^3$	$-3.32(9)\cdot 10^2$	$1.4(6)\cdot 10^0$	$-1.71(2)\cdot 10^3$	$1.09(2)\cdot 10^2$	$7.88(2)\cdot 10^1$
0.265	$3.84(7)\cdot 10^3$	$-3.19(8)\cdot 10^2$	$2.3(5)\cdot 10^0$	$-1.53(2)\cdot 10^3$	$9.7(2)\cdot 10^1$	$6.41(2)\cdot 10^1$
0.275	$3.51(6)\cdot 10^3$	$-2.92(7)\cdot 10^2$	$2.2(5)\cdot 10^0$	$-1.39(2)\cdot 10^3$	$9.2(1)\cdot 10^1$	$4.94(2)\cdot 10^1$
0.285	$3.29(6)\cdot 10^3$	$-2.71(6)\cdot 10^2$	$1.7(4)\cdot 10^0$	$-1.26(2)\cdot 10^3$	$8.4(4)\cdot 10^0$	$3.53(2)\cdot 10^1$
0.295	$3.03(5)\cdot 10^3$	$-2.38(6)\cdot 10^2$	$1.7(3)\cdot 10^0$	$-1.05(1)\cdot 10^3$	$6.5(1)\cdot 10^1$	$2.14(2)\cdot 10^1$
0.305	$2.74(4)\cdot 10^3$	$-2.17(5)\cdot 10^2$	$2.1(3)\cdot 10^0$	$-8.6(1)\cdot 10^2$	$5.96(8)\cdot 10^1$	$7.3(2)\cdot 10^0$
0.315	$2.38(3)\cdot 10^3$	$-1.99(4)\cdot 10^2$	$1.5(2)\cdot 10^0$	$-6.61(9)\cdot 10^2$	$5.03(6)\cdot 10^1$	$-6.6(1)\cdot 10^0$
0.325	$2.03(2)\cdot 10^3$	$-1.59(2)\cdot 10^2$	$1.1(1)\cdot 10^0$	$-4.65(6)\cdot 10^2$	$2.87(3)\cdot 10^1$	$-2.14(1)\cdot 10^1$
0.335	$1.39(1)\cdot 10^3$	$-1.21(1)\cdot 10^2$	$6(1)\cdot 10^{-2}$	$-2.23(3)\cdot 10^2$	$1.88(2)\cdot 10^1$	$-2.570(6)\cdot 10^1$
0.345	$4.59(5)\cdot 10^2$	$-5.91(7)\cdot 10^1$	$1.0(1)\cdot 10^{-1}$	$-9.2(1)\cdot 10^1$	$8.9(6)\cdot 10^{-2}$	$-1.165(3)\cdot 10^1$
0.355	$2.20(3)\cdot 10^2$	$-1.92(3)\cdot 10^1$	$-1(1)\cdot 10^{-4}$	$-3.99(4)\cdot 10^1$	$1.0(1)\cdot 10^{-2}$	$-5.91(2)\cdot 10^0$
0.365	$7.4(1)\cdot 10^1$	$-1.10(6)\cdot 10^0$	$-2(1)\cdot 10^{-4}$	$-1.73(2)\cdot 10^1$	$9(9)\cdot 10^{-8}$	$-2.85(1)\cdot 10^0$
0.375	$4.50(7)\cdot 10^1$	$-2.0(9)\cdot 10^{-2}$	$-8.8(7)\cdot 10^{-3}$	$-7.8(1)\cdot 10^0$	$1(1)\cdot 10^{-11}$	$-1.452(7)\cdot 10^0$
0.385	$1.17(2)\cdot 10^1$	$-1.2(3)\cdot 10^{-2}$	$-2.0(1)\cdot 10^{-3}$	$-8.0(3)\cdot 10^{-1}$	$3(3)\cdot 10^{-13}$	$-1.84(7)\cdot 10^{-2}$
0.395	$2.1(2)\cdot 10^{-1}$	$-3(1)\cdot 10^{-3}$	$-4(4)\cdot 10^{-6}$	$-3(1)\cdot 10^{-5}$	$1.0(7)\cdot 10^{-13}$	$-1.83(6)\cdot 10^{-2}$
0.405	$-1(1)\cdot 10^{-7}$	$4(4)\cdot 10^{-8}$	$-3(2)\cdot 10^{-8}$	$-5(5)\cdot 10^{-12}$	$1.1(7)\cdot 10^{-11}$	$-1.0(1)\cdot 10^{-3}$
0.415	$5(2)\cdot 10^{-5}$	$1.1(4)\cdot 10^{-7}$	$-1(1)\cdot 10^{-11}$	$-1(1)\cdot 10^{-10}$	$4(4)\cdot 10^{-8}$	$-1.951(2)\cdot 10^{-1}$
0.425	$-2(4)\cdot 10^{-3}$	$-7.1(2)\cdot 10^{-3}$	$5(7)\cdot 10^{-7}$	0	0	0
0.435	0	$-1(1)\cdot 10^{-3}$	0	0	0	0
0.445	0	0	0	0	0	0

Table 12. Individual contributions from the different colour factors to $(1-T)\frac{dC_{(1-T)}}{d(1-T)}$ for the thrust distribution.

JHEP06(2009)041

ρ	N_c^2	N_c^0	N_c^{-2}	$N_f N_c$	N_f/N_c	N_f^2
0.005	$-1.10(1)\cdot 10^4$	$6.01(2)\cdot 10^3$	$7.83(1)\cdot 10^2$	$2.82(4)\cdot 10^3$	$-6.094(5)\cdot 10^3$	$8.3694(7)\cdot 10^3$
0.015	$5.3(1)\cdot 10^3$	$3.64(3)\cdot 10^3$	$3.2(1)\cdot 10^1$	$-1.435(4)\cdot 10^4$	$-1.137(4)\cdot 10^3$	$3.4802(5)\cdot 10^3$
0.025	$9.2(1)\cdot 10^3$	$2.04(2)\cdot 10^3$	$-1.0(1)\cdot 10^1$	$-1.278(4)\cdot 10^4$	$-4.76(4)\cdot 10^2$	$2.3914(4)\cdot 10^3$
0.035	$1.03(1)\cdot 10^4$	$1.18(2)\cdot 10^3$	$-1.5(1)\cdot 10^1$	$-1.119(4)\cdot 10^4$	$-2.05(4)\cdot 10^2$	$1.8219(4)\cdot 10^3$
0.045	$1.04(1)\cdot 10^4$	$6.9(2)\cdot 10^2$	$-1.6(1)\cdot 10^1$	$-9.71(4)\cdot 10^3$	$-7.6(4)\cdot 10^1$	$1.4625(3)\cdot 10^3$
0.055	$9.7(1)\cdot 10^3$	$3.6(2)\cdot 10^2$	$-1.5(1)\cdot 10^1$	$-8.51(4)\cdot 10^3$	$4(4)\cdot 10^0$	$1.2114(3)\cdot 10^3$
0.065	$9.3(1)\cdot 10^3$	$1.7(2)\cdot 10^2$	$-1.0(1)\cdot 10^1$	$-7.48(4)\cdot 10^3$	$5.3(4)\cdot 10^1$	$1.0256(3)\cdot 10^3$
0.075	$8.4(1)\cdot 10^3$	$4(2)\cdot 10^1$	$-1.0(1)\cdot 10^1$	$-6.74(3)\cdot 10^3$	$8.0(4)\cdot 10^1$	$8.812(3)\cdot 10^2$
0.085	$7.9(1)\cdot 10^3$	$-4(2)\cdot 10^1$	$-9(1)\cdot 10^0$	$-5.87(3)\cdot 10^3$	$9.1(4)\cdot 10^1$	$7.673(3)\cdot 10^2$
0.095	$7.3(1)\cdot 10^3$	$-8(2)\cdot 10^1$	$-3(1)\cdot 10^0$	$-5.35(3)\cdot 10^3$	$1.03(4)\cdot 10^2$	$6.737(3)\cdot 10^2$
0.105	$6.5(1)\cdot 10^3$	$-1.4(2)\cdot 10^2$	$-8(1)\cdot 10^0$	$-4.75(3)\cdot 10^3$	$1.00(4)\cdot 10^2$	$5.964(3)\cdot 10^2$
0.115	$5.9(1)\cdot 10^3$	$-1.4(2)\cdot 10^2$	$-3(1)\cdot 10^0$	$-4.32(3)\cdot 10^3$	$1.05(3)\cdot 10^2$	$5.317(3)\cdot 10^2$
0.125	$5.3(1)\cdot 10^3$	$-1.6(2)\cdot 10^2$	$-4(1)\cdot 10^0$	$-3.86(3)\cdot 10^3$	$1.00(3)\cdot 10^2$	$4.764(2)\cdot 10^2$
0.135	$4.8(1)\cdot 10^3$	$-2.2(2)\cdot 10^2$	$-3.1(9)\cdot 10^0$	$-3.50(3)\cdot 10^3$	$9.7(3)\cdot 10^1$	$4.283(2)\cdot 10^2$
0.145	$4.4(1)\cdot 10^3$	$-1.6(1)\cdot 10^2$	$-1.5(9)\cdot 10^0$	$-3.09(3)\cdot 10^3$	$8.8(3)\cdot 10^1$	$3.875(2)\cdot 10^2$
0.155	$3.8(1)\cdot 10^3$	$-1.3(1)\cdot 10^2$	$-2.6(9)\cdot 10^0$	$-2.82(3)\cdot 10^3$	$8.3(3)\cdot 10^1$	$3.517(2)\cdot 10^2$
0.165	$3.45(9)\cdot 10^3$	$-1.6(1)\cdot 10^2$	$-1.1(8)\cdot 10^0$	$-2.48(2)\cdot 10^3$	$7.4(3)\cdot 10^1$	$3.194(2)\cdot 10^2$
0.175	$2.73(9)\cdot 10^3$	$-1.0(1)\cdot 10^2$	$-1.9(8)\cdot 10^0$	$-2.24(2)\cdot 10^3$	$7.1(3)\cdot 10^1$	$2.911(2)\cdot 10^2$
0.185	$2.22(9)\cdot 10^3$	$-1.0(1)\cdot 10^2$	$-1.8(8)\cdot 10^0$	$-2.04(2)\cdot 10^3$	$6.0(2)\cdot 10^1$	$2.649(2)\cdot 10^2$
0.195	$2.09(9)\cdot 10^3$	$-1.1(1)\cdot 10^2$	$-2(7)\cdot 10^{-1}$	$-1.81(2)\cdot 10^3$	$5.2(2)\cdot 10^1$	$2.410(2)\cdot 10^2$
0.205	$1.64(9)\cdot 10^3$	$-8(1)\cdot 10^1$	$-1.4(7)\cdot 10^0$	$-1.55(2)\cdot 10^3$	$4.7(2)\cdot 10^1$	$2.198(2)\cdot 10^2$
0.215	$1.33(8)\cdot 10^3$	$-5(1)\cdot 10^1$	$-7(7)\cdot 10^{-1}$	$-1.38(2)\cdot 10^3$	$4.2(2)\cdot 10^1$	$1.997(2)\cdot 10^2$
0.225	$8.7(8)\cdot 10^2$	$-5(1)\cdot 10^1$	$-2.2(6)\cdot 10^0$	$-1.22(2)\cdot 10^3$	$3.7(2)\cdot 10^1$	$1.814(2)\cdot 10^2$
0.235	$7.2(8)\cdot 10^2$	$-2.2(9)\cdot 10^1$	$-5(6)\cdot 10^{-1}$	$-1.06(2)\cdot 10^3$	$2.3(1)\cdot 10^1$	$1.632(2)\cdot 10^2$
0.245	$5.4(7)\cdot 10^2$	$-8(9)\cdot 10^0$	$-8(5)\cdot 10^{-1}$	$-9.0(2)\cdot 10^2$	$2.0(1)\cdot 10^1$	$1.469(2)\cdot 10^2$
0.255	$2.1(7)\cdot 10^2$	$-9(8)\cdot 10^0$	$-5(5)\cdot 10^{-1}$	$-7.1(2)\cdot 10^2$	$1.6(1)\cdot 10^1$	$1.309(2)\cdot 10^2$
0.265	$1.3(7)\cdot 10^2$	$9(8)\cdot 10^0$	$-7(4)\cdot 10^{-1}$	$-6.2(2)\cdot 10^2$	$9(1)\cdot 10^0$	$1.153(2)\cdot 10^2$
0.275	$-5(6)\cdot 10^1$	$1.5(7)\cdot 10^1$	$-5(4)\cdot 10^{-1}$	$-4.7(1)\cdot 10^2$	$5.5(9)\cdot 10^0$	$9.91(2)\cdot 10^1$
0.285	$-2.0(6)\cdot 10^2$	$7(6)\cdot 10^0$	$-8(3)\cdot 10^{-1}$	$-3.7(1)\cdot 10^2$	$-1(3)\cdot 10^{-1}$	$8.35(2)\cdot 10^1$
0.295	$-2.0(5)\cdot 10^2$	$2.8(5)\cdot 10^1$	$-4(2)\cdot 10^{-1}$	$-2.5(1)\cdot 10^2$	$-7(6)\cdot 10^{-1}$	$6.73(2)\cdot 10^1$
0.305	$-2.9(4)\cdot 10^2$	$1.9(4)\cdot 10^1$	$-2(2)\cdot 10^{-1}$	$-1.71(9)\cdot 10^2$	$-1.4(5)\cdot 10^0$	$4.94(1)\cdot 10^1$
0.315	$-2.1(3)\cdot 10^2$	$1.2(3)\cdot 10^1$	$-4(1)\cdot 10^{-1}$	$-1.24(6)\cdot 10^2$	$-5(3)\cdot 10^{-1}$	$2.99(1)\cdot 10^1$
0.325	$5(2)\cdot 10^1$	$5(2)\cdot 10^0$	$-2.5(6)\cdot 10^{-1}$	$-1.24(4)\cdot 10^2$	$3.2(2)\cdot 10^0$	$7.12(8)\cdot 10^0$
0.335	$1.34(5)\cdot 10^2$	$-7(7)\cdot 10^{-1}$	$-1.1(6)\cdot 10^{-3}$	$-7.5(1)\cdot 10^1$	$5.1(2)\cdot 10^{-1}$	$-1.041(4)\cdot 10^1$
0.345	$4.4(1)\cdot 10^1$	$-2.4(2)\cdot 10^0$	$-4.5(2)\cdot 10^{-2}$	$-1.57(3)\cdot 10^1$	$4(3)\cdot 10^{-5}$	$-4.52(1)\cdot 10^0$
0.355	$1.86(6)\cdot 10^1$	$-3.1(6)\cdot 10^{-1}$	$-1.2(7)\cdot 10^{-5}$	$-7.5(1)\cdot 10^0$	$3(3)\cdot 10^{-11}$	$-1.639(5)\cdot 10^0$
0.365	$3.7(2)\cdot 10^0$	$-2.4(8)\cdot 10^{-2}$	$-4.0(4)\cdot 10^{-4}$	$-7.5(3)\cdot 10^{-1}$	$1(1)\cdot 10^{-12}$	$-1.62(1)\cdot 10^{-1}$
0.375	$1.4(2)\cdot 10^{-1}$	$-3(3)\cdot 10^{-7}$	$-7(1)\cdot 10^{-5}$	$-5(5)\cdot 10^{-6}$	$4(2)\cdot 10^{-11}$	$-4.38(5)\cdot 10^{-2}$
0.385	$2.1(4)\cdot 10^{-2}$	$1.8(7)\cdot 10^{-6}$	$-3(3)\cdot 10^{-9}$	$-7(7)\cdot 10^{-14}$	$6(4)\cdot 10^{-8}$	$-9.09(2)\cdot 10^{-2}$
0.395	$3(4)\cdot 10^{-5}$	$3(2)\cdot 10^{-9}$	$-2(2)\cdot 10^{-11}$	$-1(1)\cdot 10^{-12}$	$3(2)\cdot 10^{-11}$	$-2.7(2)\cdot 10^{-3}$
0.405	$-3(2)\cdot 10^{-7}$	$9(7)\cdot 10^{-10}$	$-3(1)\cdot 10^{-11}$	$-6(4)\cdot 10^{-12}$	$9(8)\cdot 10^{-9}$	$-3.7(4)\cdot 10^{-3}$
0.415	$2(2)\cdot 10^{-8}$	$1(1)\cdot 10^{-5}$	$-4(4)\cdot 10^{-9}$	$-6(6)\cdot 10^{-4}$	0	$-1.0(4)\cdot 10^{-1}$
0.425	0	0	0	0	0	0

Table 13. Individual contributions from the different colour factors to $\rho\frac{dC_\rho}{d\rho}$ for the heavy jet mass distribution.

JHEP06(2009)041

B_W	N_c^2	N_c^0	N_c^{-2}	$N_f N_c$	N_f/N_c	N_f^2
0.005	$3.30(6)\cdot 10^4$	$-8.6(1)\cdot 10^3$	$4.845(5)\cdot 10^3$	$1.192(2)\cdot 10^5$	$-2.799(2)\cdot 10^4$	$2.2782(2)\cdot 10^4$
0.015	$-3.05(2)\cdot 10^4$	$1.169(6)\cdot 10^4$	$7.19(4)\cdot 10^2$	$-8.55(9)\cdot 10^3$	$-6.85(1)\cdot 10^3$	$1.0195(1)\cdot 10^4$
0.025	$-7.5(2)\cdot 10^3$	$8.19(6)\cdot 10^3$	$2.20(3)\cdot 10^2$	$-1.788(8)\cdot 10^4$	$-3.356(9)\cdot 10^3$	$6.8578(7)\cdot 10^3$
0.035	$3.8(2)\cdot 10^3$	$5.78(5)\cdot 10^3$	$7.1(3)\cdot 10^1$	$-1.922(7)\cdot 10^4$	$-1.908(8)\cdot 10^3$	$5.1322(6)\cdot 10^3$
0.045	$9.9(2)\cdot 10^3$	$3.95(4)\cdot 10^3$	$1.1(2)\cdot 10^1$	$-1.853(6)\cdot 10^4$	$-1.145(7)\cdot 10^3$	$4.0453(6)\cdot 10^3$
0.055	$1.25(2)\cdot 10^4$	$2.84(4)\cdot 10^3$	$0(2)\cdot 10^{-1}$	$-1.731(6)\cdot 10^4$	$-7.03(6)\cdot 10^2$	$3.2925(5)\cdot 10^3$
0.065	$1.40(2)\cdot 10^4$	$1.96(4)\cdot 10^3$	$-1.4(2)\cdot 10^1$	$-1.571(6)\cdot 10^4$	$-4.33(6)\cdot 10^2$	$2.7390(5)\cdot 10^3$
0.075	$1.40(2)\cdot 10^4$	$1.41(3)\cdot 10^3$	$-1.4(2)\cdot 10^1$	$-1.437(5)\cdot 10^4$	$-2.44(6)\cdot 10^2$	$2.3111(4)\cdot 10^3$
0.085	$1.37(2)\cdot 10^4$	$8.4(3)\cdot 10^2$	$-1.3(2)\cdot 10^1$	$-1.292(5)\cdot 10^4$	$-1.07(5)\cdot 10^2$	$1.9746(4)\cdot 10^3$
0.095	$1.33(2)\cdot 10^4$	$6.5(3)\cdot 10^2$	$-1.2(1)\cdot 10^1$	$-1.156(5)\cdot 10^4$	$-3.0(5)\cdot 10^1$	$1.7000(4)\cdot 10^3$
0.105	$1.26(2)\cdot 10^4$	$3.3(2)\cdot 10^2$	$-1.4(1)\cdot 10^1$	$-1.047(4)\cdot 10^4$	$2.2(5)\cdot 10^1$	$1.4749(4)\cdot 10^3$
0.115	$1.14(2)\cdot 10^4$	$1.8(2)\cdot 10^2$	$-9(1)\cdot 10^0$	$-9.47(4)\cdot 10^3$	$5.6(5)\cdot 10^1$	$1.2858(3)\cdot 10^3$
0.125	$1.08(2)\cdot 10^4$	$6(2)\cdot 10^1$	$-7(1)\cdot 10^0$	$-8.38(4)\cdot 10^3$	$9.5(4)\cdot 10^1$	$1.1265(3)\cdot 10^3$
0.135	$9.8(1)\cdot 10^3$	$-5(2)\cdot 10^1$	$-6(1)\cdot 10^0$	$-7.50(4)\cdot 10^3$	$1.02(4)\cdot 10^2$	$9.905(3)\cdot 10^2$
0.145	$8.6(1)\cdot 10^3$	$-1.2(2)\cdot 10^2$	$-5(1)\cdot 10^0$	$-6.70(4)\cdot 10^3$	$1.03(4)\cdot 10^2$	$8.725(3)\cdot 10^2$
0.155	$8.0(1)\cdot 10^3$	$-1.7(2)\cdot 10^2$	$-2.3(9)\cdot 10^0$	$-5.95(4)\cdot 10^3$	$1.24(4)\cdot 10^2$	$7.710(3)\cdot 10^2$
0.165	$7.0(1)\cdot 10^3$	$-1.5(2)\cdot 10^2$	$-3.8(8)\cdot 10^0$	$-5.25(3)\cdot 10^3$	$1.13(3)\cdot 10^2$	$6.831(3)\cdot 10^2$
0.175	$5.8(1)\cdot 10^3$	$-1.8(2)\cdot 10^2$	$-2(8)\cdot 10^{-1}$	$-4.67(3)\cdot 10^3$	$1.06(3)\cdot 10^2$	$6.068(3)\cdot 10^2$
0.185	$4.8(1)\cdot 10^3$	$-1.7(1)\cdot 10^2$	$-4(7)\cdot 10^{-1}$	$-4.09(3)\cdot 10^3$	$9.8(3)\cdot 10^1$	$5.386(2)\cdot 10^2$
0.195	$3.9(1)\cdot 10^3$	$-1.3(1)\cdot 10^2$	$-1.5(7)\cdot 10^0$	$-3.48(3)\cdot 10^3$	$8.3(3)\cdot 10^1$	$4.795(2)\cdot 10^2$
0.205	$3.2(1)\cdot 10^3$	$-1.2(1)\cdot 10^2$	$-2.1(6)\cdot 10^0$	$-3.00(3)\cdot 10^3$	$7.7(2)\cdot 10^1$	$4.269(2)\cdot 10^2$
0.215	$2.0(1)\cdot 10^3$	$-7(1)\cdot 10^1$	$-3(6)\cdot 10^{-1}$	$-2.46(3)\cdot 10^3$	$5.6(2)\cdot 10^1$	$3.790(2)\cdot 10^2$
0.225	$1.28(9)\cdot 10^3$	$-2(1)\cdot 10^1$	$-1.5(5)\cdot 10^0$	$-1.99(2)\cdot 10^3$	$4.1(2)\cdot 10^1$	$3.348(2)\cdot 10^2$
0.235	$6.2(9)\cdot 10^2$	$-2(1)\cdot 10^1$	$-5(5)\cdot 10^{-1}$	$-1.58(2)\cdot 10^3$	$2.3(2)\cdot 10^1$	$2.937(2)\cdot 10^2$
0.245	$-3.1(8)\cdot 10^2$	$3.8(9)\cdot 10^1$	$-8(4)\cdot 10^{-1}$	$-1.17(2)\cdot 10^3$	$1.3(1)\cdot 10^1$	$2.529(2)\cdot 10^2$
0.255	$-6.2(7)\cdot 10^2$	$6.3(8)\cdot 10^1$	$-9(3)\cdot 10^{-1}$	$-7.3(2)\cdot 10^2$	$-6(1)\cdot 10^0$	$2.123(2)\cdot 10^2$
0.265	$-1.11(6)\cdot 10^3$	$7.4(6)\cdot 10^1$	$4(3)\cdot 10^{-1}$	$-3.4(1)\cdot 10^2$	$-1.06(6)\cdot 10^1$	$1.678(2)\cdot 10^2$
0.275	$-1.23(4)\cdot 10^3$	$7.0(4)\cdot 10^1$	$8(2)\cdot 10^{-1}$	$-3(1)\cdot 10^1$	$-2.37(5)\cdot 10^1$	$1.136(1)\cdot 10^2$
0.285	$-4.1(2)\cdot 10^2$	$1.2(2)\cdot 10^1$	$1.5(6)\cdot 10^{-1}$	$-2.7(5)\cdot 10^1$	$-6.7(2)\cdot 10^0$	$2.952(8)\cdot 10^1$
0.295	$1.9(1)\cdot 10^1$	$-2.0(2)\cdot 10^0$	$-5.9(2)\cdot 10^{-2}$	$-3.17(4)\cdot 10^1$	$3(2)\cdot 10^{-5}$	$-5.73(1)\cdot 10^0$
0.305	$1.53(9)\cdot 10^0$	$-7(7)\cdot 10^{-5}$	$-1.31(8)\cdot 10^{-3}$	$-2(1)\cdot 10^{-3}$	$5(3)\cdot 10^{-12}$	$-1.13(1)\cdot 10^{-1}$
0.315	$1.9(6)\cdot 10^{-3}$	$4(3)\cdot 10^{-8}$	$-5(3)\cdot 10^{-10}$	$-9(9)\cdot 10^{-11}$	$9(5)\cdot 10^{-12}$	$-2.8(2)\cdot 10^{-3}$
0.325	$1.5(8)\cdot 10^{-2}$	$3(3)\cdot 10^{-4}$	$-3(3)\cdot 10^{-9}$	$-4(4)\cdot 10^{-4}$	0	$-7(3)\cdot 10^{-2}$
0.335	0	0	0	0	0	0

Table 14. Individual contributions from the different colour factors to $B_W \frac{dC_{B_W}}{dB_W}$ for the wide jet broadening distribution.

JHEP06(2009)041

B_T	N_c^2	N_c^0	N_c^{-2}	$N_f N_c$	N_f/N_c	N_f^2
0.005	$-2.9(7)\cdot 10^3$	$-3.2(1)\cdot 10^3$	$4.480(8)\cdot 10^3$	$9.64(2)\cdot 10^4$	$-2.592(2)\cdot 10^4$	$2.2742(2)\cdot 10^4$
0.015	$-5.33(5)\cdot 10^4$	$1.97(1)\cdot 10^4$	$-1.1(1)\cdot 10^2$	$-2.75(2)\cdot 10^4$	$-4.92(2)\cdot 10^3$	$1.01489(9)\cdot 10^4$
0.025	$-1.23(5)\cdot 10^4$	$1.32(1)\cdot 10^4$	$-3.8(1)\cdot 10^2$	$-3.34(2)\cdot 10^4$	$-1.69(2)\cdot 10^3$	$6.8099(7)\cdot 10^3$
0.035	$7.1(4)\cdot 10^3$	$9.3(1)\cdot 10^3$	$-3.83(9)\cdot 10^2$	$-3.31(2)\cdot 10^4$	$-4.4(2)\cdot 10^2$	$5.0819(6)\cdot 10^3$
0.045	$1.70(4)\cdot 10^4$	$6.2(1)\cdot 10^3$	$-3.46(8)\cdot 10^2$	$-3.08(2)\cdot 10^4$	$1.6(2)\cdot 10^2$	$3.9942(5)\cdot 10^3$
0.055	$2.26(4)\cdot 10^4$	$4.1(1)\cdot 10^3$	$-2.95(7)\cdot 10^2$	$-2.85(1)\cdot 10^4$	$4.6(2)\cdot 10^2$	$3.2413(5)\cdot 10^3$
0.065	$2.58(4)\cdot 10^4$	$2.92(9)\cdot 10^3$	$-2.57(6)\cdot 10^2$	$-2.59(1)\cdot 10^4$	$6.5(2)\cdot 10^2$	$2.6872(5)\cdot 10^3$
0.075	$2.65(4)\cdot 10^4$	$1.82(8)\cdot 10^3$	$-2.20(6)\cdot 10^2$	$-2.37(1)\cdot 10^4$	$7.4(1)\cdot 10^2$	$2.2583(5)\cdot 10^3$
0.085	$2.64(4)\cdot 10^4$	$8.8(7)\cdot 10^2$	$-1.81(5)\cdot 10^2$	$-2.16(1)\cdot 10^4$	$8.3(1)\cdot 10^2$	$1.9214(5)\cdot 10^3$
0.095	$2.69(3)\cdot 10^4$	$4.9(7)\cdot 10^2$	$-1.60(5)\cdot 10^2$	$-1.96(1)\cdot 10^4$	$8.3(1)\cdot 10^2$	$1.6464(5)\cdot 10^3$
0.105	$2.56(3)\cdot 10^4$	$-0(6)\cdot 10^0$	$-1.41(4)\cdot 10^2$	$-1.78(1)\cdot 10^4$	$8.3(1)\cdot 10^2$	$1.4206(5)\cdot 10^3$
0.115	$2.49(3)\cdot 10^4$	$-3.3(6)\cdot 10^2$	$-1.15(4)\cdot 10^2$	$-1.66(1)\cdot 10^4$	$8.3(1)\cdot 10^2$	$1.2309(5)\cdot 10^3$
0.125	$2.37(3)\cdot 10^4$	$-6.3(5)\cdot 10^2$	$-9.9(4)\cdot 10^1$	$-1.52(1)\cdot 10^4$	$8.0(1)\cdot 10^2$	$1.0699(5)\cdot 10^3$
0.135	$2.28(3)\cdot 10^4$	$-6.7(5)\cdot 10^2$	$-7.9(3)\cdot 10^1$	$-1.352(9)\cdot 10^4$	$7.8(1)\cdot 10^2$	$9.316(5)\cdot 10^2$
0.145	$2.09(3)\cdot 10^4$	$-8.3(5)\cdot 10^2$	$-7.3(3)\cdot 10^1$	$-1.251(9)\cdot 10^4$	$7.2(1)\cdot 10^2$	$8.118(5)\cdot 10^2$
0.155	$2.03(3)\cdot 10^4$	$-1.03(4)\cdot 10^3$	$-6.4(3)\cdot 10^1$	$-1.152(8)\cdot 10^4$	$7.1(1)\cdot 10^2$	$7.091(5)\cdot 10^2$
0.165	$1.90(2)\cdot 10^4$	$-1.03(4)\cdot 10^3$	$-5.6(3)\cdot 10^1$	$-1.045(8)\cdot 10^4$	$6.63(9)\cdot 10^2$	$6.171(6)\cdot 10^2$
0.175	$1.78(2)\cdot 10^4$	$-1.01(4)\cdot 10^3$	$-4.0(2)\cdot 10^1$	$-9.77(7)\cdot 10^3$	$6.30(8)\cdot 10^2$	$5.373(6)\cdot 10^2$
0.185	$1.64(2)\cdot 10^4$	$-1.12(4)\cdot 10^3$	$-3.5(2)\cdot 10^1$	$-8.74(7)\cdot 10^3$	$6.09(8)\cdot 10^2$	$4.632(6)\cdot 10^2$
0.195	$1.53(2)\cdot 10^4$	$-1.05(3)\cdot 10^3$	$-3.8(2)\cdot 10^1$	$-7.94(7)\cdot 10^3$	$5.50(7)\cdot 10^2$	$3.985(6)\cdot 10^2$
0.205	$1.46(2)\cdot 10^4$	$-1.09(3)\cdot 10^3$	$-2.6(2)\cdot 10^1$	$-7.42(7)\cdot 10^3$	$5.47(7)\cdot 10^2$	$3.382(7)\cdot 10^2$
0.215	$1.36(2)\cdot 10^4$	$-1.05(3)\cdot 10^3$	$-2.2(2)\cdot 10^1$	$-6.66(6)\cdot 10^3$	$4.95(6)\cdot 10^2$	$2.827(7)\cdot 10^2$
0.225	$1.26(2)\cdot 10^4$	$-9.4(3)\cdot 10^2$	$-2.4(2)\cdot 10^1$	$-6.12(6)\cdot 10^3$	$4.71(6)\cdot 10^2$	$2.304(7)\cdot 10^2$
0.235	$1.17(2)\cdot 10^4$	$-9.4(2)\cdot 10^2$	$-1.6(1)\cdot 10^1$	$-5.66(6)\cdot 10^3$	$4.34(5)\cdot 10^2$	$1.774(7)\cdot 10^2$
0.245	$1.09(2)\cdot 10^4$	$-9.2(2)\cdot 10^2$	$-1.4(1)\cdot 10^1$	$-5.12(5)\cdot 10^3$	$4.11(5)\cdot 10^2$	$1.263(7)\cdot 10^2$
0.255	$1.02(1)\cdot 10^4$	$-8.4(2)\cdot 10^2$	$-1.3(1)\cdot 10^1$	$-4.76(5)\cdot 10^3$	$3.80(4)\cdot 10^2$	$7.01(7)\cdot 10^1$
0.265	$9.7(1)\cdot 10^3$	$-8.1(2)\cdot 10^2$	$-1.12(9)\cdot 10^1$	$-4.47(4)\cdot 10^3$	$3.58(3)\cdot 10^2$	$7.7(6)\cdot 10^0$
0.275	$9.4(1)\cdot 10^3$	$-7.2(1)\cdot 10^2$	$-1.09(7)\cdot 10^1$	$-4.24(3)\cdot 10^3$	$3.46(3)\cdot 10^2$	$-6.79(6)\cdot 10^1$
0.285	$9.11(7)\cdot 10^3$	$-6.12(9)\cdot 10^2$	$-1.28(5)\cdot 10^1$	$-4.17(2)\cdot 10^3$	$3.43(2)\cdot 10^2$	$-1.722(4)\cdot 10^2$
0.295	$8.52(4)\cdot 10^3$	$-6.91(5)\cdot 10^2$	$-8(3)\cdot 10^{-1}$	$-2.77(1)\cdot 10^3$	$2.35(1)\cdot 10^2$	$-1.570(2)\cdot 10^2$
0.305	$6.26(3)\cdot 10^3$	$-5.47(3)\cdot 10^2$	$2.3(2)\cdot 10^0$	$-1.741(9)\cdot 10^3$	$8.57(6)\cdot 10^1$	$-1.046(1)\cdot 10^2$
0.315	$4.55(2)\cdot 10^3$	$-4.14(3)\cdot 10^2$	$1.9(1)\cdot 10^0$	$-1.215(7)\cdot 10^3$	$3.32(3)\cdot 10^1$	$-7.413(9)\cdot 10^1$
0.325	$3.24(2)\cdot 10^3$	$-3.03(2)\cdot 10^2$	$1.5(1)\cdot 10^0$	$-8.52(5)\cdot 10^2$	$3.42(8)\cdot 10^0$	$-5.275(6)\cdot 10^1$
0.335	$2.24(1)\cdot 10^3$	$-2.20(2)\cdot 10^2$	$1.03(7)\cdot 10^0$	$-5.65(3)\cdot 10^2$	$1.99(5)\cdot 10^0$	$-3.615(5)\cdot 10^1$
0.345	$1.337(9)\cdot 10^3$	$-1.36(1)\cdot 10^2$	$4.5(4)\cdot 10^{-1}$	$-3.23(2)\cdot 10^2$	$7.7(3)\cdot 10^{-1}$	$-2.237(3)\cdot 10^1$
0.355	$6.37(5)\cdot 10^2$	$-6.24(6)\cdot 10^1$	$8(4)\cdot 10^{-3}$	$-1.470(9)\cdot 10^2$	$2.5(1)\cdot 10^{-1}$	$-1.226(2)\cdot 10^1$
0.365	$2.81(3)\cdot 10^2$	$-2.50(3)\cdot 10^1$	$-1.3(3)\cdot 10^{-2}$	$-6.80(4)\cdot 10^1$	$1.2(2)\cdot 10^{-2}$	$-6.38(2)\cdot 10^0$
0.375	$1.01(1)\cdot 10^2$	$-3.0(3)\cdot 10^{-1}$	$-1.6(1)\cdot 10^{-2}$	$-2.75(2)\cdot 10^1$	$7(6)\cdot 10^{-12}$	$-2.90(1)\cdot 10^0$
0.385	$4.7(1)\cdot 10^0$	$-3.8(2)\cdot 10^{-1}$	$-2.2(4)\cdot 10^{-4}$	$-2.0(1)\cdot 10^{-1}$	$9(6)\cdot 10^{-14}$	$-1.80(2)\cdot 10^{-1}$
0.395	$1.0(1)\cdot 10^{-1}$	$4(4)\cdot 10^{-8}$	$-2(2)\cdot 10^{-9}$	$-2(1)\cdot 10^{-7}$	$1.4(8)\cdot 10^{-12}$	$-1.17(5)\cdot 10^{-2}$
0.405	$-1.3(6)\cdot 10^{-5}$	$9(6)\cdot 10^{-10}$	$-3(1)\cdot 10^{-12}$	$-1(1)\cdot 10^{-10}$	$3(2)\cdot 10^{-4}$	$-7.38(4)\cdot 10^{-2}$
0.415	0	0	0	0	0	0

Table 15. Individual contributions from the different colour factors to $B_T \frac{dC_{B_T}}{dB_T}$ for the total jet broadening distribution.

JHEP06(2009)041

C	N_c^2	N_c^0	N_c^{-2}	$N_f N_c$	N_f/N_c	N_f^2
0.005	$-2.82(3)\cdot 10^4$	$4.28(9)\cdot 10^3$	$2.583(6)\cdot 10^3$	$5.10(1)\cdot 10^4$	$-1.578(1)\cdot 10^4$	$1.6764(2)\cdot 10^4$
0.015	$-3.60(3)\cdot 10^4$	$1.22(1)\cdot 10^4$	$4.7(1)\cdot 10^2$	$-1.04(2)\cdot 10^4$	$-5.45(2)\cdot 10^3$	$8.808(1)\cdot 10^3$
0.025	$-1.76(4)\cdot 10^4$	$9.8(1)\cdot 10^3$	$1.6(1)\cdot 10^2$	$-1.73(2)\cdot 10^4$	$-3.27(2)\cdot 10^3$	$6.697(1)\cdot 10^3$
0.035	$-7.3(4)\cdot 10^3$	$8.6(1)\cdot 10^3$	$2(1)\cdot 10^1$	$-1.94(2)\cdot 10^4$	$-2.23(2)\cdot 10^3$	$5.522(1)\cdot 10^3$
0.045	$-1.0(4)\cdot 10^3$	$6.6(1)\cdot 10^3$	$-6(1)\cdot 10^1$	$-1.99(2)\cdot 10^4$	$-1.59(2)\cdot 10^3$	$4.7388(9)\cdot 10^3$
0.055	$4.2(4)\cdot 10^3$	$5.8(1)\cdot 10^3$	$-6(1)\cdot 10^1$	$-2.05(2)\cdot 10^4$	$-1.16(2)\cdot 10^3$	$4.1679(9)\cdot 10^3$
0.065	$6.8(4)\cdot 10^3$	$5.2(1)\cdot 10^3$	$-9(1)\cdot 10^1$	$-2.01(2)\cdot 10^4$	$-8.3(2)\cdot 10^2$	$3.7300(9)\cdot 10^3$
0.075	$9.4(4)\cdot 10^3$	$4.3(1)\cdot 10^3$	$-1.1(1)\cdot 10^2$	$-1.91(2)\cdot 10^4$	$-6.2(2)\cdot 10^2$	$3.3755(9)\cdot 10^3$
0.085	$1.12(5)\cdot 10^4$	$3.6(1)\cdot 10^3$	$-9(1)\cdot 10^1$	$-1.89(2)\cdot 10^4$	$-4.3(2)\cdot 10^2$	$3.0855(9)\cdot 10^3$
0.095	$1.20(5)\cdot 10^4$	$3.3(1)\cdot 10^3$	$-1.1(1)\cdot 10^2$	$-1.85(2)\cdot 10^4$	$-3.1(2)\cdot 10^2$	$2.8420(8)\cdot 10^3$
0.105	$1.44(5)\cdot 10^4$	$2.6(1)\cdot 10^3$	$-1.1(1)\cdot 10^2$	$-1.78(2)\cdot 10^4$	$-1.7(2)\cdot 10^2$	$2.6327(8)\cdot 10^3$
0.115	$1.42(5)\cdot 10^4$	$2.6(1)\cdot 10^3$	$-9(1)\cdot 10^1$	$-1.77(1)\cdot 10^4$	$-7(2)\cdot 10^1$	$2.4504(8)\cdot 10^3$
0.125	$1.45(5)\cdot 10^4$	$2.1(1)\cdot 10^3$	$-1.1(1)\cdot 10^2$	$-1.70(1)\cdot 10^4$	$-3(2)\cdot 10^1$	$2.2893(8)\cdot 10^3$
0.135	$1.59(5)\cdot 10^4$	$1.9(1)\cdot 10^3$	$-1.1(1)\cdot 10^2$	$-1.66(1)\cdot 10^4$	$7(2)\cdot 10^1$	$2.1488(8)\cdot 10^3$
0.145	$1.62(5)\cdot 10^4$	$1.7(1)\cdot 10^3$	$-6(1)\cdot 10^1$	$-1.63(1)\cdot 10^4$	$8(2)\cdot 10^1$	$2.0234(8)\cdot 10^3$
0.155	$1.65(5)\cdot 10^4$	$1.4(1)\cdot 10^3$	$-9(1)\cdot 10^1$	$-1.56(1)\cdot 10^4$	$1.3(2)\cdot 10^2$	$1.9086(8)\cdot 10^3$
0.165	$1.65(5)\cdot 10^4$	$1.2(1)\cdot 10^3$	$-9.2(9)\cdot 10^1$	$-1.54(1)\cdot 10^4$	$1.8(2)\cdot 10^2$	$1.8064(8)\cdot 10^3$
0.175	$1.67(5)\cdot 10^4$	$1.0(1)\cdot 10^3$	$-9.0(9)\cdot 10^1$	$-1.48(1)\cdot 10^4$	$2.2(2)\cdot 10^2$	$1.7110(8)\cdot 10^3$
0.185	$1.70(5)\cdot 10^4$	$8(1)\cdot 10^2$	$-6.0(9)\cdot 10^1$	$-1.42(1)\cdot 10^4$	$2.8(2)\cdot 10^2$	$1.6272(8)\cdot 10^3$
0.195	$1.63(5)\cdot 10^4$	$6(1)\cdot 10^2$	$-5.6(9)\cdot 10^1$	$-1.43(1)\cdot 10^4$	$2.7(2)\cdot 10^2$	$1.5478(8)\cdot 10^3$
0.205	$1.67(5)\cdot 10^4$	$6(1)\cdot 10^2$	$-6.4(9)\cdot 10^1$	$-1.36(1)\cdot 10^4$	$3.2(2)\cdot 10^2$	$1.4751(8)\cdot 10^3$
0.215	$1.72(5)\cdot 10^4$	$4(1)\cdot 10^2$	$-7.1(8)\cdot 10^1$	$-1.34(1)\cdot 10^4$	$3.0(2)\cdot 10^2$	$1.4074(8)\cdot 10^3$
0.225	$1.68(5)\cdot 10^4$	$3(1)\cdot 10^2$	$-5.1(8)\cdot 10^1$	$-1.29(1)\cdot 10^4$	$3.5(2)\cdot 10^2$	$1.3450(8)\cdot 10^3$
0.235	$1.72(5)\cdot 10^4$	$1(1)\cdot 10^2$	$-4.1(8)\cdot 10^1$	$-1.26(1)\cdot 10^4$	$3.4(2)\cdot 10^2$	$1.2865(8)\cdot 10^3$
0.245	$1.71(5)\cdot 10^4$	$2(1)\cdot 10^2$	$-7.2(8)\cdot 10^1$	$-1.21(1)\cdot 10^4$	$3.2(2)\cdot 10^2$	$1.2336(8)\cdot 10^3$
0.255	$1.70(5)\cdot 10^4$	$-6(9)\cdot 10^1$	$-4.3(7)\cdot 10^1$	$-1.22(1)\cdot 10^4$	$3.9(2)\cdot 10^2$	$1.1829(8)\cdot 10^3$
0.265	$1.65(5)\cdot 10^4$	$-1(9)\cdot 10^1$	$-5.1(8)\cdot 10^1$	$-1.17(1)\cdot 10^4$	$3.7(2)\cdot 10^2$	$1.1354(8)\cdot 10^3$
0.275	$1.67(5)\cdot 10^4$	$-3(9)\cdot 10^1$	$-4.3(7)\cdot 10^1$	$-1.15(1)\cdot 10^4$	$3.7(2)\cdot 10^2$	$1.0907(8)\cdot 10^3$
0.285	$1.59(5)\cdot 10^4$	$-2.8(9)\cdot 10^2$	$-4.3(7)\cdot 10^1$	$-1.11(1)\cdot 10^4$	$3.6(2)\cdot 10^2$	$1.0482(8)\cdot 10^3$
0.295	$1.65(5)\cdot 10^4$	$-2.4(9)\cdot 10^2$	$-3.1(7)\cdot 10^1$	$-1.08(1)\cdot 10^4$	$3.8(2)\cdot 10^2$	$1.0099(8)\cdot 10^3$
0.305	$1.61(5)\cdot 10^4$	$-2.2(9)\cdot 10^2$	$-4.3(7)\cdot 10^1$	$-1.07(1)\cdot 10^4$	$3.7(2)\cdot 10^2$	$9.723(8)\cdot 10^2$
0.315	$1.63(5)\cdot 10^4$	$-3.6(9)\cdot 10^2$	$-2.9(7)\cdot 10^1$	$-1.04(1)\cdot 10^4$	$3.9(2)\cdot 10^2$	$9.347(8)\cdot 10^2$
0.325	$1.55(5)\cdot 10^4$	$-3.9(9)\cdot 10^2$	$-3.1(7)\cdot 10^1$	$-9.8(1)\cdot 10^3$	$3.8(2)\cdot 10^2$	$9.033(8)\cdot 10^2$
0.335	$1.53(5)\cdot 10^4$	$-3.1(8)\cdot 10^2$	$-1.7(7)\cdot 10^1$	$-9.9(1)\cdot 10^3$	$3.9(2)\cdot 10^2$	$8.704(8)\cdot 10^2$
0.345	$1.51(5)\cdot 10^4$	$-4.2(8)\cdot 10^2$	$-2.8(7)\cdot 10^1$	$-9.8(1)\cdot 10^3$	$3.9(2)\cdot 10^2$	$8.412(8)\cdot 10^2$
0.355	$1.48(5)\cdot 10^4$	$-4.6(8)\cdot 10^2$	$-2.7(6)\cdot 10^1$	$-9.3(1)\cdot 10^3$	$3.8(2)\cdot 10^2$	$8.126(8)\cdot 10^2$
0.365	$1.50(4)\cdot 10^4$	$-5.7(8)\cdot 10^2$	$-2.7(6)\cdot 10^1$	$-9.2(1)\cdot 10^3$	$3.9(2)\cdot 10^2$	$7.836(8)\cdot 10^2$
0.375	$1.54(4)\cdot 10^4$	$-5.2(8)\cdot 10^2$	$-1.8(6)\cdot 10^1$	$-9.0(1)\cdot 10^3$	$4.0(2)\cdot 10^2$	$7.592(8)\cdot 10^2$
0.385	$1.44(4)\cdot 10^4$	$-5.3(8)\cdot 10^2$	$-2.0(6)\cdot 10^1$	$-8.6(1)\cdot 10^3$	$3.9(2)\cdot 10^2$	$7.343(8)\cdot 10^2$
0.395	$1.44(4)\cdot 10^4$	$-5.8(8)\cdot 10^2$	$-2.5(6)\cdot 10^1$	$-8.8(1)\cdot 10^3$	$3.9(2)\cdot 10^2$	$7.092(8)\cdot 10^2$
0.405	$1.40(4)\cdot 10^4$	$-5.6(8)\cdot 10^2$	$-1.1(6)\cdot 10^1$	$-8.3(1)\cdot 10^3$	$3.8(1)\cdot 10^2$	$6.859(8)\cdot 10^2$
0.415	$1.48(4)\cdot 10^4$	$-6.8(7)\cdot 10^2$	$-1.3(6)\cdot 10^1$	$-8.1(1)\cdot 10^3$	$3.3(1)\cdot 10^2$	$6.657(8)\cdot 10^2$
0.425	$1.34(4)\cdot 10^4$	$-6.5(7)\cdot 10^2$	$-2.2(5)\cdot 10^1$	$-7.9(1)\cdot 10^3$	$3.8(1)\cdot 10^2$	$6.445(8)\cdot 10^2$
0.435	$1.35(4)\cdot 10^4$	$-6.6(7)\cdot 10^2$	$-1.4(5)\cdot 10^1$	$-7.8(1)\cdot 10^3$	$4.0(1)\cdot 10^2$	$6.234(8)\cdot 10^2$
0.445	$1.35(4)\cdot 10^4$	$-6.5(7)\cdot 10^2$	$-2.6(5)\cdot 10^1$	$-7.6(1)\cdot 10^3$	$3.5(1)\cdot 10^2$	$6.052(8)\cdot 10^2$
0.455	$1.36(4)\cdot 10^4$	$-9.0(7)\cdot 10^2$	$-6(5)\cdot 10^0$	$-7.6(1)\cdot 10^3$	$3.6(1)\cdot 10^2$	$5.859(8)\cdot 10^2$
0.465	$1.33(4)\cdot 10^4$	$-6.2(7)\cdot 10^2$	$-1.3(5)\cdot 10^1$	$-7.1(1)\cdot 10^3$	$3.9(1)\cdot 10^2$	$5.683(8)\cdot 10^2$
0.475	$1.27(4)\cdot 10^4$	$-6.7(7)\cdot 10^2$	$-1.1(5)\cdot 10^1$	$-7.3(1)\cdot 10^3$	$3.7(1)\cdot 10^2$	$5.506(8)\cdot 10^2$
0.485	$1.27(4)\cdot 10^4$	$-8.4(7)\cdot 10^2$	$-1.2(5)\cdot 10^1$	$-6.8(1)\cdot 10^3$	$3.6(1)\cdot 10^2$	$5.366(8)\cdot 10^2$
0.495	$1.26(4)\cdot 10^4$	$-7.0(7)\cdot 10^2$	$-1.3(5)\cdot 10^1$	$-6.9(1)\cdot 10^3$	$3.4(1)\cdot 10^2$	$5.190(8)\cdot 10^2$

Table 16. Individual contributions from the different colour factors to $\rho\frac{dC_C}{dC}$ for the C parameter distribution.

JHEP06(2009)041

C	N_c^2	N_c^0	N_c^{-2}	$N_f N_c$	N_f/N_c	N_f^2
0.505	$1.24(4)\cdot 10^4$	$-8.6(7)\cdot 10^2$	$-4(5)\cdot 10^0$	$-6.6(1)\cdot 10^3$	$3.6(1)\cdot 10^2$	$5.051(8)\cdot 10^2$
0.515	$1.20(4)\cdot 10^4$	$-6.7(6)\cdot 10^2$	$-9(4)\cdot 10^0$	$-6.7(1)\cdot 10^3$	$3.8(1)\cdot 10^2$	$4.909(8)\cdot 10^2$
0.525	$1.24(4)\cdot 10^4$	$-7.0(6)\cdot 10^2$	$-5(4)\cdot 10^0$	$-6.4(1)\cdot 10^3$	$3.4(1)\cdot 10^2$	$4.762(8)\cdot 10^2$
0.535	$1.13(4)\cdot 10^4$	$-8.5(6)\cdot 10^2$	$-1.5(4)\cdot 10^1$	$-6.2(1)\cdot 10^3$	$3.5(1)\cdot 10^2$	$4.619(8)\cdot 10^2$
0.545	$1.15(4)\cdot 10^4$	$-7.3(6)\cdot 10^2$	$-6(4)\cdot 10^0$	$-6.1(1)\cdot 10^3$	$3.3(1)\cdot 10^2$	$4.473(8)\cdot 10^2$
0.555	$1.16(4)\cdot 10^4$	$-7.9(6)\cdot 10^2$	$-4(4)\cdot 10^0$	$-5.9(1)\cdot 10^3$	$3.2(1)\cdot 10^2$	$4.370(8)\cdot 10^2$
0.565	$1.16(4)\cdot 10^4$	$-7.6(6)\cdot 10^2$	$-7(4)\cdot 10^0$	$-5.9(1)\cdot 10^3$	$3.5(1)\cdot 10^2$	$4.225(8)\cdot 10^2$
0.575	$1.14(4)\cdot 10^4$	$-8.3(6)\cdot 10^2$	$-6(4)\cdot 10^0$	$-5.7(1)\cdot 10^3$	$3.3(1)\cdot 10^2$	$4.109(8)\cdot 10^2$
0.585	$1.09(4)\cdot 10^4$	$-7.6(6)\cdot 10^2$	$-4(4)\cdot 10^0$	$-5.5(1)\cdot 10^3$	$3.4(1)\cdot 10^2$	$3.997(8)\cdot 10^2$
0.595	$1.07(4)\cdot 10^4$	$-8.1(6)\cdot 10^2$	$1(3)\cdot 10^0$	$-5.4(1)\cdot 10^3$	$3.2(1)\cdot 10^2$	$3.885(8)\cdot 10^2$
0.605	$1.04(4)\cdot 10^4$	$-7.4(6)\cdot 10^2$	$-5(3)\cdot 10^0$	$-5.4(1)\cdot 10^3$	$3.3(1)\cdot 10^2$	$3.794(8)\cdot 10^2$
0.615	$1.08(4)\cdot 10^4$	$-7.7(5)\cdot 10^2$	$2(3)\cdot 10^0$	$-5.5(1)\cdot 10^3$	$3.2(1)\cdot 10^2$	$3.680(8)\cdot 10^2$
0.625	$9.8(4)\cdot 10^3$	$-8.3(5)\cdot 10^2$	$-2(3)\cdot 10^0$	$-5.0(1)\cdot 10^3$	$3.0(1)\cdot 10^2$	$3.573(9)\cdot 10^2$
0.635	$1.02(4)\cdot 10^4$	$-7.3(5)\cdot 10^2$	$3(3)\cdot 10^0$	$-5.0(1)\cdot 10^3$	$3.1(1)\cdot 10^2$	$3.484(9)\cdot 10^2$
0.645	$1.01(4)\cdot 10^4$	$-8.0(5)\cdot 10^2$	$-2(3)\cdot 10^0$	$-4.9(1)\cdot 10^3$	$3.1(1)\cdot 10^2$	$3.392(9)\cdot 10^2$
0.655	$9.4(4)\cdot 10^3$	$-7.8(5)\cdot 10^2$	$-5(3)\cdot 10^0$	$-4.9(1)\cdot 10^3$	$2.65(9)\cdot 10^2$	$3.293(9)\cdot 10^2$
0.665	$1.00(4)\cdot 10^4$	$-7.5(5)\cdot 10^2$	$0(3)\cdot 10^{-1}$	$-4.9(1)\cdot 10^3$	$2.91(9)\cdot 10^2$	$3.182(9)\cdot 10^2$
0.675	$9.6(3)\cdot 10^3$	$-8.4(5)\cdot 10^2$	$-3(3)\cdot 10^0$	$-4.7(1)\cdot 10^3$	$3.18(9)\cdot 10^2$	$3.132(9)\cdot 10^2$
0.685	$9.7(3)\cdot 10^3$	$-7.3(5)\cdot 10^2$	$1.0(3)\cdot 10^1$	$-4.4(1)\cdot 10^3$	$2.80(9)\cdot 10^2$	$3.012(9)\cdot 10^2$
0.695	$9.2(3)\cdot 10^3$	$-7.7(5)\cdot 10^2$	$2(3)\cdot 10^0$	$-4.5(1)\cdot 10^3$	$2.12(7)\cdot 10^2$	$2.947(9)\cdot 10^2$
0.705	$8.8(3)\cdot 10^3$	$-7.4(5)\cdot 10^2$	$-1(2)\cdot 10^0$	$-4.4(1)\cdot 10^3$	$2.75(9)\cdot 10^2$	$2.852(9)\cdot 10^2$
0.715	$8.3(3)\cdot 10^3$	$-7.8(4)\cdot 10^2$	$2(2)\cdot 10^0$	$-4.2(1)\cdot 10^3$	$2.86(8)\cdot 10^2$	$2.78(1)\cdot 10^2$
0.725	$8.9(3)\cdot 10^3$	$-7.7(4)\cdot 10^2$	$6(2)\cdot 10^0$	$-4.2(1)\cdot 10^3$	$2.71(8)\cdot 10^2$	$2.70(1)\cdot 10^2$
0.735	$8.9(3)\cdot 10^3$	$-7.9(4)\cdot 10^2$	$3(2)\cdot 10^0$	$-4.3(1)\cdot 10^3$	$2.56(7)\cdot 10^2$	$2.65(1)\cdot 10^2$
0.745	$7.8(3)\cdot 10^3$	$-7.2(4)\cdot 10^2$	$5(2)\cdot 10^0$	$-4.4(1)\cdot 10^3$	$2.57(7)\cdot 10^2$	$2.54(1)\cdot 10^2$
0.755	$2.43(2)\cdot 10^4$	$-6.2(3)\cdot 10^2$	$-5.2(1)\cdot 10^1$	$-1.106(7)\cdot 10^4$	$8.14(5)\cdot 10^2$	$-6.780(8)\cdot 10^2$
0.765	$1.97(1)\cdot 10^4$	$-1.58(1)\cdot 10^3$	$1.06(7)\cdot 10^1$	$-4.36(3)\cdot 10^3$	$3.55(2)\cdot 10^2$	$-3.520(3)\cdot 10^2$
0.775	$1.418(8)\cdot 10^4$	$-1.25(1)\cdot 10^3$	$1.53(6)\cdot 10^1$	$-2.78(2)\cdot 10^3$	$7.40(9)\cdot 10^1$	$-2.490(2)\cdot 10^2$
0.785	$1.072(7)\cdot 10^4$	$-9.93(9)\cdot 10^2$	$1.01(4)\cdot 10^1$	$-2.00(2)\cdot 10^3$	$1.17(1)\cdot 10^2$	$-1.892(2)\cdot 10^2$
0.795	$8.53(6)\cdot 10^3$	$-8.09(7)\cdot 10^2$	$1.07(4)\cdot 10^1$	$-1.52(2)\cdot 10^3$	$1.066(8)\cdot 10^2$	$-1.488(2)\cdot 10^2$
0.805	$6.68(5)\cdot 10^3$	$-6.86(6)\cdot 10^2$	$8.7(3)\cdot 10^0$	$-1.22(1)\cdot 10^3$	$3.4(4)\cdot 10^{-1}$	$-1.191(1)\cdot 10^2$
0.815	$5.09(4)\cdot 10^3$	$-5.56(5)\cdot 10^2$	$6.7(3)\cdot 10^0$	$-9.6(1)\cdot 10^2$	$1.16(7)\cdot 10^0$	$-9.65(1)\cdot 10^1$
0.825	$4.34(4)\cdot 10^3$	$-4.54(5)\cdot 10^2$	$4.7(2)\cdot 10^0$	$-7.91(8)\cdot 10^2$	$7(1)\cdot 10^{-2}$	$-7.87(1)\cdot 10^1$
0.835	$3.52(3)\cdot 10^3$	$-3.59(4)\cdot 10^2$	$2.4(1)\cdot 10^0$	$-6.45(6)\cdot 10^2$	$4.62(4)\cdot 10^1$	$-6.448(9)\cdot 10^1$
0.845	$2.84(3)\cdot 10^3$	$-3.15(3)\cdot 10^2$	$2.3(1)\cdot 10^0$	$-5.48(5)\cdot 10^2$	$6.3(1)\cdot 10^0$	$-5.297(8)\cdot 10^1$
0.855	$1.56(2)\cdot 10^3$	$-2.58(3)\cdot 10^2$	$1.22(9)\cdot 10^0$	$-4.50(4)\cdot 10^2$	$1.32(2)\cdot 10^1$	$-4.356(7)\cdot 10^1$
0.865	$1.87(2)\cdot 10^3$	$-2.09(3)\cdot 10^2$	$3.7(5)\cdot 10^{-1}$	$-3.65(3)\cdot 10^2$	$7.6(4)\cdot 10^{-1}$	$-3.551(6)\cdot 10^1$
0.875	$1.39(2)\cdot 10^3$	$-1.38(2)\cdot 10^2$	$2.6(4)\cdot 10^{-1}$	$-2.88(3)\cdot 10^2$	$3.63(7)\cdot 10^0$	$-2.904(6)\cdot 10^1$
0.885	$1.02(1)\cdot 10^3$	$-9.7(2)\cdot 10^1$	$2.1(4)\cdot 10^{-1}$	$-2.18(2)\cdot 10^2$	$2(1)\cdot 10^{-3}$	$-2.343(5)\cdot 10^1$
0.895	$8.6(1)\cdot 10^2$	$-7.7(1)\cdot 10^1$	$1.7(3)\cdot 10^{-1}$	$-1.74(2)\cdot 10^2$	$2(3)\cdot 10^{-4}$	$-1.880(4)\cdot 10^1$
0.905	$6.78(9)\cdot 10^2$	$-6.1(1)\cdot 10^1$	$0(2)\cdot 10^{-3}$	$-1.45(1)\cdot 10^2$	$2(2)\cdot 10^{-5}$	$-1.481(4)\cdot 10^1$
0.915	$5.05(7)\cdot 10^2$	$-3.33(7)\cdot 10^1$	$-1(1)\cdot 10^{-2}$	$-1.106(9)\cdot 10^2$	$2(1)\cdot 10^{-4}$	$-1.149(3)\cdot 10^1$
0.925	$3.26(5)\cdot 10^2$	$-2.13(5)\cdot 10^1$	$-8(5)\cdot 10^{-4}$	$-7.68(7)\cdot 10^1$	$1(1)\cdot 10^{-9}$	$-8.68(3)\cdot 10^0$
0.935	$7.3(2)\cdot 10^1$	$-6.2(7)\cdot 10^{-1}$	$-1.3(2)\cdot 10^{-2}$	$-5.62(5)\cdot 10^1$	$2(1)\cdot 10^{-11}$	$-6.18(2)\cdot 10^0$
0.945	$1.40(2)\cdot 10^2$	$-4.8(2)\cdot 10^0$	$-1.1(1)\cdot 10^{-2}$	$-2.99(3)\cdot 10^1$	$2(1)\cdot 10^{-9}$	$-4.22(2)\cdot 10^0$
0.955	$3.19(8)\cdot 10^1$	$-8.8(7)\cdot 10^{-1}$	$-3.7(5)\cdot 10^{-3}$	$-2.60(9)\cdot 10^0$	$1.3(9)\cdot 10^{-11}$	$-2.51(1)\cdot 10^0$
0.965	$2.28(5)\cdot 10^1$	$-1.6(6)\cdot 10^{-2}$	$-2(2)\cdot 10^{-5}$	$-1(1)\cdot 10^{-6}$	$1.7(9)\cdot 10^{-11}$	$-1.98(4)\cdot 10^{-1}$
0.975	$4.0(1)\cdot 10^0$	$1(1)\cdot 10^{-4}$	$-1.05(9)\cdot 10^{-3}$	$-6(2)\cdot 10^{-3}$	$3(1)\cdot 10^{-13}$	$-1.22(3)\cdot 10^{-1}$
0.985	$1(1)\cdot 10^{-4}$	$1(1)\cdot 10^{-7}$	$2(2)\cdot 10^{-10}$	$-8(7)\cdot 10^{-9}$	$1(1)\cdot 10^{-12}$	$-4.88684(2)\cdot 10^{-1}$
0.995	$-2(1)\cdot 10^{-5}$	$1(1)\cdot 10^{-11}$	$-2(3)\cdot 10^{-10}$	$-2(2)\cdot 10^{-12}$	$6(4)\cdot 10^{-9}$	$-1.443(2)\cdot 10^{-1}$

Table 17. Individual contributions from the different colour factors to $\rho\frac{dC_C}{dC}$ for the C parameter distribution.

JHEP06(2009)041

$\ln y_{23}$	N_c^2	N_c^0	N_c^{-2}	$N_f N_c$	N_f/N_c	N_f^2
-9.875	$-2.6(1)\cdot 10^4$	$3.1(2)\cdot 10^3$	$1.426(9)\cdot 10^3$	$1.89(3)\cdot 10^4$	$-8.30(2)\cdot 10^3$	$8.762(3)\cdot 10^3$
-9.625	$-2.63(9)\cdot 10^4$	$3.7(2)\cdot 10^3$	$1.208(8)\cdot 10^3$	$1.49(3)\cdot 10^4$	$-7.51(2)\cdot 10^3$	$8.164(2)\cdot 10^3$
-9.375	$-2.44(8)\cdot 10^4$	$3.9(1)\cdot 10^3$	$1.046(7)\cdot 10^3$	$1.19(3)\cdot 10^4$	$-6.74(2)\cdot 10^3$	$7.594(2)\cdot 10^3$
-9.125	$-2.34(7)\cdot 10^4$	$4.7(1)\cdot 10^3$	$9.18(7)\cdot 10^2$	$8.2(2)\cdot 10^3$	$-6.04(1)\cdot 10^3$	$7.048(2)\cdot 10^3$
-8.875	$-2.04(7)\cdot 10^4$	$4.7(1)\cdot 10^3$	$7.41(6)\cdot 10^2$	$5.2(2)\cdot 10^3$	$-5.40(1)\cdot 10^3$	$6.535(2)\cdot 10^3$
-8.625	$-1.94(6)\cdot 10^4$	$4.9(1)\cdot 10^3$	$6.49(5)\cdot 10^2$	$3.2(2)\cdot 10^3$	$-4.79(1)\cdot 10^3$	$6.040(2)\cdot 10^3$
-8.375	$-1.70(6)\cdot 10^4$	$4.7(1)\cdot 10^3$	$5.33(5)\cdot 10^2$	$5(2)\cdot 10^2$	$-4.25(1)\cdot 10^3$	$5.578(1)\cdot 10^3$
-8.125	$-1.41(5)\cdot 10^4$	$4.85(9)\cdot 10^3$	$4.52(4)\cdot 10^2$	$-1.1(2)\cdot 10^3$	$-3.73(1)\cdot 10^3$	$5.137(1)\cdot 10^3$
-7.875	$-1.26(5)\cdot 10^4$	$4.53(8)\cdot 10^3$	$3.68(4)\cdot 10^2$	$-2.8(1)\cdot 10^3$	$-3.268(9)\cdot 10^3$	$4.719(1)\cdot 10^3$
-7.625	$-1.03(4)\cdot 10^4$	$4.56(7)\cdot 10^3$	$3.06(3)\cdot 10^2$	$-4.1(1)\cdot 10^3$	$-2.829(8)\cdot 10^3$	$4.329(1)\cdot 10^3$
-7.375	$-8.9(4)\cdot 10^3$	$4.09(7)\cdot 10^3$	$2.33(3)\cdot 10^2$	$-5.0(1)\cdot 10^3$	$-2.434(8)\cdot 10^3$	$3.9575(9)\cdot 10^3$
-7.125	$-6.0(4)\cdot 10^3$	$3.85(6)\cdot 10^3$	$1.94(3)\cdot 10^2$	$-5.8(1)\cdot 10^3$	$-2.096(7)\cdot 10^3$	$3.6097(8)\cdot 10^3$
-6.875	$-4.5(3)\cdot 10^3$	$3.50(5)\cdot 10^3$	$1.51(2)\cdot 10^2$	$-6.56(9)\cdot 10^3$	$-1.783(6)\cdot 10^3$	$3.2822(7)\cdot 10^3$
-6.625	$-3.1(3)\cdot 10^3$	$3.19(5)\cdot 10^3$	$1.15(2)\cdot 10^2$	$-6.88(8)\cdot 10^3$	$-1.501(5)\cdot 10^3$	$2.9761(6)\cdot 10^3$
-6.375	$-1.4(3)\cdot 10^3$	$2.89(4)\cdot 10^3$	$8.4(2)\cdot 10^1$	$-7.13(7)\cdot 10^3$	$-1.261(5)\cdot 10^3$	$2.6907(6)\cdot 10^3$
-6.125	$-1(2)\cdot 10^2$	$2.47(4)\cdot 10^3$	$6.6(2)\cdot 10^1$	$-7.28(7)\cdot 10^3$	$-1.052(4)\cdot 10^3$	$2.4229(5)\cdot 10^3$
-5.875	$1.5(2)\cdot 10^3$	$2.17(3)\cdot 10^3$	$4.7(1)\cdot 10^1$	$-7.37(6)\cdot 10^3$	$-8.68(4)\cdot 10^2$	$2.1753(5)\cdot 10^3$
-5.625	$2.2(2)\cdot 10^3$	$1.93(3)\cdot 10^3$	$3.3(1)\cdot 10^1$	$-7.24(5)\cdot 10^3$	$-6.94(4)\cdot 10^2$	$1.9439(4)\cdot 10^3$
-5.375	$2.9(2)\cdot 10^3$	$1.65(2)\cdot 10^3$	$2.4(1)\cdot 10^1$	$-7.03(5)\cdot 10^3$	$-5.50(3)\cdot 10^2$	$1.7302(4)\cdot 10^3$
-5.125	$3.4(2)\cdot 10^3$	$1.30(2)\cdot 10^3$	$1.38(9)\cdot 10^1$	$-6.73(4)\cdot 10^3$	$-4.38(3)\cdot 10^2$	$1.5330(3)\cdot 10^3$
-4.875	$3.9(1)\cdot 10^3$	$1.14(2)\cdot 10^3$	$8.3(8)\cdot 10^0$	$-6.31(4)\cdot 10^3$	$-3.36(3)\cdot 10^2$	$1.3512(3)\cdot 10^3$
-4.625	$4.1(1)\cdot 10^3$	$8.8(2)\cdot 10^2$	$4.6(7)\cdot 10^0$	$-5.94(3)\cdot 10^3$	$-2.50(2)\cdot 10^2$	$1.1843(3)\cdot 10^3$
-4.375	$4.4(1)\cdot 10^3$	$7.1(1)\cdot 10^2$	$1.7(6)\cdot 10^0$	$-5.56(3)\cdot 10^3$	$-1.80(2)\cdot 10^2$	$1.0315(2)\cdot 10^3$
-4.125	$4.27(9)\cdot 10^3$	$5.3(1)\cdot 10^2$	$-5(5)\cdot 10^{-1}$	$-5.03(2)\cdot 10^3$	$-1.23(2)\cdot 10^2$	$8.926(2)\cdot 10^2$
-3.875	$4.35(8)\cdot 10^3$	$4.0(1)\cdot 10^2$	$-1.3(4)\cdot 10^0$	$-4.53(2)\cdot 10^3$	$-7.6(2)\cdot 10^1$	$7.661(2)\cdot 10^2$
-3.625	$3.87(7)\cdot 10^3$	$2.70(8)\cdot 10^2$	$-1.7(4)\cdot 10^0$	$-4.05(2)\cdot 10^3$	$-4.2(1)\cdot 10^1$	$6.527(2)\cdot 10^2$
-3.375	$3.52(6)\cdot 10^3$	$1.82(7)\cdot 10^2$	$-2.0(3)\cdot 10^0$	$-3.53(2)\cdot 10^3$	$-1.6(1)\cdot 10^1$	$5.501(1)\cdot 10^2$
-3.125	$3.29(5)\cdot 10^3$	$1.09(6)\cdot 10^2$	$-2.1(3)\cdot 10^0$	$-3.09(1)\cdot 10^3$	$3(1)\cdot 10^0$	$4.586(1)\cdot 10^2$
-2.875	$2.75(5)\cdot 10^3$	$4.5(5)\cdot 10^1$	$-1.4(2)\cdot 10^0$	$-2.62(1)\cdot 10^3$	$1.72(9)\cdot 10^1$	$3.773(1)\cdot 10^2$
-2.625	$2.36(4)\cdot 10^3$	$7(4)\cdot 10^0$	$-1.5(2)\cdot 10^0$	$-2.17(1)\cdot 10^3$	$2.31(8)\cdot 10^1$	$3.056(1)\cdot 10^2$
-2.375	$1.98(3)\cdot 10^3$	$-2.1(3)\cdot 10^1$	$-7(2)\cdot 10^{-1}$	$-1.779(9)\cdot 10^3$	$2.81(6)\cdot 10^1$	$2.4251(9)\cdot 10^2$
-2.125	$1.49(3)\cdot 10^3$	$-3.0(3)\cdot 10^1$	$-1.0(1)\cdot 10^0$	$-1.417(7)\cdot 10^3$	$2.79(5)\cdot 10^1$	$1.8729(7)\cdot 10^2$
-1.875	$1.10(2)\cdot 10^3$	$-3.5(2)\cdot 10^1$	$-4(1)\cdot 10^{-1}$	$-1.043(6)\cdot 10^3$	$2.44(4)\cdot 10^1$	$1.3890(6)\cdot 10^2$
-1.625	$7.9(2)\cdot 10^2$	$-3.0(2)\cdot 10^1$	$-3.2(8)\cdot 10^{-1}$	$-7.33(4)\cdot 10^2$	$1.86(3)\cdot 10^1$	$9.514(5)\cdot 10^1$
-1.375	$4.0(1)\cdot 10^2$	$-2.0(1)\cdot 10^1$	$-2.2(5)\cdot 10^{-1}$	$-4.12(3)\cdot 10^2$	$1.07(2)\cdot 10^1$	$5.267(4)\cdot 10^1$
-1.125	$7(4)\cdot 10^0$	$6(4)\cdot 10^{-1}$	$-0(1)\cdot 10^{-3}$	$-5.80(9)\cdot 10^1$	$7.7(5)\cdot 10^{-1}$	$1.028(2)\cdot 10^1$
-0.875	0	0	0	0	0	0

Table 18. Individual contributions from the different colour factors to $y_{23}\frac{dC_{y_{23}}}{dy_{23}}$ for the three-to-two jet transition distribution.

JHEP06(2009)041

$y_{\rm cut}$	N_c^2	N_c^0	N_c^{-2}	$N_f N_c$	N_f/N_c	N_f^2
0.3	$-2(3)\cdot 10^{0}$	$4(2)\cdot 10^{-1}$	$-7(4)\cdot 10^{-3}$	$-5.9(7)\cdot 10^{0}$	$2(4)\cdot 10^{-2}$	$1.48(3)\cdot 10^{0}$
0.15	$4.4(1)\cdot 10^{2}$	$-1.82(8)\cdot 10^{1}$	$-2.7(3)\cdot 10^{-1}$	$-4.47(4)\cdot 10^{2}$	$1.13(2)\cdot 10^{1}$	$5.93(2)\cdot 10^{1}$
0.1	$1.05(2)\cdot 10^{3}$	$-3.1(1)\cdot 10^{1}$	$-4.9(3)\cdot 10^{-1}$	$-1.000(6)\cdot 10^{3}$	$2.19(3)\cdot 10^{1}$	$1.336(3)\cdot 10^{2}$
0.06	$2.16(3)\cdot 10^{3}$	$-2.0(2)\cdot 10^{1}$	$-1.20(6)\cdot 10^{0}$	$-2.048(8)\cdot 10^{3}$	$3.19(4)\cdot 10^{1}$	$2.843(4)\cdot 10^{2}$
0.03	$3.84(5)\cdot 10^{3}$	$1.23(3)\cdot 10^{2}$	$-2.71(6)\cdot 10^{0}$	$-4.09(2)\cdot 10^{3}$	$1.08(8)\cdot 10^{1}$	$6.238(9)\cdot 10^{2}$
0.015	$4.83(8)\cdot 10^{3}$	$5.78(5)\cdot 10^{2}$	$-3.1(2)\cdot 10^{0}$	$-6.59(3)\cdot 10^{3}$	$-1.10(1)\cdot 10^{2}$	$1.183(2)\cdot 10^{3}$
0.01	$4.4(1)\cdot 10^{3}$	$1.060(7)\cdot 10^{3}$	$2(2)\cdot 10^{-1}$	$-8.12(3)\cdot 10^{3}$	$-2.66(2)\cdot 10^{2}$	$1.646(2)\cdot 10^{3}$
0.006	$2.4(2)\cdot 10^{3}$	$1.96(1)\cdot 10^{3}$	$1.35(4)\cdot 10^{1}$	$-9.68(5)\cdot 10^{3}$	$-6.22(3)\cdot 10^{2}$	$2.409(3)\cdot 10^{3}$
0.003	$-4.7(3)\cdot 10^{3}$	$3.76(2)\cdot 10^{3}$	$6.54(4)\cdot 10^{1}$	$-1.050(9)\cdot 10^{4}$	$-1.499(5)\cdot 10^{3}$	$3.862(5)\cdot 10^{3}$
0.0015	$-1.74(4)\cdot 10^{4}$	$6.13(3)\cdot 10^{3}$	$1.95(2)\cdot 10^{2}$	$-8.1(1)\cdot 10^{3}$	$-3.064(9)\cdot 10^{3}$	$5.899(9)\cdot 10^{3}$
0.001	$-2.84(6)\cdot 10^{4}$	$7.61(4)\cdot 10^{3}$	$3.38(1)\cdot 10^{2}$	$-4.1(2)\cdot 10^{3}$	$-4.43(1)\cdot 10^{3}$	$7.41(1)\cdot 10^{3}$
0.0006	$-4.60(8)\cdot 10^{4}$	$9.38(6)\cdot 10^{3}$	$6.17(3)\cdot 10^{2}$	$4.7(2)\cdot 10^{3}$	$-6.79(2)\cdot 10^{3}$	$9.74(2)\cdot 10^{3}$
0.0003	$-7.1(1)\cdot 10^{4}$	$1.070(9)\cdot 10^{4}$	$1.273(3)\cdot 10^{3}$	$2.58(3)\cdot 10^{4}$	$-1.142(3)\cdot 10^{4}$	$1.380(3)\cdot 10^{4}$
0.00015	$-9.2(3)\cdot 10^{4}$	$9.0(2)\cdot 10^{3}$	$2.406(8)\cdot 10^{3}$	$6.22(6)\cdot 10^{4}$	$-1.821(4)\cdot 10^{4}$	$1.906(5)\cdot 10^{4}$
0.0001	$-9.4(4)\cdot 10^{4}$	$5.4(2)\cdot 10^{3}$	$3.413(7)\cdot 10^{3}$	$9.13(7)\cdot 10^{4}$	$-2.341(6)\cdot 10^{4}$	$2.271(5)\cdot 10^{4}$

Table 19. Individual contributions from the different colour factors to the NNLO coefficient $C_{3-jet,Durham}$ for the three-jet rate with the Durham jet algorithm for various values of $y_{\rm cut}$.

$y_{\rm cut}$	N_c^2	N_c^0	N_c^{-2}	$N_f N_c$	N_f/N_c	N_f^2
0.3	$4.3(6)\cdot 10^{1}$	$-3(2)\cdot 10^{0}$	$-6(4)\cdot 10^{-2}$	$-6.5(2)\cdot 10^{1}$	$1.68(9)\cdot 10^{0}$	$1.091(1)\cdot 10^{1}$
0.15	$1.17(5)\cdot 10^{3}$	$6(1)\cdot 10^{1}$	$-4(2)\cdot 10^{-1}$	$-2.05(3)\cdot 10^{3}$	$2(9)\cdot 10^{-1}$	$3.835(2)\cdot 10^{2}$
0.1	$1.33(9)\cdot 10^{3}$	$3.5(2)\cdot 10^{2}$	$2.0(4)\cdot 10^{0}$	$-3.74(4)\cdot 10^{3}$	$-9.8(2)\cdot 10^{1}$	$8.788(4)\cdot 10^{2}$
0.06	$-2.0(2)\cdot 10^{3}$	$1.16(3)\cdot 10^{3}$	$1.82(8)\cdot 10^{1}$	$-5.66(8)\cdot 10^{3}$	$-4.95(5)\cdot 10^{2}$	$1.9342(9)\cdot 10^{3}$
0.03	$-1.49(3)\cdot 10^{4}$	$3.07(5)\cdot 10^{3}$	$1.20(2)\cdot 10^{2}$	$-4.2(2)\cdot 10^{3}$	$-1.94(1)\cdot 10^{3}$	$4.461(2)\cdot 10^{3}$
0.015	$-4.24(7)\cdot 10^{4}$	$5.2(1)\cdot 10^{3}$	$4.60(2)\cdot 10^{2}$	$7.8(3)\cdot 10^{3}$	$-5.17(3)\cdot 10^{3}$	$8.808(3)\cdot 10^{3}$
0.01	$-6.44(7)\cdot 10^{4}$	$6.1(1)\cdot 10^{3}$	$8.78(3)\cdot 10^{2}$	$2.47(4)\cdot 10^{4}$	$-8.34(4)\cdot 10^{3}$	$1.2472(5)\cdot 10^{4}$
0.006	$-9.7(1)\cdot 10^{4}$	$4.3(2)\cdot 10^{3}$	$1.783(5)\cdot 10^{3}$	$6.09(6)\cdot 10^{4}$	$-1.427(6)\cdot 10^{4}$	$1.8585(8)\cdot 10^{4}$
0.003	$-1.33(2)\cdot 10^{5}$	$-6.1(3)\cdot 10^{3}$	$4.055(9)\cdot 10^{3}$	$1.46(1)\cdot 10^{5}$	$-2.68(1)\cdot 10^{4}$	$3.015(1)\cdot 10^{4}$
0.0015	$-1.19(3)\cdot 10^{5}$	$-3.48(5)\cdot 10^{4}$	$8.18(2)\cdot 10^{3}$	$2.98(1)\cdot 10^{5}$	$-4.63(2)\cdot 10^{4}$	$4.655(2)\cdot 10^{4}$
0.001	$-8.7(5)\cdot 10^{4}$	$-6.47(6)\cdot 10^{4}$	$1.169(2)\cdot 10^{4}$	$4.24(2)\cdot 10^{5}$	$-6.16(3)\cdot 10^{4}$	$5.875(3)\cdot 10^{4}$

Table 20. Individual contributions from the different colour factors to the NNLO coefficient $C_{3-jet,Geneva}$ for the three-jet rate with the the Geneva jet algorithm for various values of $y_{\rm cut}$.

$y_{\rm cut}$	N_c^2	N_c^0	N_c^{-2}	$N_f N_c$	N_f/N_c	N_f^2
0.3	$3.5(8)\cdot 10^{1}$	$-3(1)\cdot 10^{0}$	$-5(3)\cdot 10^{-2}$	$-2.7(1)\cdot 10^{1}$	$1.0(1)\cdot 10^{0}$	$2.770(5)\cdot 10^{0}$
0.15	$1.85(3)\cdot 10^{3}$	$-8.9(9)\cdot 10^{1}$	$-2.4(3)\cdot 10^{0}$	$-1.41(1)\cdot 10^{3}$	$5.4(1)\cdot 10^{1}$	$1.3607(9)\cdot 10^{2}$
0.1	$3.86(9)\cdot 10^{3}$	$-1.1(2)\cdot 10^{2}$	$-8.9(5)\cdot 10^{0}$	$-3.33(2)\cdot 10^{3}$	$1.10(2)\cdot 10^{2}$	$3.349(2)\cdot 10^{2}$
0.06	$7.2(2)\cdot 10^{3}$	$1.4(3)\cdot 10^{2}$	$-2.7(1)\cdot 10^{1}$	$-6.83(5)\cdot 10^{3}$	$1.54(4)\cdot 10^{2}$	$7.945(4)\cdot 10^{2}$
0.03	$9.2(3)\cdot 10^{3}$	$1.48(6)\cdot 10^{3}$	$-5.8(2)\cdot 10^{1}$	$-1.33(1)\cdot 10^{4}$	$-3(1)\cdot 10^{1}$	$1.9819(9)\cdot 10^{3}$
0.015	$2.6(5)\cdot 10^{3}$	$4.7(2)\cdot 10^{3}$	$-7.1(3)\cdot 10^{1}$	$-1.95(2)\cdot 10^{4}$	$-9.4(2)\cdot 10^{2}$	$4.116(2)\cdot 10^{3}$
0.01	$-8.9(5)\cdot 10^{3}$	$7.7(1)\cdot 10^{3}$	$-2.1(5)\cdot 10^{1}$	$-2.13(3)\cdot 10^{4}$	$-2.12(3)\cdot 10^{3}$	$5.947(2)\cdot 10^{3}$
0.006	$-2.74(9)\cdot 10^{4}$	$1.18(3)\cdot 10^{4}$	$1.88(7)\cdot 10^{2}$	$-1.77(4)\cdot 10^{4}$	$-4.55(8)\cdot 10^{3}$	$9.025(4)\cdot 10^{3}$
0.003	$-6.8(1)\cdot 10^{4}$	$1.67(6)\cdot 10^{4}$	$1.02(1)\cdot 10^{3}$	$3(6)\cdot 10^{2}$	$-1.08(1)\cdot 10^{4}$	$1.4875(6)\cdot 10^{4}$
0.0015	$-1.16(2)\cdot 10^{5}$	$1.81(6)\cdot 10^{4}$	$2.99(2)\cdot 10^{3}$	$4.6(1)\cdot 10^{4}$	$-2.02(3)\cdot 10^{4}$	$2.311(1)\cdot 10^{4}$
0.001	$-1.38(4)\cdot 10^{5}$	$1.41(7)\cdot 10^{4}$	$4.84(2)\cdot 10^{3}$	$9.1(1)\cdot 10^{4}$	$-2.93(3)\cdot 10^{4}$	$2.923(1)\cdot 10^{4}$
0.0006	$-1.45(4)\cdot 10^{5}$	$0(1)\cdot 10^{2}$	$8.03(2)\cdot 10^{3}$	$1.74(2)\cdot 10^{5}$	$-4.36(3)\cdot 10^{4}$	$3.855(2)\cdot 10^{4}$
0.0003	$-7.1(7)\cdot 10^{4}$	$-4.5(1)\cdot 10^{4}$	$1.414(4)\cdot 10^{4}$	$3.47(3)\cdot 10^{5}$	$-6.93(5)\cdot 10^{4}$	$5.455(3)\cdot 10^{4}$

Table 21. Individual contributions from the different colour factors to the NNLO coefficient $C_{3-jet,Jade-E0}$ for the three-jet rate with the the Jade-E0 jet algorithm for various values of $y_{\rm cut}$.

JHEP06(2009)041

$y_{\rm cut}$	N_c^2	N_c^0	N_c^{-2}	$N_f N_c$	N_f/N_c	N_f^2
0.3	$-2(3)\cdot 10^{0}$	$3(6)\cdot 10^{-1}$	$-5(2)\cdot 10^{-2}$	$-6.5(6)\cdot 10^{0}$	$-1.5(4)\cdot 10^{-1}$	$1.475(3)\cdot 10^{0}$
0.15	$4.3(3)\cdot 10^{2}$	$-2.5(4)\cdot 10^{1}$	$0(9)\cdot 10^{-3}$	$-4.48(7)\cdot 10^{2}$	$1.01(5)\cdot 10^{1}$	$5.986(4)\cdot 10^{1}$
0.1	$9.3(6)\cdot 10^{2}$	$-2.1(6)\cdot 10^{1}$	$-4(2)\cdot 10^{-1}$	$-9.7(1)\cdot 10^{2}$	$1.67(7)\cdot 10^{1}$	$1.364(1)\cdot 10^{2}$
0.06	$1.62(9)\cdot 10^{3}$	$1(1)\cdot 10^{1}$	$-4(4)\cdot 10^{-1}$	$-1.90(2)\cdot 10^{3}$	$1.4(1)\cdot 10^{1}$	$2.915(2)\cdot 10^{2}$
0.03	$2.6(2)\cdot 10^{3}$	$2.2(2)\cdot 10^{2}$	$2(6)\cdot 10^{-1}$	$-3.70(5)\cdot 10^{3}$	$-3.8(2)\cdot 10^{1}$	$6.431(4)\cdot 10^{2}$
0.015	$2.9(2)\cdot 10^{3}$	$5.9(3)\cdot 10^{2}$	$6(1)\cdot 10^{0}$	$-5.61(9)\cdot 10^{3}$	$-1.98(4)\cdot 10^{2}$	$1.2207(6)\cdot 10^{3}$
0.01	$2.1(2)\cdot 10^{3}$	$1.12(3)\cdot 10^{3}$	$1.31(9)\cdot 10^{1}$	$-6.8(1)\cdot 10^{3}$	$-3.82(6)\cdot 10^{2}$	$1.6975(9)\cdot 10^{3}$
0.006	$2(4)\cdot 10^{2}$	$1.91(6)\cdot 10^{3}$	$3.6(1)\cdot 10^{1}$	$-7.8(2)\cdot 10^{3}$	$-7.93(8)\cdot 10^{2}$	$2.485(1)\cdot 10^{3}$
0.003	$-8.1(5)\cdot 10^{3}$	$3.53(7)\cdot 10^{3}$	$1.12(3)\cdot 10^{2}$	$-7.4(2)\cdot 10^{3}$	$-1.76(2)\cdot 10^{3}$	$3.960(2)\cdot 10^{3}$
0.0015	$-1.89(7)\cdot 10^{4}$	$5.5(2)\cdot 10^{3}$	$2.78(4)\cdot 10^{2}$	$-3.5(3)\cdot 10^{3}$	$-3.42(2)\cdot 10^{3}$	$6.034(3)\cdot 10^{3}$
0.001	$-2.79(9)\cdot 10^{4}$	$6.6(1)\cdot 10^{3}$	$4.47(3)\cdot 10^{2}$	$1.3(3)\cdot 10^{3}$	$-4.89(3)\cdot 10^{3}$	$7.590(3)\cdot 10^{3}$
0.0006	$-4.0(1)\cdot 10^{4}$	$7.9(1)\cdot 10^{3}$	$7.69(5)\cdot 10^{2}$	$1.06(4)\cdot 10^{4}$	$-7.27(6)\cdot 10^{3}$	$9.959(5)\cdot 10^{3}$
0.0003	$-5.9(1)\cdot 10^{4}$	$7.8(3)\cdot 10^{3}$	$1.505(7)\cdot 10^{3}$	$3.44(7)\cdot 10^{4}$	$-1.207(8)\cdot 10^{4}$	$1.4070(6)\cdot 10^{4}$
0.00015	$-7.3(2)\cdot 10^{4}$	$4.6(4)\cdot 10^{3}$	$2.76(1)\cdot 10^{3}$	$7.46(8)\cdot 10^{4}$	$-1.92(1)\cdot 10^{4}$	$1.9362(9)\cdot 10^{4}$
0.0001	$-7.5(2)\cdot 10^{4}$	$-1(4)\cdot 10^{2}$	$3.81(1)\cdot 10^{3}$	$1.06(1)\cdot 10^{5}$	$-2.45(1)\cdot 10^{4}$	$2.312(1)\cdot 10^{4}$

Table 22. Individual contributions from the different colour factors to the NNLO coefficient $C_{3-jet,Cambridge}$ for the three-jet rate with the the Cambridge jet algorithm for various values of $y_{\rm cut}$.

References

[1] A. Gehrmann-De Ridder, T. Gehrmann, E.W.N. Glover and G. Heinrich, *NNLO corrections to event shapes in e^+e^- annihilation*, *JHEP* **12** (2007) 094 [arXiv:0711.4711] [SPIRES].

[2] A. Gehrmann-De Ridder, T. Gehrmann, E.W.N. Glover and G. Heinrich, *Jet rates in electron-positron annihilation at $O(\alpha_s^3)$ in QCD*, *Phys. Rev. Lett.* **100** (2008) 172001 [arXiv:0802.0813] [SPIRES].

[3] A. Gehrmann-De Ridder, T. Gehrmann, E.W.N. Glover and G. Heinrich, *NNLO moments of event shapes in e^+e^- annihilation*, *JHEP* **05** (2009) 106 [arXiv:0903.4658] [SPIRES].

[4] S. Weinzierl, *NNLO corrections to 3-jet observables in electron-positron annihilation*, *Phys. Rev. Lett.* **101** (2008) 162001 [arXiv:0807.3241] [SPIRES].

[5] S. Weinzierl and D.A. Kosower, *QCD corrections to four-jet production and three-jet structure in e^+e^- annihilation*, *Phys. Rev.* **D 60** (1999) 054028 [hep-ph/9901277] [SPIRES].

[6] S. Weinzierl, *The infrared structure of $e^+e^- \to 3$ jets at NNLO reloaded*, arXiv:0904.1145 [SPIRES].

[7] T. Becher and M.D. Schwartz, *A Precise determination of α_s from LEP thrust data using effective field theory*, *JHEP* **07** (2008) 034 [arXiv:0803.0342] [SPIRES].

[8] S. Catani, L. Trentadue, G. Turnock and B.R. Webber, *Resummation of large logarithms in e^+e^- event shape distributions*, *Nucl. Phys.* **B 407** (1993) 3 [SPIRES].

[9] S. Catani and B.R. Webber, *Resummed C-parameter distribution in e^+e^- annihilation*, *Phys. Lett.* **B 427** (1998) 377 [hep-ph/9801350] [SPIRES].

[10] T. Gehrmann, G. Luisoni and H. Stenzel, *Matching NLLA+NNLO for event shape distributions*, *Phys. Lett.* **B 664** (2008) 265 [arXiv:0803.0695] [SPIRES].

[11] Y.L. Dokshitzer and B.R. Webber, *Power corrections to event shape distributions*, *Phys. Lett.* **B 404** (1997) 321 [hep-ph/9704298] [SPIRES].

[12] R.A. Davison and B.R. Webber, *Non-perturbative contribution to the thrust distribution in e^+e^- annihilation*, *Eur. Phys. J.* **C 59** (2009) 13 [arXiv:0809.3326] [SPIRES].

JHEP06(2009)041

[13] T. Gehrmann and E. Remiddi, *Differential equations for two-loop four-point functions*, *Nucl. Phys.* **B 580** (2000) 485 [hep-ph/9912329] [SPIRES].

[14] T. Gehrmann and E. Remiddi, *Two-loop master integrals for $\gamma^* \to 3$ jets: the planar topologies*, *Nucl. Phys.* **B 601** (2001) 248 [hep-ph/0008287] [SPIRES].

[15] T. Gehrmann and E. Remiddi, *Two-loop master integrals for $\gamma^* \to 3$ jets: the non-planar topologies*, *Nucl. Phys.* **B 601** (2001) 287 [hep-ph/0101124] [SPIRES].

[16] S. Moch, P. Uwer and S. Weinzierl, *Nested sums, expansion of transcendental functions and multi-scale multi-loop integrals*, *J. Math. Phys.* **43** (2002) 3363 [hep-ph/0110083] [SPIRES].

[17] F.A. Berends, W.T. Giele and H. Kuijf, *Exact expressions for processes involving a vector boson and up to five partons*, *Nucl. Phys.* **B 321** (1989) 39 [SPIRES].

[18] K. Hagiwara and D. Zeppenfeld, *Amplitudes for multiparton processes involving a current at e^+e^-, $e^\pm p$ and hadron colliders*, *Nucl. Phys.* **B 313** (1989) 560 [SPIRES].

[19] N.K. Falck, D. Graudenz and G. Kramer, *Cross-section for five jet production in e^+e^- annihilation*, *Nucl. Phys.* **B 328** (1989) 317 [SPIRES].

[20] G.A. Schuler, S. Sakakibara and J.G. Körner, *Use of four-dimensional spin methods in the calculation of radiative QCD corrections*, *Phys. Lett.* **B 194** (1987) 125 [SPIRES].

[21] J.G. Körner and P. Sieben, *Use of helicity methods in evaluating loop integrals: a QCD example*, *Nucl. Phys.* **B 363** (1991) 65 [SPIRES].

[22] W.T. Giele and E.W.N. Glover, *Higher order corrections to jet cross-sections in e^+e^- annihilation*, *Phys. Rev.* **D 46** (1992) 1980 [SPIRES].

[23] Z. Bern, L.J. Dixon, D.A. Kosower and S. Weinzierl, *One-loop amplitudes for $e^+e^- \to \bar{q}q\bar{Q}Q$*, *Nucl. Phys.* **B 489** (1997) 3 [hep-ph/9610370] [SPIRES].

[24] Z. Bern, L.J. Dixon and D.A. Kosower, *One-loop amplitudes for e^+e^- to four partons*, *Nucl. Phys.* **B 513** (1998) 3 [hep-ph/9708239] [SPIRES].

[25] J.M. Campbell, E.W.N. Glover and D.J. Miller, *The one-loop QCD corrections for $\gamma^* \to q\bar{q}gg$*, *Phys. Lett.* **B 409** (1997) 503 [hep-ph/9706297] [SPIRES].

[26] E.W.N. Glover and D.J. Miller, *The one-loop QCD corrections for $\gamma^* \to Q\bar{Q}q\bar{q}$*, *Phys. Lett.* **B 396** (1997) 257 [hep-ph/9609474] [SPIRES].

[27] L.W. Garland, T. Gehrmann, E.W.N. Glover, A. Koukoutsakis and E. Remiddi, *The two-loop QCD matrix element for $e^+e^- \to 3$ jets*, *Nucl. Phys.* **B 627** (2002) 107 [hep-ph/0112081] [SPIRES].

[28] L.W. Garland, T. Gehrmann, E.W.N. Glover, A. Koukoutsakis and E. Remiddi, *Two-loop QCD helicity amplitudes for $e^+e^- \to 3$ jets*, *Nucl. Phys.* **B 642** (2002) 227 [hep-ph/0206067] [SPIRES].

[29] S. Moch, P. Uwer and S. Weinzierl, *Two-loop amplitudes with nested sums: fermionic contributions to $e^+e^- \to q\bar{q}g$*, *Phys. Rev.* **D 66** (2002) 114001 [hep-ph/0207043] [SPIRES].

[30] T. Gehrmann and E. Remiddi, *Numerical evaluation of harmonic polylogarithms*, *Comput. Phys. Commun.* **141** (2001) 296 [hep-ph/0107173] [SPIRES].

[31] T. Gehrmann and E. Remiddi, *Numerical evaluation of two-dimensional harmonic polylogarithms*, *Comput. Phys. Commun.* **144** (2002) 200 [hep-ph/0111255] [SPIRES].

[32] J. Vollinga and S. Weinzierl, *Numerical evaluation of multiple polylogarithms*, *Comput. Phys. Commun.* **167** (2005) 177 [hep-ph/0410259] [SPIRES].

JHEP06(2009)041

[33] D.A. Kosower, *Multiple singular emission in gauge theories*, *Phys. Rev.* **D 67** (2003) 116003 [hep-ph/0212097] [SPIRES].

[34] D.A. Kosower, *All-orders singular emission in gauge theories*, *Phys. Rev. Lett.* **91** (2003) 061602 [hep-ph/0301069] [SPIRES].

[35] S. Weinzierl, *Subtraction terms at NNLO*, *JHEP* **03** (2003) 062 [hep-ph/0302180] [SPIRES].

[36] S. Weinzierl, *Subtraction terms for one-loop amplitudes with one unresolved parton*, *JHEP* **07** (2003) 052 [hep-ph/0306248] [SPIRES].

[37] W.B. Kilgore, *Subtraction terms for hadronic production processes at Next-to-Next-to-Leading Order*, *Phys. Rev.* **D 70** (2004) 031501 [hep-ph/0403128] [SPIRES].

[38] S. Frixione and M. Grazzini, *Subtraction at NNLO*, *JHEP* **06** (2005) 010 [hep-ph/0411399] [SPIRES].

[39] A. Gehrmann-De Ridder, T. Gehrmann and G. Heinrich, *Four-particle phase space integrals in massless QCD*, *Nucl. Phys.* **B 682** (2004) 265 [hep-ph/0311276] [SPIRES].

[40] A. Gehrmann-De Ridder, T. Gehrmann and E.W.N. Glover, *Infrared structure of* $e^+e^- \to 2$ *jets at NNLO*, *Nucl. Phys.* **B 691** (2004) 195 [hep-ph/0403057] [SPIRES].

[41] A. Gehrmann-De Ridder, T. Gehrmann and E.W.N. Glover, *Quark-gluon antenna functions from neutralino decay*, *Phys. Lett.* **B 612** (2005) 36 [hep-ph/0501291] [SPIRES].

[42] A. Gehrmann-De Ridder, T. Gehrmann and E.W.N. Glover, *Gluon-gluon antenna functions from Higgs boson decay*, *Phys. Lett.* **B 612** (2005) 49 [hep-ph/0502110] [SPIRES].

[43] A. Gehrmann-De Ridder, T. Gehrmann and E.W.N. Glover, *Antenna subtraction at NNLO*, *JHEP* **09** (2005) 056 [hep-ph/0505111] [SPIRES].

[44] A. Gehrmann-De Ridder, T. Gehrmann, E.W.N. Glover and G. Heinrich, *Infrared structure of* $e^+e^- \to 3$ *jets at NNLO*, *JHEP* **11** (2007) 058 [arXiv:0710.0346] [SPIRES].

[45] G. Somogyi, Z. Trócsányi and V. Del Duca, *Matching of singly- and doubly-unresolved limits of tree-level QCD squared matrix elements*, *JHEP* **06** (2005) 024 [hep-ph/0502226] [SPIRES].

[46] G. Somogyi, Z. Trócsányi and V. Del Duca, *A subtraction scheme for computing QCD jet cross sections at NNLO: regularization of doubly-real emissions*, *JHEP* **01** (2007) 070 [hep-ph/0609042] [SPIRES].

[47] G. Somogyi and Z. Trócsányi, *A subtraction scheme for computing QCD jet cross sections at NNLO: regularization of real-virtual emission*, *JHEP* **01** (2007) 052 [hep-ph/0609043] [SPIRES].

[48] S. Catani and M. Grazzini, *An NNLO subtraction formalism in hadron collisions and its application to Higgs boson production at the LHC*, *Phys. Rev. Lett.* **98** (2007) 222002 [hep-ph/0703012] [SPIRES].

[49] G. Somogyi and Z. Trócsányi, *A subtraction scheme for computing QCD jet cross sections at NNLO: integrating the subtraction terms I*, *JHEP* **08** (2008) 042 [arXiv:0807.0509] [SPIRES].

[50] G. Somogyi, *Subtraction with hadronic initial states: an NNLO-compatible scheme*, arXiv:0903.1218 [SPIRES].

[51] U. Aglietti, V. Del Duca, C. Duhr, G. Somogyi and Z. Trócsányi, *Analytic integration of real-virtual counterterms in NNLO jet cross sections I*, *JHEP* **09** (2008) 107 [arXiv:0807.0514] [SPIRES].

JHEP06(2009)041

[52] C. Anastasiou, K. Melnikov and F. Petriello, *Real radiation at NNLO: $e^+e^- \to 2$ jets through $O(\alpha_s^2)$*, *Phys. Rev. Lett.* **93** (2004) 032002 [hep-ph/0402280] [SPIRES].

[53] S. Weinzierl, *NNLO corrections to 2-jet observables in electron positron annihilation*, *Phys. Rev.* **D 74** (2006) 014020 [hep-ph/0606008] [SPIRES].

[54] S. Weinzierl, *The forward-backward asymmetry at NNLO revisited*, *Phys. Lett.* **B 644** (2007) 331 [hep-ph/0609021] [SPIRES].

[55] C. Anastasiou and K. Melnikov, *Higgs boson production at hadron colliders in NNLO QCD*, *Nucl. Phys.* **B 646** (2002) 220 [hep-ph/0207004] [SPIRES].

[56] C. Anastasiou, L.J. Dixon, K. Melnikov and F. Petriello, *Dilepton rapidity distribution in the Drell-Yan process at NNLO in QCD*, *Phys. Rev. Lett.* **91** (2003) 182002 [hep-ph/0306192] [SPIRES].

[57] C. Anastasiou, L.J. Dixon, K. Melnikov and F. Petriello, *High precision QCD at hadron colliders: electroweak gauge boson rapidity distributions at NNLO*, *Phys. Rev.* **D 69** (2004) 094008 [hep-ph/0312266] [SPIRES].

[58] C. Anastasiou, K. Melnikov and F. Petriello, *Higgs boson production at hadron colliders: differential cross sections through Next-to-Next-to-Leading Order*, *Phys. Rev. Lett.* **93** (2004) 262002 [hep-ph/0409088] [SPIRES].

[59] C. Anastasiou, K. Melnikov and F. Petriello, *Fully differential Higgs boson production and the di-photon signal through Next-to-Next-to-Leading Order*, *Nucl. Phys.* **B 724** (2005) 197 [hep-ph/0501130] [SPIRES].

[60] C. Anastasiou, G. Dissertori and F. Stockli, *NNLO QCD predictions for the $H \to WW \to ll\nu\nu$ signal at the LHC*, *JHEP* **09** (2007) 018 [arXiv:0707.2373] [SPIRES].

[61] K. Melnikov and F. Petriello, *The W boson production cross section at the LHC through $O(\alpha_s^2)$*, *Phys. Rev. Lett.* **96** (2006) 231803 [hep-ph/0603182] [SPIRES].

[62] C. Anastasiou, K. Melnikov and F. Petriello, *The electron energy spectrum in muon decay through $O(\alpha^2)$*, *JHEP* **09** (2007) 014 [hep-ph/0505069] [SPIRES].

[63] S. Catani, D. de Florian and M. Grazzini, *Higgs production in hadron collisions: soft and virtual QCD corrections at NNLO*, *JHEP* **05** (2001) 025 [hep-ph/0102227] [SPIRES].

[64] S. Catani, D. de Florian and M. Grazzini, *Direct Higgs production and jet veto at the Tevatron and the LHC in NNLO QCD*, *JHEP* **01** (2002) 015 [hep-ph/0111164] [SPIRES].

[65] M. Grazzini, *NNLO predictions for the Higgs boson signal in the $H \to WW \to l\nu l\nu$ and $H \to ZZ \to 4l$ decay channels*, *JHEP* **02** (2008) 043 [arXiv:0801.3232] [SPIRES].

[66] R.V. Harlander and W.B. Kilgore, *Soft and virtual corrections to $pp \to H + X$ at NNLO*, *Phys. Rev.* **D 64** (2001) 013015 [hep-ph/0102241] [SPIRES].

[67] R.V. Harlander and W.B. Kilgore, *Next-to-Next-to-Leading Order Higgs production at hadron colliders*, *Phys. Rev. Lett.* **88** (2002) 201801 [hep-ph/0201206] [SPIRES].

[68] R.V. Harlander and W.B. Kilgore, *Higgs boson production in bottom quark fusion at Next-to-Next-to-Leading Order*, *Phys. Rev.* **D 68** (2003) 013001 [hep-ph/0304035] [SPIRES].

[69] S. Brandt, C. Peyrou, R. Sosnowski and A. Wroblewski, *The principal axis of jets. An attempt to analyze high-energy collisions as two-body processes*, *Phys. Lett.* **12** (1964) 57 [SPIRES].

[70] E. Farhi, *A QCD test for jets*, *Phys. Rev. Lett.* **39** (1977) 1587 [SPIRES].

JHEP06(2009)041

[71] L. Clavelli and D. Wyler, *Kinematical bounds on jet variables and the heavy jet mass distribution*, *Phys. Lett.* **B 103** (1981) 383 [SPIRES].

[72] P.E.L. Rakow and B.R. Webber, *Transverse momentum moments of hadron distributions in QCD jets*, *Nucl. Phys.* **B 191** (1981) 63 [SPIRES].

[73] S. Catani, G. Turnock and B.R. Webber, *Jet broadening measures in e^+e^- annihilation*, *Phys. Lett.* **B 295** (1992) 269 [SPIRES].

[74] G. Parisi, *Super inclusive cross-sections*, *Phys. Lett.* **B 74** (1978) 65 [SPIRES].

[75] J.F. Donoghue, F.E. Low and S.-Y. Pi, *Tensor analysis of hadronic jets in quantum chromodynamics*, *Phys. Rev.* **D 20** (1979) 2759 [SPIRES].

[76] S. Catani and B.R. Webber, *Infrared safe but infinite: soft gluon divergences inside the physical region*, *JHEP* **10** (1997) 005 [hep-ph/9710333] [SPIRES].

[77] W.J. Stirling, *Hard QCD working group: theory summary*, *J. Phys.* **G 17** (1991) 1567 [SPIRES].

[78] S. Bethke, Z. Kunszt, D.E. Soper and W.J. Stirling, *New jet cluster algorithms: Next-to-Leading Order QCD and hadronization corrections*, *Nucl. Phys.* **B 370** (1992) 310 [SPIRES].

[79] JADE collaboration, W. Bartel et al., *Experimental studies on multi-jet production in e^+e^- annihilation at PETRA energies*, *Z. Phys.* **C 33** (1986) 23 [SPIRES].

[80] Y.L. Dokshitzer, G.D. Leder, S. Moretti and B.R. Webber, *Better jet clustering algorithms*, *JHEP* **08** (1997) 001 [hep-ph/9707323] [SPIRES].

[81] M. Dine and J.R. Sapirstein, *Higher order QCD corrections in e^+e^- annihilation*, *Phys. Rev. Lett.* **43** (1979) 668 [SPIRES].

[82] K.G. Chetyrkin, A.L. Kataev and F.V. Tkachov, *Higher order corrections to Σ-t ($e^+e^- \to$ hadrons) in quantum chromodynamics*, *Phys. Lett.* **B 85** (1979) 277 [SPIRES].

[83] W. Celmaster and R.J. Gonsalves, *An analytic calculation of higher order quantum chromodynamic corrections in e^+e^- annihilation*, *Phys. Rev. Lett.* **44** (1980) 560 [SPIRES].

[84] S.G. Gorishnii, A.L. Kataev and S.A. Larin, *The $O(\alpha - S^3)$ corrections to Σ-tot ($e^+e^- \to$ hadrons) and gamma ($\tau^- \to \tau$-neutrino + hadrons) in QCD*, *Phys. Lett.* **B 259** (1991) 144 [SPIRES].

[85] L.R. Surguladze and M.A. Samuel, *Total hadronic cross-section in e^+e^- annihilation at the four loop level of perturbative QCD*, *Phys. Rev. Lett.* **66** (1991) 560 [SPIRES].

[86] L.J. Dixon and A. Signer, *Complete $O(\alpha_s^3)$ results for $e^+e^- \to (\gamma, Z) \to$ four jets*, *Phys. Rev.* **D 56** (1997) 4031 [hep-ph/9706285] [SPIRES].

[87] J.J. van der Bij and E.W.N. Glover, *Z boson production and decay via gluons*, *Nucl. Phys.* **B 313** (1989) 237 [SPIRES].

[88] ALEPH collaboration, A. Heister et al., *Studies of QCD at e^+e^- centre-of-mass energies between 91 GeV and 209 GeV*, *Eur. Phys. J.* **C 35** (2004) 457 [SPIRES].

[89] A. Banfi, G. Marchesini, Y.L. Dokshitzer and G. Zanderighi, *QCD analysis of near-to-planar 3-jet events*, *JHEP* **07** (2000) 002 [hep-ph/0004027] [SPIRES].

JHEP06(2009)041